Thermal deconsolidation of thermoplastic prepreg tapes during Laser-Assisted Fiber Placement

An experimental investigation into the effects of rapid laser heating on the deconsolidation state of carbon-fiber reinforced thermoplastic prepreg tapes

A. Choudhary

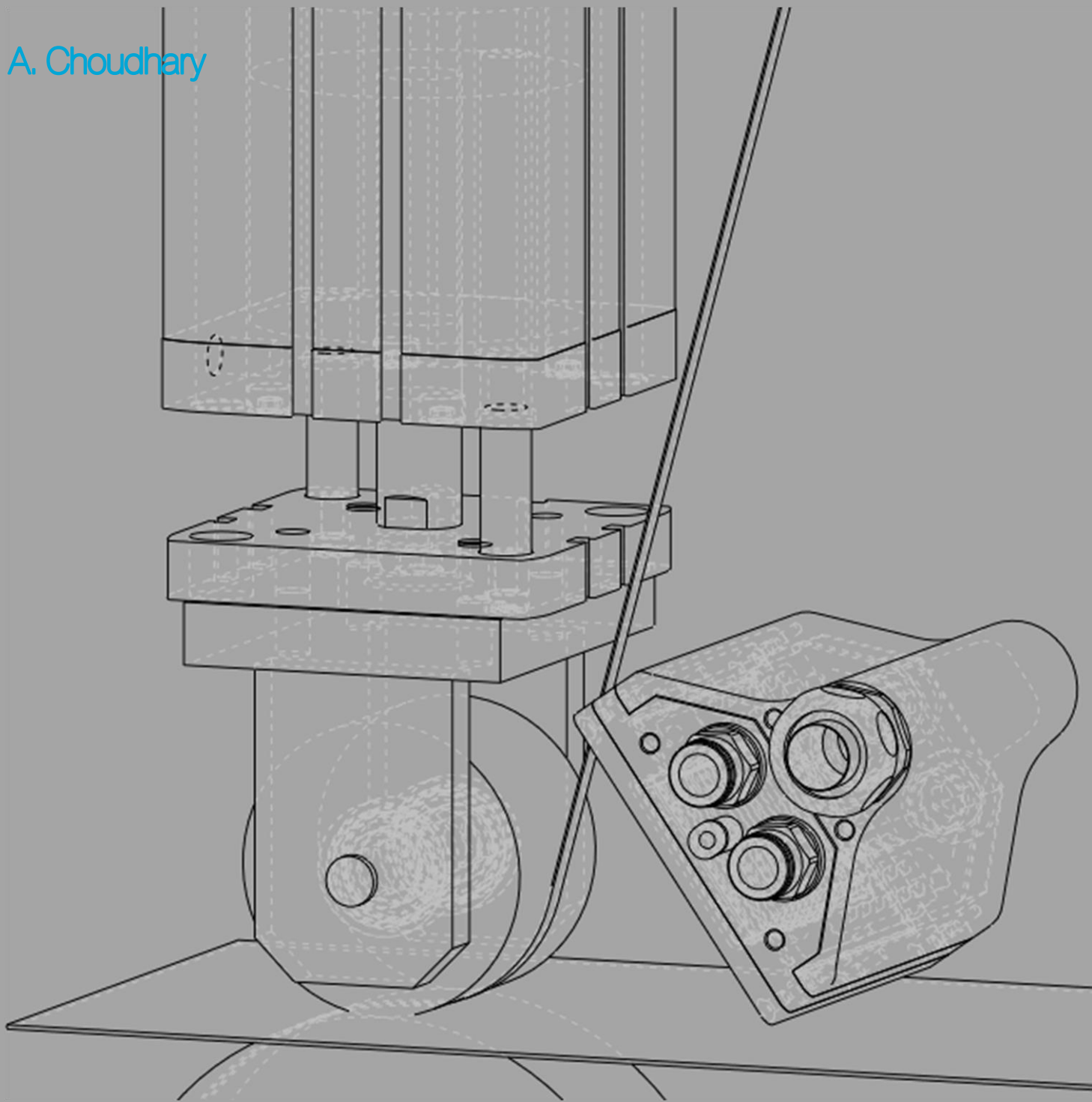

TU Delft

Thermal deconsolidation of thermoplastic prepreg tapes during Laser-Assisted Fiber Placement

An experimental investigation into the effects of rapid laser heating on the deconsolidation state of carbon-fiber reinforced thermoplastic prepreg tapes

by

Abhas Choudhary

in partial fulfillment of the requirements for the degree of

Master of Science
in Aerospace Engineering

at the Delft University of Technology.

To be publicly defended on Wednesday, 24^{th} July 2019 at 10:00 AM.

Student number:	4722434
Project duration:	January 7, 2019 – July 24, 2019
Supervisor:	Dr. Julie Teuwen
Additional Supervisors:	Dr. Daniël Peeters
	Ozan Çelik, M.Sc.

TU Delft Delft University of Technology

Delft University of Technology

Faculty of Aerospace Engineering

Department of Aerospace Structures and Materials

GRADUATION COMMITTEE

Date of graduation: July 24, 2019

Chair Holder:

Prof. dr. Clemens Dransfeld

Committee members:

Dr. Irene Fernandez Villegas

Dr. Julie Teuwen

Dr. Boyang Chen

Acknowledgement

First of all, I would like to convey my deepest gratitude to my supervisor, Julie Teuwen. Her constant support, encouragement and wisdom over the last 9 months has played a major role in helping me complete this thesis on time. Her feedback and critical questions have helped me strengthen my propositions. I am very grateful to her for giving me an opportunity to work on this topic and for having such a keen interest in my work. Furthermore, I would like to thank Daniël Peeters and Ozan Çelik for their support and feedback, and for being present in every update meeting. Ozan helped me look at my findings more critically and provided a lot of useful tips when I got stuck with specific problems. I am grateful to Daniël for his critical feedback that helped not only improve my arguments but also understand the relevance of my work in the bigger picture. Having a diverse set of expert opinion in every update meeting, helped me look at my research from different perspectives and was one of the highlights of my research journey. It has been a great pleasure and learning experience working with all of you.

A great amount of time and effort for this research was spent in the Delft Aerospace Structures and Materials Laboratory (DASML). I would like to thank Frans Oostrum, Durga Mainali, Misja Huizinga, Ed Roessen and Berthil Grashof for all their support. Furthermore, I am grateful to the members of the NDT research group for letting me borrow sensors and space.

I would also like to thank all of the members of the assessment committee for taking the time to review my work and for their interest in my research. Thank you Irene Fernandez Villegas, Boyang Chen and Julie Tuewen.

Special thanks to friends and colleagues for being there through the tough times. Thanks to Khushboo and Shubhonil for being great friends and for their constant support in the last two years. Thanks to fellow ASM colleagues: Lisette, André, Karthik, Tom, Moh, João, Niels, Bart, Dries, Caroline and others in room NB1.07 for sharing ideas, scientific resources and brainstorming sessions.

Finally and most importantly, I would like to thank my family back home for their constant love and support. They inspire and motivate me every single day. This thesis would not have been completed without their encouragement.

Abhas Choudhary
Delft, July 2019

Abstract

The automation of thermoplastic composite production and the drive towards out-of-autoclave processes, is of great relevance in the aerospace and lightweight composite structures industry. Hence, there is a crucial need for developing the current state of material and process understanding, in order to increase the technology readiness levels of automated, out-of-autoclave production processes.

Laser assisted fiber placement (LAFP) is a well-researched, automated production process which has been used in developing various thermoplastic composite demonstrators. Theoretically, this process does not require an autoclave consolidation cycle. However, one of the remaining challenge in the process, is the relatively high void content in the produced laminates (>1%). This high void content is impeding the development of thermoplastic composite structures with mechanical strength comparable to structures produced through traditional processing techniques such as an autoclave. One of the main reasons for the remaining void content in the laminates after consolidation by the roller, is thermal deconsolidation during the rapid heating phase of the process. This is a very less researched aspect of LAFP, due to which, not much is known about the changes that the incoming material undergoes, due to the rapid laser heating and which mechanisms govern these changes. Due to this, thermal deconsolidation is also not included in predictive models for the process and hence the accuracy of these models in predicting the final part quality is poor. Therefore, this research focuses on gaining a better understanding of thermal deconsolidation, in the context of rapid laser heating during LAFP, through experimental investigation.

The influence of five process variables was studied in this work: heating time, heated spot length, cooling rate, nip point temperature and the polymer type in carbon-fiber reinforced thermoplastic pre-impregnated (prepreg) tapes. The deconsolidated state of prepreg tape specimens was captured after rapid laser heating and the changes were characterized. The main results revealed that thermal deconsolidation due to rapid laser heating is governed by multiple mechanisms. Some previously unreported and non-intuitive results were observed in the material response to rapid laser heating, which are suspected to have a strong influence on the quality of the laminates produced through LAFP. Based on a qualitative and quantitative study of the influence of studied process variables on thermal deconsolidation, some mechanisms were identified and later verified with confirmatory experiments.

The results of this study can be used as a starting point to develop predictive models for estimating the deconsolidated state of thermoplastic prepreg tapes, at the end of the rapid heating phase, in future work. Various topics for further research prevail. These include: studying the influence of tool temperature on the deconsolidation response of the prepreg material, evaluation of the deconsolidated state with superior characterization techniques in order to obtain in-situ microstructural data, simulating the influence of boundary conditions that would be applied on incoming tape due to a compaction roller and studying the influence of the deconsolidated tape state on intimate contact development, under roller compaction pressure. By investigating these additional aspects, a robust and accurate predictive model for thermal deconsolidation can be developed in future work, which shall help improve the accuracy of a high-fidelity process model for LAFP, which is currently in development at TU Delft.

Contents

List of Figures

List of Tables

Nomenclature

Abbreviations

ANOVA	Analysis of variance
CF/PEEK	Carbon-fiber reinforced Polyether-ether-ketone
CF/PEKK	Carbon-fiber reinforced Polyether-ketone-ketone
CFRP	Carbon-fiber reinforced polymer
CTE	Coefficient of thermal expansion
DoE	Design of Experiments
FEM	Finite element modeling
LAFP	Laser assisted fiber placement
LATP	Laser assisted tape placement
LLS	Laser line scanner
LSCM	Laser scanning confocal microscope
PEEK	Polyether-ether-ketone
PEKK	Polyether-ketone-ketone
ROI	Region of interest
SEM	Scanning electron microscope
VCSEL	Vertical cavity surface emitting laser

Symbols

μ_f	Critical maximum fiber volume fraction
E_{net}	Net energy of decompaction
E_{void}	Energy of decompaction due to void evolution
F_d	Damping force
F_s	Elastic force
F_v	Energy of forced thermal expansion of gas
L_H	Length of heated spot
T_g	Glass-transition temperature
T_H	Heating time
T_m	Melting temperature

1 Introduction

1.1. Background

The development of fiber-reinforced composites in the aerospace industry has been rapidly increasing over the past few decades and is slowly but steadily replacing metals in the production of critical airframe parts. This is due to the higher specific properties of composites, higher chemical resistance, great fatigue performance and possibility of tailorable properties, which result in lighter structures as compared to traditional metal structures. This can be clearly seen by the successful introduction and operation of aircrafts such as the Airbus A350XWB and Boeing 787, both of whose structures contain at-least 50% by weight of advanced composites, resulting in about 20% weight saving in both aircraft [1, 2]. The development and integration of these light-weight composite structures into the newer airframes, is partially responsible for the the increased operational efficiency in terms of a 25% decrease in fuel consumption and an improved performance.

Thermoset composites have been developed and adopted in composite airframe structures more commonly than thermoplastic composites. These composites typically require long production cycle times, have limited recyclability and the raw materials often have a limited shelf life. Due to the pressing need of increasing production rates of civil aircraft, cycle times must be reduced. Therefore, the use of thermoplastic composites is being developed further, for cost-effectiveness and high-production rates, for large scale composite structures. These composites can be processed by heating the fiber-polymer network of input raw material, in the form of prepreg [1] tapes, to the polymer processing temperature[2], resulting in softening of the matrix. This is followed by consolidation and cooling processes. The absence of the need for additional curing, allows for shorter cycle times. Furthermore, thermoplastic raw materials have infinite shelf life, bring about the possibility of fusion bonding and allow for relatively easier automation concepts for the production process.

Thermoplastic fiber-reinforced composites have already been adopted for structural applications in the aircraft industry; such as the fuselage clips and cleats of Airbus A350 XWB [3], the J-nose of the Airbus A380, over-wing pressure bulkhead for the Gulfstream G500 aircraft and floor beams of various aircraft, such as in the Airbus Beluga airframe [4]. However, the production rate is greatly limited by the size of the components and only small parts such as the aforementioned fuselage clips and cleats have been produced at high production rates. This is because, to date, all thermoplastic structural components that have been certified as 'air-worthy' in the civil aviation industry, have been manufactured through an extra consolidation step that involves either an autoclave or a hot press. These steps has proven to be very time and resource consuming and hence act as a bottleneck to the use of thermoplastic composites for production of large-structures, that need a short cycle time. To this end, one promising technology for out-of-autoclave processing is 'in-situ consolidation' through laser assisted fiber or tape placement. Since, thermoplastic polymers are made up of linear polymer chains

[1] Continuous fibers tows impregnated with a suitable resin in the form of tapes that can be readily collated to form a composite laminate part.

[2] The processing temperature is generally slightly higher than the polymer melting temperature (T_m).

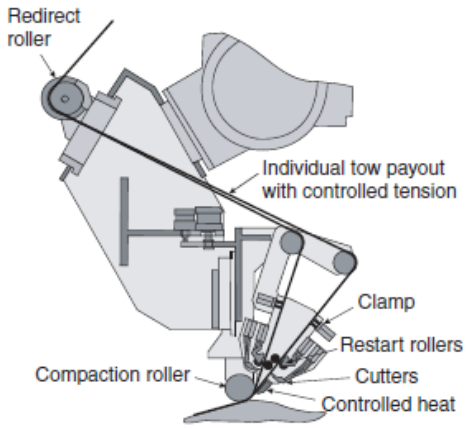

Figure 1.1: Automated fiber placement end-effector [7]

that can be melted and solidified multiple times, they can be fusion bonded i.e. when heat and pressure are simultaneously applied to the interface of the adjoining surfaces, the polymer chains diffuse across the interface to form a bond. This technique is referred to as in-situ consolidation [5]. What differentiates this manufacturing process from traditional thermoplastic composite manufacturing techniques is the rapid heating and cooling cycles and most importantly, relatively short consolidation times. Hence, in-situ laser assisted fiber or tape placement process has the potential to reduce production costs and time due to rapid consolidation [6].

In automated fiber placement, prepreg fiber tows are fed through storage spools and are guided through a delivery system to the deposition end-effector, as shown in figure 1.1. The end-effector consists of multiple components, that ensure that the tape and substrate are heated, the tape is guided to the right place on the tool and finally compacted on the tool surface through a compaction roller, which may be made of rigid or deformable materials. This action of pressing tows onto the work surface (or a previously laid ply) 'bonds' the tows to the lay-up surface and removes trapped air, minimizing the need for vacuum debulking.

Full in-situ consolidation[3], has not yet been achieved, especially at the rapid layup speeds required from the process to be qualified as a rapid manufacturing process [8, 9]. However, the technology is being slowly, but steadily developed for industrialization.

1.2. Motivation

In structural applications and particularly in the case of development of primary-load structures for the aerospace industry; the final consolidation quality of fiber reinforced thermoplastic composites plays a very important role as it influences the mechanical performance of the laminate. The achieved consolidation quality can be characterized by physical parameters such as the void percentage in the microstructure of the composite, the degree of crystallanity in the microstructure, the dimensional accuracy and bond strengths of the intralaminar interfaces. One of the challenges that is faced by the technology, that prohibits it from achieving full 'in-situ consolidation', is the presence of interlaminar and intralaminar voids in the obtained composite parts. The current state-of-the-art is at a minimum void content of 1.6% voids through an in-situ placement process [10], which is higher than the maximum allowable limit of around 1% void content set by aerospace standards.

The formation of interlaminar voids can be associated with the degree of intimate contact development between two fiber tows or between the roller and fiber tow, during placement. Better intimate contact is facilitated by smoother tape surface. Furthermore, intralaminar voids may be formed due to volatiles or air trapped in the microstructure. Earlier studies on this topic indicate that the thermoplastic tapes exhibit thermal deconsolidation when rapidly heated and this leads to an increase in surface roughness and other physical effects such as void content increase and dimensional inaccuracies.

[3]Achieving a thermoplastic composite part with less than 1% global void content and perfect bonding between plies, that does not require another consolidation step

Hence, an initial definition of thermal deconsolidation can be expressed as: "*Meso-structure disintegration as well as the resulting deterioration in macro-performance of the initially well-consolidated composites during post-thermal processing*" [11]. Deconsolidation has been reported in literature to be a combination of effects, which include decompaction of the consolidated ply or laminate, as well as changes in micro-structure (void content) and surface morphology. Decompaction of the thermoplastic composite can be defined as the *inverse of consolidation*, i.e. the fiber reinforcements are released from their frozen state due to residual stresses trapped in the ply or laminate, when heated above melting temperature. Deconsolidation has been demonstrated to have an affect on intimate contact development between plies and hence resulting in poorer bonding quality [12, 13] in addition to a higher void content in the microstructure of the laminate [13]. Hence, it is important to gain a deeper understanding of the thermal deconsolidation mechanism and its effect on the morphological properties of the prepreg tapes in the laser assisted in-situ consolidation process. This forms the main motivation for this work. This document presents the work performed as part of the master thesis project and highlights the main outcomes of the research and how they are used to answer the main research questions proposed at the beginning of the study and described in chapter 4.

1.3. Outline

In this report, the research activities conducted as part of the Master thesis is presented in detail. The report is split up into four parts. Part I forms the literature review on the current understanding of thermal deconsolidation in thermoplastic composites and the known information on thermal deconsolidation under rapid heating, in the context of laser assisted fiber placement. Following this overview, gaps in knowledge are identified and finally, the research questions that are to be answered in this work are presented.

In part II, the research activities conducted as part of this study are presented. First, the experimental setup designed for this study is described and the choices made are motivated. This is followed by a description of techniques used for characterizing the deconsolidation effects in thermoplastic prepreg tapes. Then, experimental results are presented and discussed. Finally, based on experimental observations, the dominant mechanisms for the observed deconsolidation effects are presented and motivated.

In part III, the outcomes of the performed research activities are reviewed, their relevance to the in-situ LAFP process are discussed and the author's recommendations for further research is presented. Finally, in part IV supplementary material to support the ideas presented in this thesis are given in the form of appendices.

I

Literature Review

2

State-of-the-art

2.1. Laser-assisted fiber placement

In-situ consolidation through automated fiber placement (AFP) or automated tape laying (ATP)[1] is a promising production technology that is being developed to achieve automated production of large-scale and lightweight structures. One of the key aspects of in-situ consolidation through fiber placement, is the temperature applied on the incoming tape, as it has a significant impact on bonding quality as highlighted by Schell et al. [14]. Hence, by inference the heating source on the AFP end-effector plays a crucial role. Some of the commonly used heating sources are hot-gas, infra-red and laser devices; with advancements taking place in the development and characterization of in-situ consolidation assisted by ultrasonic-vibration heating as demonstrated by [15]. Hot-gas devices have been rigorously investigated in literature as a heating source for AFP, where correlations have been drawn between the process parameters and achieved mechanical properties through single-lap shear testing, interlaminar shear strength (ILSS) and fracture toughness tests [15]. However, hot-gas heating method for an in-situ AFP process suffers drawbacks such as limited heat delivery due to convective heat losses and expensive to operate in an industrial environment, since the setup requires inert gas to prevent oxidation of the composite surface

Research has been performed by Comer et al. [10] on the use of laser-assisted tape laying process to achieve in-situ consolidation of carbon fiber (CF)/Polyether-ether-ketone (PEEK) blanks. It was found that laminates produced by the laser-assisted production process performed better than laminates produced through an autoclave in terms of interlaminar toughness. However, they performed worse in flexural strength and stiffness, interlaminar shear strength and open-hole compression tests. Fresh impetus to research on LAFP has be given due to the further development of laser technology. With the use of advanced lasers, Grouve et al. [16, 17] have demonstrated in their work on in-situ consolidation of semi-crystalline CF/Polyphenyl sulfide (PPS) tapes, that excellent toughness and high weld strengths can be achieved at high nip-point temperatures coupled with high placement speeds, in laser assisted tape placement of quarter-inch tapes. High nip-point temperatures could be reached with lower input energy using laser heaters as compared to with hot gas heaters. Schledjewski and Miaris [18] also demonstrated through experimental work, that among 13 different heat sources for the thermoplastic tape placement process, laser systems performed most efficiently in terms of temperatures achieved vs input power required. Also, in recent research and industrial application, the use of laser heating is preferred over other heat sources. The reasons for this can be summarized as [19, 20]:

- higher achievable temperatures due to better heat transfer
- better temperature control in a flat heating zone
- uniform heating projection
- can be easily integrated on an end-effector due to their compact design
- prevention of chemical reactions on the surface being heated

[1] Identical processes, with the main difference being the width of the tapes placed by the robot head. Wider tapes are placed in ATP and narrower in AFP

Because of the advantages of laser heating, the focus of research and development activities in recent time has been on LAFP. At slow placement rates of prepreg tapes (25mm/sec), it has been observed that Laser-assisted automated tape placement, is capable of producing high-quality components with full in-situ consolidation [21]. However, as stated earlier, the quality of laminates produced by the process at *high-deposition rates*, is not of sufficient standards yet and research is ongoing to develop this process capability.

2.2. Bonding mechanism

The LAFP process involves the use of a material deposition end-effector like the one shown in figure 1.1. The end-effector is mounted on a robot that traverses over the tool surface in the required layup direction and speed to deposit the thermoplastic tapes 'ply-by-ply'. In order to achieve the required thickness and geometry of the part, usually multiple traverses of the robot over the tool is required. The function of the end-effector can be illustrated with the schematic representation of the process, shown in figure 2.1a. As can be seen in the figure, a material heater (which comprises of a laser heat source in case of LAFP), heats up the incoming unidirectional thermoplastic tape material and substrate. Simultaneously, the tape is guided in between the tool/substrate and the consolidation roller. The point where the consolidation roller compacts the incoming tape and substrate together is called the 'nip-point'. Due to the applied heat and consolidation pressure, the tape is bonded to the previously laid substrate. Since, this process is similar to thermoplastic fusion bonding or welding, the mechanisms that describe the in-situ consolidation process and welding process are the same and can be illustrated as in figure 2.1b. In this figure, it can be seen that after the tape and substrate are compacted by roller pressure at the nip-point, the first step of bond development is intimate contact between the substrate and the incoming tape and this step is followed by inter-molecular diffusion of the polymer chains to achieve healing or autohesion in the laminate. Hence, the two mechanisms can be summarized as:

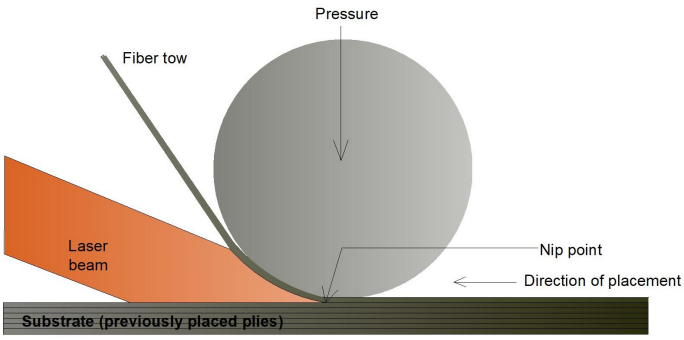

(a) Schematic representation of the LAFP process

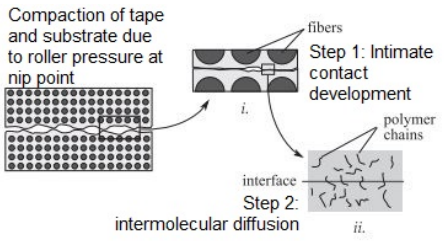

(b) Mechanisms of bond development: i. Intimate contact and ii. Inter-molecular diffusion (Adapted from [17])

Figure 2.1: Laser assisted fiber placement process schematics

1. Intimate contact development at the interface
2. Autohesion/inter-molecular diffusion which facilitates healing of the polymer molecules in the bond interface

The in-situ consolidation process is realized by completing three processing steps: heating up the material above the polymer melting temperature for a short duration, applying pressure to achieve intimate contact and rapid cooling under the application of pressure to achieve consolidation. In this way, theoretically, an expensive and slow consolidation step (such as autoclave processing) can be avoided, even for large and complex geometry parts [10].

2.3. Phases of the in-situ consolidation process

The different phases of the in-situ thermoplastic fiber placement process, which have an influence on the final part quality are the heating phase, consolidation phase and release, as illustrated in figure 2.2.

In the **heating phase**, the incoming tape and the substrate are rapidly heated by the laser to the processing temperature of the polymer. During this phase, no external pressure is applied. The intensity of heat input required is dependent on the material placement rate, the inclination of the heater, boundary conditions and parameters such as tool temperature. However, the rate of heating is always

higher than that of processes such as autoclave or press consolidation. During the heating phase, the voids and volatile present in the material microstructure are allowed to expand, since no consolidation pressure is applied to the tape at this stage [22]. At the end of the heating phase and just prior to the nip-point, the tape is heated to a temperature above the melting temperature (T_g), which is known as the processing temperature of the polymer. Here, it is suspected that some amount of thermal deconsolidation of the tape takes place, resulting in an increased void content and deformation of the tape. Although overheating of the tape may initiate the onset of thermal degradation of the PEEK polymer, full-degradation would not happen at very short heating time (in the order of milliseconds) as can be concluded from the study by Tsotra et al. [23].

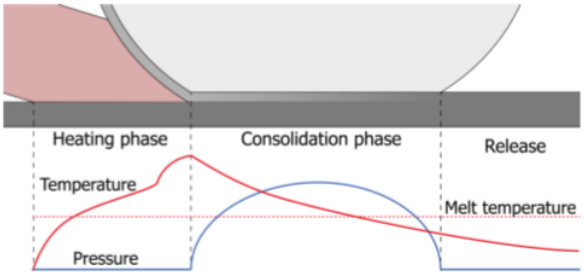

Figure 2.2: Different phases of LAFP process [13]

Following the heating phase, in the **consolidation phase**, asperities on the surface of the heated tape are flattened by the application of pressure; and intimate contact is developed between the substrate and the tape. Once intimate contact is achieved, polymer chains can diffuse between the lower tape surface and the upper surface of the substrate, gradually creating a fusion bond or weld at the interface. This process is called autohesion. Ideally at this stage, the tape and substrate should be fully consolidated into a single laminate and have close to zero void content and good inter-facial bonds between the layers. However, as can be seen in figure 2.2, the temperature drops rapidly in the laminate due to heat dissipation and hence the matrix starts becoming more viscous. As a consequence, the intimate contact development, healing and void compression is inhibited and some voids may get trapped in the interface.

Immediately after the heating phase, is the **release phase** of the process, where the part is released from the compaction pressure of the roller. Depending on the temperature of the placed tape section at release, the process of crystallization and build up of residual stresses may continue during this stage. Furthermore, it is suspected that if the compaction pressure is released while the placed tape is close to or above the processing temperature of the polymer, some deconsolidation can take place which adversely affects the quality of the part. This may happen at very high placement speeds, such that the tape temperature might not reduce below the melt temperature. Hence, some of the state-of-the-art placement heads incorporate a chilling module which follows the consolidation roller [24], that ensure that the placed tape is cooled to a temperature below the glass transition temperature of the polymer (T_g), before the compaction pressure is removed.

2.4. Process parameters and their influence

The LAFP process is a challenging production process to optimize, since it involves a large number of variables that range from (1) hardware variables, (2) processing variables to (3) material variables. Some of the common factors that affect the part quality obtained through the process are presented in table 2.1. Out of the various influencing variables, this study focuses on the heating source, heat input, material deposition speed, heating length and tape quality. While other variables are important to the process as well, investigation into them is beyond the scope of the project. Hence, in this section, the variables mentioned above are reviewed.

1. *Heat input*
   The heat input provided to the tape and substrate is crucial in determining the quality of the finally produced part after placement of the prepreg material. In order to achieve good intimate contact and autohesion, it is necessary for the the tape and substrate surfaces to be heated to the polymer processing temperature which is slightly higher than the polymer melting temperature (T_m). This

Table 2.1: Influencing variables of the LAFP process

Hardware Variables	Process Variables	Material Variables
•Heating source	•Heat input	•Fiber volume content of prepreg
•Roller geometry and number of rollers	•Consolidation pressure •Cooling rate	•Polymer matrix processing parameters
•Roller hardness and deformation	•Material deposition speed	•Surface roughness of tape
	•Distance of heat source from tape and substrate •Tool temperature •Laminate thickness	•Tape quality and composition Viscosity
	•Heated spot length	

ensures that the matrix material melts and hence its viscosity decreases. This aids flattening of asperities leading to intimate contact and subsequently polymer healing.

2. *Material deposition speed*
   The deposition speed also plays an important role in the achieved laminate quality through the process. Due to industrialization demands, higher speeds are constantly sought from the in-situ consolidation process. As the parameter is still being investigated and no standard has been defined yet, it is common to find values ranging from 10 mm/s to 400 mm/s. However, the upper limit of achievable speeds for *good consolidation quality* in parts is limited to 25 - 100 mm/s at the current technology readiness level. This is due to high interlaminar and intralaminar void content obtained at higher deposition speeds. Furthermore, the speed of material placement also affects the heating and cooling rate as well as heat flux that is applied on the incoming tape. This is subsequently expected to affect the deconsolidation behavior of the thermoplastic material. Hence, for static experimental tests, the effect of material deposition speeds can be evaluated by incorporating the heating times that correspond to the range of deposition speeds; considering a constant heated spot length.
3. *Cooling rate*
   The influence of cooling rate on the mechanical properties of laminates produced through LAFP has been extensively studied and it has been established by various authors that cooling rate has a strong influence of the crystallanity of the placed tapes. In general, lower (optimized) cooling rates, result in better crystallization in the tapes, leading to higher mechanical properties [10, 15]. However, an interesting aspect of cooling rates in terms of thermal deconsolidation is that, with lower cooling rates after the rapid heating phase in automated fiber placement, it is suspected by Kok et al. [13] and Kok [25], that since the placed tape remains at higher temperatures for a longer time, the deconsolidation effects could be exacerbated. Hence, since the influence of cooling rate seems to influence crystallization and deconsolidation in different ways, studying this factor is deemed to be necessary.
4. *Heated spot length*
   The size of the heated section of the tape has been proven to have an influence on the quality of bonds achieved in the in-situ consolidation process. Since, the width of input prepreg tapes theoretically remain constant, variation in spot size is brought about by varying the length of the heated spot. Khan et al. [12] have demonstrated that with an increase in heated spot length, better degree of bonding between plies could be achieved for hot-gas placement. Furthermore, the influence of heated spot length on the heat transfer process at the nip-point is studied by Han et al. [26] and the results indicate that the length of the heated spot length has an influence on the temperature gradient on the tape surface along the length of the tape and this in turn influences the bond quality. However, to the author's knowledge, the influence of heated spot length has not been studied on thermal deconsolidation due to laser heating in LAFP and hence this is a parameter chosen to be investigated in this study.

5. *Tape quality and composition*
   During the LAFP process, the state of the tape evolves due to the various physical processes and this plays an important role on the final consolidation quality. Ideally, the in-situ consolidation process requires rectangular geometry with a homogeneous distribution of the fibers over the width of the material and all perfectly impregnated by the thermoplastic matrix material. Furthermore, the void content of the tapes should be as low as possible, since it is quite difficult to compress interlaminar and intralaminar voids during the extremely short time of the tape under consolidation pressure. It is also required that the incoming tapes have a smooth matrix-rich layer on both surfaces, to aid intimate contact development as well as result in better interlaminar bonds. After extensive effort in improving tape quality for the in-situ placement process, considerable improvements have been made in tape parameters such as thickness variation over width, fiber distribution, surface roughness and level of fiber impregnation. However, the tapes are not yet ideal for the process and further research is required.
   Various researchers have investigated the affect of tape quality on the in-situ consolidation process and have proposed further improvement to tapes [24, 27, 28]. To evaluate the quality of incoming tapes, Schledjewski and Schlarb [28] have proposed a quality index which allows comparison of different tape materials and can be used to identify the areas that require further development. Furthermore, Lamontia et al. [29] developed critical specifications for placement-grade thermoplastic tapes. Some of the most important attributes are presented in table 2.2.

Table 2.2: Critical specifications for placement-grade tapes and tows [29]

Tape Attribute	Specification
Tow width	6.35 mm, +0.0 mm, -0.10 mm
Tape width	150 mm or 75 mm, +0.00 mm, -0.10 mm
Thickness variation	Less than 6% of material thickness
Void Content	Less than 1%
Fiber-matrix distribution	Uniform throughout cross-section with pure resin at top surface with thickness = 1x fiber diameter

   Furthermore, the composition of prepreg tape, in terms of the type of the thermoplastic polymer, is an interesting aspect to be studied. The variation in as-received properties and polymer composition, and its influence on thermal deconsolidation can be investigated by varying the tape polymer material (as long as the polymer matrix material for both types remains in the same family of polymers).

2.5. Thermal deconsolidation

The phenomenon of deconsolidation in the in-situ consolidation process through LAFP is a temperature-induced deformation of the incoming tape or deposited substrate. It has been identified in literature, that this deformation of the thermoplastic prepreg material results in voids in the microstructure and development of a rough, fiber-rich surface [13]. Furthermore, deconsolidation during the heating phase is also suspected to contribute to increase in the width of the incoming tapes, which is a major contributor to overlaps and poor pressure application in the laminate [25]. However, the influence of thermal deconsolidation on width increase, has not been experimentally verified, yet. Deconsolidation in the heating phase of LAFP is undesirable, since the presence of voids in the produced laminate results in a decrease in mechanical performance, such as loss of strength and stiffness of the laminates produced [10]. Studies performed by Ageorges et al. [30] and Brzeski and Mitschang [31] indicate that a very low external pressure of 0.2 MPa is sufficient to prevent deconsolidation of carbon fiber reinforced composites when they are heated to processing temperatures. Hence, deconsolidation does not take place in conventional thermoplastic production technologies such as press forming or autoclave processing since, some amount of pressure is applied constantly on the material, while it is at a temperature above the processing temperature of the polymer. However, in the case of LAFP, deconsolidation can take place during two points of the process:

- During the heating phase, the tape and substrate are heated at the nip-point as illustrated in figure 2.1a and 2.3. Although the time of heating is in the order of milliseconds, the tape and substrate

reach melting temperature during the short time and since no pressure is being applied, they show deconsolidation effects. This deconsolidation is characterized (based on literature) by an increase in the surface roughness of the heated surface of the tape, increase in thickness due to fiber reinforcement decompaction and increase in void content. Various authors have assessed the severity of deconsolidation based on the latter effect, i.e.: increase in void content [32, 33], however most of the research focus has been on deconsolidation during conventional processing techniques and not rapid in-situ consolidation via LAFP.

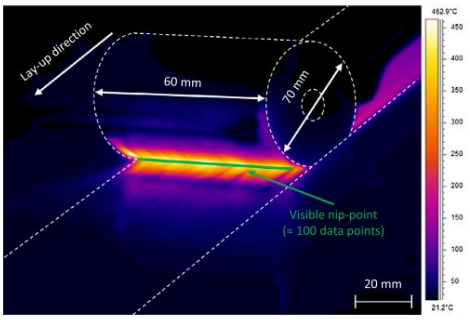

Figure 2.3: Nip-point of interest in LAFP heating process [34]

- During the release phase, as identified in literature [22]; both experiments and predictive models show that deconsolidation plays a role in determination of the final void content in the laminate, after the consolidation pass. This is because at high placement rates, the placed ply may remain at a temperature higher than the T_m, even after the roller pressure is removed; resulting in deconsolidation of the placed ply. The authors identified that although deconsolidation is somewhat mitigated due to multiple passes of the compaction roller, the effect was not completely removed and hence some sort of quench cooling is required after the consolidation pass of the roller, to freeze the consolidation state of the placed ply. To this end, a deposition head concept proposed by Lamontia and Gruber [24] would be useful as it incorporates a 'cold area module' in the thermoplastic tape placement head, which chills the laminate leaving the first compaction head, while still applying pressure to prevent deconsolidation.

A substantial amount of work has been done on characterizing the deconsolidation behavior of consolidated laminates when they are heated during a post consolidation process (in the absence of external pressure application). However, there is very less research performed on characterizing deconsolidation of thermoplastic prepreg tapes during rapid heating and cooling during LAFP. Furthermore, the effect of deconsolidation during the heating phase of LAFP, on the intimate contact development and the final part quality obtained through the LAFP process is not well-studied or incorporated in predictive process models.

2.5.1. Deconsolidation mechanisms

The severity of thermal deconsolidation in conventional processes is commonly characterized by the void content in the produced laminate. Based on literature, four interdependent physical mechanisms that contribute to deconsolidation *during reheating and post-processing of thermoplastic composites* were identified. It is important to note that these mechanisms have not been verified for deconsolidation of thermoplastic prepreg tapes/tows and substrate, due to a lack of work done on this topic. The mechanisms identified for deconsolidation of 'consolidated' laminates can be briefly stated as follows:

1. Decompaction in the thickness direction of the fiber-matrix network due to release of residual stresses
2. Viscoelastic behavior of the matrix; causing thermal expansion
3. Thermal expansion of the voids
4. Shrinkage of voids and subsequent coalescence into larger diameter voids

Decompaction is a widely investigated deconsolidation mechanism for deconsolidation of thermoplastic composite laminates in a post-consolidation thermal treatment such as induction heating and

fusion bonding. The decompaction mechanism can be described as a 'spring-back' effect wherein trapped elastic stresses in the fiber-matrix bed are released, resulting in increase in laminate thickness as well as change in the fiber-matrix distribution [32]. Decompaction in the fiber-matrix interface results in increase in void content as well as increase in the thickness of the laminate. The latter effect can be seen in figure 2.4. Various researchers have identified that void growth in the laminate takes place simultaneously with the decompaction of the fiber-matrix network. Hence, in order to gain more knowledge about the mechanism, it is important to evaluate the compressibility of the fiber reinforcement under consolidation pressure. The compressibility of the reinforcement network is determined by multiple parameters such as the critical maximum volume fraction of fibers (μ_f), architecture of the fiber network and the elastic properties of the fibers. Hence the pressure required to compress a reinforcement network to the maximum fiber volume fraction during consolidation can be expressed as:

$$p|_c = f(\mu_f, \text{fiber network architecture}, \text{elastic properties of fiber}) \tag{2.1}$$

Due to this compaction pressure, during consolidation and solidification of the laminate, residual stresses are stored. When the laminate is heated above the melting temperature of the semi-crystalline polymer, these stresses are released in the form of laminate decompaction. The decompaction pressure can be considered proportional to the $p|_c$.

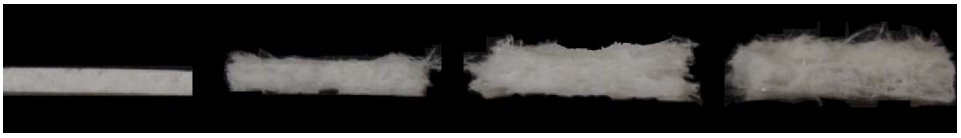

Figure 2.4: Thickness increase due to decompaction in a glass mat thermoplastic (GMT) composite at deconsolidation times: 0s, 50s, 200s and 500s respectively [32]

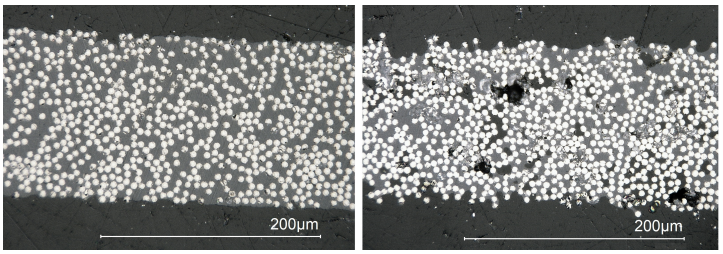

Figure 2.5: Comparison of as-received and deconsolidated prepreg tape specimen cross-section. Deconsolidated tape specimen exhibiting increased void content and dry-fiber rich surface

In addition to void growth because of the decompaction pressure, as discussed above; the viscous and elastic properties of the polymer also play an important role in the void content development. Viscoelastic expansion is a mechanism through which decompaction of amorphous and semi-crystalline polymers takes place. When the polymer is heated above its glass transition temperature (T_g), the viscosity decreases rapidly. This is generally taken as the point of onset towards a truly liquid melt. However, when the temperature remains between the (T_g) and the liquid melt temperature (melting temperature T_m in case of semi-crystalline polymers), the polymer retains some elastic and viscous properties, and hence can deform continually under stress. In these condition, not only do microscopic voids expand due to elastic traction but new voids are also created due to cavitation in the matrix [35]. As the temperature increases and approaches liquid melt temperature, the elastic properties of the polymer decreases and hence traction becomes a decreasingly dominant driver of deconsolidation. The viscoelastic effect of the polymer also results in 'migration of voids' from one region of the microstructure to another. This phenomenon is particularly important in the case of in-situ consolidation as it explains the development of voids in regions of the tape that were identified as 'void-free' initially. As the temperature of the polymer rises and the elastic properties disappear, the voids present in the microstructure collapse as soon as some external pressure is applied. However, in some cases, due to a particular direction of the heat flux, the voids may propagate in the same direction within the material, resulting in a change in location of the voids. An example of the migration of void can be seen in figure

2.6, where a carbon-fiber reinforced PEI laminate is heated to observe the effect of deconsolidation on the void content and distribution. As can be seen in the figure, the location of the void (distance 'd' from the edge) changes after the deconsolidation treatment.

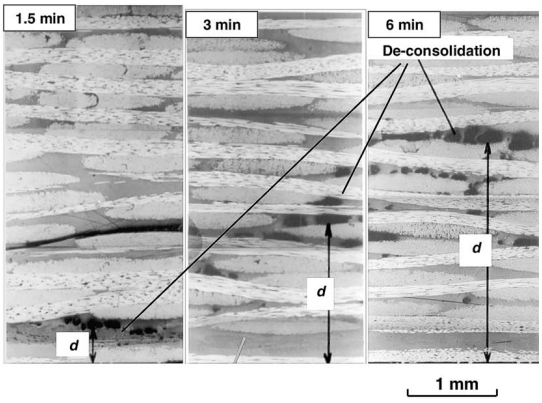

Figure 2.6: Migration of void in CF/PEI laminate after deconsolidation treatment [33]

Higher surface tension between the air and the thermoplastic matrix melt, is found to decrease the effect of deconsolidation in fiber reinforced thermoplastic composites [31], while increase in the deconsolidation effect is associated with thermal expansion of the void due to increased internal pressure at high temperatures. However, Ye et al. [35] estimated that the thermal expansion of voids (in a dried laminate) results in only an increase of 0.7 times the initial average void volume. The increase in void volume determined in the study was the upper bound of the range, since the effect of elasticity of the polymer matrix as well as surface tension was not incorporated in the calculation. The trivial contribution of void volume increase due to thermal expansion compared to the fact that void content increase of 10-20% has been observed due to thermal deconsolidation, indicates that thermal gas expansion does not have a dominant effect on the deconsolidation phenomenon [36]. However, this cannot be assumed to be true for the LAFP heating process due to very different heat flux and heating times.

The shrinkage and coalescence of voids into larger ones, is considered to be an minor contributor to the void content increase, as coalescence of voids itself does not add to the global void content in the material. In reality, coalescence, like the word suggests converts smaller voids into larger ones, while correspondingly also reducing the total number of voids. As the result, the global void content is not considerably influenced. Thus, it appears that the increase of void content due to decompaction of the fiber reinforcement network plays a major role for void growth in thermal deconsolidation, which was verified experimentally by Ye et al. [35]. Furthermore, experimental observations indicate that that no significant void growth has been observed in re-heating processes for pure thermoplastic matrix material. This indicates and reinforces the observation made by Wolfrath et al. [32] that spring-back of the fiber reinforcement plays a major role in the deconsolidation of thermoplastic composites. Furthermore, this supports the idea that the mechanisms that play a major role in deconsolidation of consolidated laminates may not play a major role in the deconsolidation of prepreg tapes, since the latter is subjected to lower compaction pressures due to incomplete consolidation. This is identified as one of the aspects to be investigated in the proposed research.

2.5.2. Theoretical Models

Studies indicate that due to deconsolidation, some of the LAFP sub-processes are affected, which subsequently affect the final part quality. In literature, various models are proposed which evaluate the degree of deconsolidation during thermal treatment of consolidated laminates under no external pressure application. In this section, a brief review of some relevant models proposed in literature, which address the effect of deconsolidation on the void evolution and thickness change due to decompaction are presented.

1. Brzeski and Mitschang [31] developed a deconsolidation model based on the first law of thermodynamics, incorporating the combination of energies related to: decompaction of the fiber-matrix network, the void thermal expansion, internal void pressure and surface tension, among other

mechanisms. The input and output parameters of the model can be schematically described as in figure 2.7.

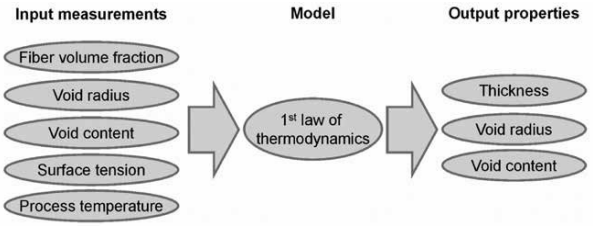

Figure 2.7: Input and output parameters of model proposed by Brzeski and Mitschang [31]

The decompaction of the fiber-matrix network is considered analogous to a spring-damper system with settling effects. According to the authors, since during the compaction process, friction and fiber rearrangement works against the compaction force, the residual stresses stored in the laminate result in lower forces (during deconsolidation) than the applied compaction force. For an elastic force F_s (depending on specimen thickness x) and a damping force F_d depending on velocity v, the energy associated with decompaction can be expressed as:

$$E_{net} = \int F_s(x)dx + \int F_d(v)dt \tag{2.2}$$

where the expression is integrated over the specimen thickness x and time of fiber rearrangement. Furthermore, void evolution was described in terms of void growth due to thermal expansion and internal void pressure. The thermal expansion, as stated before, has a small effect on deconsolidation, since it is an order of magnitude lower than the total observed void increase. Furthermore, the authors proposed that there is some energy consumption due to the forced thermal expansion of the gas which is represented as F_v. The energy of the decompaction due to void evolution was described as follows:

$$E_{void} = \int -F_v dx = \int -(p_i - p_e) * A_v dx \tag{2.3}$$

where p_i and p_e are the internal pressure of the void and the atmospheric pressure respectively, A_v is the area of voids at any cut area in the in-place direction and A_{spe} is the specimen area. Only the void area is considered in the expression for void energy. The expression is evaluated over the specimen thickness x. By incorporating the ideal gas law in Equation 2.3 (initial void pressure, volume and temperature represented as p_o, V_o and T_o) and x_c, x and T being the theoretical thickness of the composite, current thickness and temperature respectively, the following formulation was proposed:

$$E_{void} = -\int \left[\frac{p_o * V_o * T}{x * T_o} - p_e * A_{spe} * \left(1 - \frac{x_c}{x}\right) \right] dx \tag{2.4}$$

The surface energy in the model was described in terms of the surface tension factor γ and evolved surface area of the void. Furthermore, dA_vo was defined as the new surface area of the void at any cut in the in-plane direction. The surface tension factor was determined experimentally by an optical tensiometer. The relation for the surface energy was given as follows:

$$E_{surface} = -\int \gamma dA_{vo} \tag{2.5}$$

The surface tension factor is considered to contribute to void shrinkage and coalescence and hence is considered to oppose the deconsolidation effects. The deconsolidation behavior was finally formulated as a sum of the energy contributions from the various interactions which in addition to the parameters defined above, includes energy of composite due to heat capacity, thermal expansion, external compaction pressure and crystallanity. In the proposed model all of these energy contributions were considered to be zero and no external pressure was applied. The results obtained from the model showed good correlation to physical measurements in terms of specimen thickness, void content and void radius.

2. In a different approach to model deconsolidation behavior, Ye et al. [35] considered the effect of thermal expansion of voids, coalescence of small voids into larger ones and the growth of voids due to decompaction of the laminate. It was identified that void growth during deconsolidation is primarily due to the decompaction, wherein the existing voids are expanded due to traction and new voids are created through cavitation. The model proposed by the authors considered that a void in the composite can be modeled as a representative volume element (RVE) as shown in figure 2.8 and the mathematical description was established in terms of homogenization of the voids and an averaging technique to obtain trends that would give further insight into thermal deconsolidation. In the model, α was defined as the average void content in N voids and μ_f

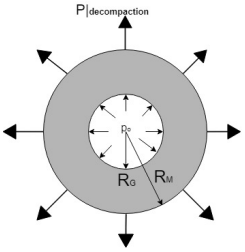

Figure 2.8: Schematics of representative volume element

as the average volume fraction with regards to the fiber volume fraction in the numerous RVE's that make up the composite. The model assumed that the effect of coalescence of void is not significant and hence it was omitted in the model. Based on this assumption, the term 'volume equivalent radius' was defined, as shown below:

$$R^o_{g_m} = \sqrt[3]{\frac{V^o_{g_m}}{\frac{4}{3}\pi}} \tag{2.6}$$

$$R_{g_m} = \sqrt[3]{\frac{V_{g_m}}{\frac{4}{3}\pi}} \tag{2.7}$$

and the initial and deconsolidated void content as:

$$\alpha^o_m = \frac{V^o_{g_m}}{V_{g_m}} = \alpha^o \tag{2.8}$$

and

$$\alpha_m = \frac{V_g}{V_m} = \alpha \tag{2.9}$$

where, $V^o_{g_m}$ is the initial volume of the m-th void, V_{g_m} the global volume counterpart, V^o_m is the initial volume of the whole RVE and V_m the current global counterpart. Hence the variation in void content of the RVE was used to represent the void content in the composite.
The authors described the decompaction behavior by defining the elastic and viscous properties in the model with the constitutive description:

$$\sigma_{ij} = -p\delta_{ij} + (S_{ij})_{elastic} + (\tau_{ij})_{viscous} \tag{2.10}$$

where, p is the hydrostatic stress, $(\tau_{ij})_{viscous}$ the viscous stress and $(S_{ij})_{elastic}$ the elastic stress which relates to elastic shear deformation in the composite. The elastic properties were defined using a linear law whereas non-linear viscous effects were considered for the material using the power-law, due to the observation that in the material, the viscosity decreased with an increase in shear rate of the material during decompaction. The complete formulation of the model can be found in [35], since it is too mathematically intensive to be presented in this report. Using the finally obtained relation, the variation in void content α for the laminate can be determined by the equation 2.9 which can be used to determine the average degree of deconsolidation. The results obtained from the model showed good correlation with experimental measurements

of a deconsolidated glass fiber reinforced thermoplastic composite. Furthermore based on the results, the authors concluded that the 'driving force' for void growth is the decompaction of the fiber reinforcement network and the elasticity of the matrix is responsible for further carrying the 'traction' force and hence contributing to the void growth.

2.5.3. Literature on thermal deconsolidation during LAFP

An inital study on the effects of rapid laser heating on deconsolidation of thermoplastic prepreg tapes has been performed by Kok et al. [13] and Kok [25]. The studies demonstrated that rapid laser heating during LAFP heating phase does indeed result in deconsolidation effects. The authors have characterized deconsolidation in terms of increase in void content, thickness and surface roughness of the placed tapes. Furthermore, based on the inaccuracy of existing models to predict final tape widths after placement, the authors proposed that deconsolidation may also result in increase of width during the heating phase (before pressure is applied to compact prepreg tapes). This proposition however remains to be experimentally confirmed and explained.

2.5.4. Relevance of current understanding for LAFP process

All of the mechanisms and models reviewed in this chapter have at least one thing in common: they are all based on the deconsolidation of pre-consolidated thermoplastic laminates, which underwent a re-heating process at relatively low heating rates. One of the main mechanisms that has been identified and implemented in the models proposed in literature, are the spring-back effect of the fiber reinforcements and thermal expansion of voids. The former has been explained to be responsible for decompaction of the laminate in the thickness direction. Since, decompaction of the fiber reinforcement and the resultant fiber-rich (rough) surface has been observed in thermoplastic prepreg tape material, the models on the spring-back effect are an important point to begin at to understand the underlying mechanisms of thermal deconsolidation and trying to model the behavior for the prepreg material in LAFP. Furthermore, due to rapid heating and very limited consolidation time for the LAFP process, it is also suspected that void thermal growth influences the deconsolidation state of prepreg tapes. The result of experimental investigations shall help identify whether the same mechanisms and models as described in this chapter, are applicable to the prepreg materials as well. Hence the relevance of the work done in this thesis is to experimentally investigate the deconsolidation phenomenon in tapes and identify underlying mechanisms; which can be further used to model the behavior in future work. However, it must be noted that these mechanisms do not take place individually and do have an influence on the other mechanisms. Since, the focus of the models proposed in literature is to predict void content development and thickness change, these models need to be broadened to investigate all other effects of deconsolidation (in future work), such as the development of surface roughness, possible increase in width and other possible effects which shall be revealed by experimental characterization of thermal deconsolidation of prepreg tapes.

2.6. Conclusion

In this chapter, the state-of-the-art in 'in-situ consolidation' through LAFP was presented and the influencing processing parameters considered in this study were introduced and the choices motivated. The phenomenon of thermal deconsolidation of thermoplastic composites was discussed and the information presented in literature regarding deconsolidation of consolidated laminates was reviewed. It was discovered that deconsolidation has been studied extensively in the context of consolidated laminates, when they are subjected to post-consolidation heating processes where no pressure or reduced pressure is applied. However, very little work is focused on thermal deconsolidation of prepreg tapes in the context of rapid heating during LAFP. Hence, a major gap is identified in the understanding of the phenomenon in the context of LAFP and hence a need was felt to perform research on this topic. The gaps identified based on the literature reviewed is presented in chapter 3 and the research questions that shall be answered in this study are presented in chapter 4.

3

Gaps identified in literature

Major efforts have been spent on research in the topic of thermal deconsolidation in consolidated laminates when they are subjected to temperatures near the polymer processing temperature. The high interest in this area has been due to the effect of deconsolidation on the final quality of parts that undergo processes such as fusion bonding(resistance welding, inductive welding and ultrasonic welding) or inductive heating. However, the deconsolidation of thermoplastic prepreg tapes, during the rapid heating process of LAFP, when no consolidation pressure is being applied on the tape for a short duration, is a recent observation. Hence, not much research has been performed on this topic.

3.1. Research gaps

The mechanisms of deconsolidation that have been identified by various researchers through experimental testing, have been used to develop theoretical models to describe the void evolution and laminate decompaction due to deconsolidation. However, it is important to note that the mechanisms and models discussed in chapter 2, have the following drawbacks with regards to deconsolidation of prepreg material in the context of LAFP process:

- Since, the majority of investigative work on deconsolidation of thermoplastic composites, has been performed in the context of post-consolidation heat treatment processes for thermoplastic laminates, it is not known whether the same mechanisms and theoretical models proposed hold true for the prepreg thermoplastic material as well. This is due to the incomplete consolidation state of prepreg tapes, which may result in lesser fiber decompaction and possibly lesser void growth due to lesser 'spring-back' effect, for instance.
- The rapid heating and cooling rates that are characteristic of the LAFP process, are not accurately represented in the experimental information, proposed mechanisms and theoretical models available in literature. This is due to the fact that previous studies on deconsolidation were done at much lower heating rates and hence longer heating times. Therefore, the kinetics of LAFP thermal treatment are different from the kinetics of traditional deconsolidation treatment of composite samples and the influence of this change is unknown.
- Development of surface roughness has not been quantitatively addressed in the models available in literature and no mechanisms have been identified *explicitly*, which explain the fiber-rich surface of the tape after deconsolidation. However, it can be assumed that fiber-reinforcement decompaction due to spring-back effect may play a role in the development of surface roughness as well. One of the common way of modeling intimate contact during LAFP, is by modeling the process in the form of flattening of surface asperities when pressure is applied. Some authors also propose that intimate contact requires matrix impregnation of a dry fiber bed (due to deconsolidation). Hence, the models presented in literature, require to depict surface profile either in the form of asperities or as a dry (and rough) fiber bed; in order to model the intimate contact development between tape and substrate. Therefore, the state of surface roughness at the end of the heating phase in LAFP is an important aspect to understand and be able to predict.

- The most common materials used to characterize deconsolidation and propose underlying mechanisms that govern deconsolidation effects, were glass mat thermoplastic composites, as reviewed in chapter 2. This was motivated by the fact that glass mat composites are known to compress and loft significantly, which aided in understanding the fundamental mechanism due to the exacerbated decompaction effects. The same fundamental mechanism may apply to other thermoplastic composite materials as well, however, since woven fabrics are known to store more elastic energy than other fiber architectures, it is expected that the effect is significantly less pronounced for laminates made from uni-directional prepregs [37]. Furthermore, the response of carbon fiber reinforced thermoplastic prepreg tapes is not known, and since the material is currently being developed for large-scale in-situ LAFP process, this knowledge is deemed to be important to attain.
- One of the major remaining challenges is the knowledge on how and to what extent the consolidation quality of the pre-impregnated thermoplastic tapes is affected by the laser heating process; before the compaction roller applies pressure on the heated area. Although some work on quantifying the deconsolidation behavior is done by Kok et al. [13] and Kok [25], their work did not incorporate a study of the influence of varying process parameters (quantitatively and qualitatively) on the tape quality and hence, conclusive evidence of dominant mechanisms of deconsolidation was not found. Furthermore, it was suggested by the authors that tape deformation in the width direction could be a function of heated spot length, in addition to the heating temperature. However, this has never been proven experimentally and no possible governing mechanisms are proposed for the tape width increase other than the fiber-spreading induced by roller pressure. This aspect needs to be investigated further in order to 1) verify whether tape deformation indeed takes place before the application of pressure and 2) identify dominant mechanisms that govern the width increase.

Hence, in general, more experimental investigation is required on the deconsolidation effects in prepreg material, at rapid heating and cooling rates. This shall help identify the mechanisms which are dominant in the process. Based on these experimental trends, predictive models may be developed in future work, which shall help increasing the accuracy of process models used to predict final part quality for the LAFP process.

3.2. Summary

In this chapter, the main research gaps identified from a literature review on the topic of thermal deconsolidation of thermoplastic composites, are presented. Most of the gaps in knowledge are a result of the fact that thermal deconsolidation of thermoplastic prepreg tapes due to rapid laser heating has not been sufficiently researched and the hence the results published in literature and the general mechanisms proposed, may differ from the case of LAFP; in terms of the following key aspects:

- The influence of rapid heating and cooling rates that are characteristic of LAFP, have not been investigated experimentally.
- The influence of initial material consolidation state (semi-consolidated in case of prepreg tapes and fully consolidated state in literature) on the deconsolidation response has not been studied.
- Influence of LAFP process parameters on the deconsolidation state of prepreg tape has not been experimentally investigated.

Hence, the basis of this work was focused on filling these knowledge gaps. In order to do that some research questions were proposed that the study aims to answer. The research question are presented in chapter 4.

4

Research questions and hypothesis

Based on the literature presented in the preceding chapters, certain gaps were identified in the knowledge on thermal deconsolidation effects on thermoplastic prepreg tapes, during the rapid heating phase of the LAFP process. In chapter 2, the main influencing variables of the LAFP process were identified in table 2.1. However, in order to develop a fundamental understanding of the phenomenon, some research boundaries need to be defined. Hence, it was decided to only focus on the influence of the heat input (dictated by input power of the laser), the heating time to reach the processing temperature (corresponding to varying material deposition speeds), cooling rate (after the heating phase ends), heated spot length and the type of polymer matrix in the prepreg tapes; while other variables mentioned in the LAFP context were kept constant. The other main variables, whose influence was not studied and left constant are: tool temperature, influence of consolidation pressure and distance of target from laser source.

The purpose of the proposed research is to develop a deeper understanding about the influence of the variables identified (which are relevant in the context of LAFP), on the degree of deconsolidation. The term degree of deconsolidation in this study, can be initially defined as the evolution of changes in the microstructure (decompaction and void development), morphology (surface roughness and waviness) and deformation (width increase) of the prepreg material.

4.1. Research Questions

The main research question that is expected to be answered through the proposed research can be stated as follows:

How can the relationship between the selected process parameters and the degree of deconsolidation of thermoplastic prepreg tapes, during the rapid heating phase of the LAFP process be defined?

To answer the main research question, the following questions and sub-questions are framed:

I. How can the physical changes in thermoplastic prepreg tapes, due to thermal deconsolidation during rapid laser heating, be characterized experimentally?

1. How can a static VCSEL laser heating setup be designed to simulate thermal deconsolidation of thermoplastic prepreg tape, at rapid heating rates?
2. How can the deconsolidation phenomenon be studied 'in-situ', during the rapid laser heating phase?
3. What previously unreported deconsolidation effects can be observed in thermoplastic prepreg tapes?
4. At what temperature does the onset of thermal deconsolidation during LAFP begin?
5. What are the qualitative and quantitative relationships between changes in surface roughness,

void content development[1], decompaction and other tape deformation effects of deconsolidated prepreg specimens, due to the following variable parameters:

- Heating time
- Length of heated segment
- Cooling rate
- Temperature at the nip-point
- Type of polymer matrix (linked to as-received material quality and composition)

II. What are the main physical mechanisms that influence thermal deconsolidation in prepreg thermoplastic material?

1. What is the common primary governing mechanism (if one all-explaining mechanism exists) of thermal deconsolidation effects?
2. What is the relevance of theories proposed in literature (as reviewed in chapter 2), in explaining thermal deconsolidation of thermoplastic prepreg tapes, in the context of LAFP?
3. How can the fiber-rich, rough surface in the deconsolidated prepreg tape be explained, based on either previously identified mechanisms or possible new mechanisms identified through experimental investigation?
4. What is the dominant mechanism explaining void formation?
5. What is the effect of changing prepreg tape polymer type on the observed deconsolidation effects?

III. What is the relevance of this work in the context of LAFP process and prepreg tape material development?
IV. What are the limitations of this work and recommendation for further studies?

4.2. Hypotheses

The main hypotheses proposed are presented in this section. These hypotheses were made, based on an initial understanding from available literature. However, since some previously unreported material responses were observed during the experimental investigation, further propositions are introduced and discussed in later chapters. The testing of proposed hypotheses as well as the description and motivation for the further propositions is presented in chapter 8.

1. Out-of-plane fiber decompaction due to residual stresses is the main mechanism describing surface roughness development and results in void formation near the heated surface (in the microstructure) due to traction and cavitation.

2. Out-of-plane fiber decompaction is the main contributor to increase in thickness of the tape specimen at *rapid heating rates*, since less time is available for thermal expansion of voids through-the-thickness of the specimen.

3. The deconsolidation effect is less pronounced for shorter heating times with higher heat intensity.

[1] Changes in void percentage, distribution and average void size

II

Research Activities

5

Experimental details: Materials and Setup

This chapter deals mainly with the research question: *"How can a static VCSEL laser heating setup be designed to simulate thermal deconsolidation of thermoplastic prepreg tape, at rapid heating rates?"* To answer this question, the materials used for the study, the experimental setup designed to simulate rapid laser heating conditions and the techniques used to monitor the process conditions are described in detail.

5.1. Materials

The experimental work was conducted using carbon-fiber reinforced Polyether-ether-ketone (CF/PEEK) prepreg tapes (TC1200 AS4D/PEEK). Further confirmatory experiments were also conducted using carbon-fiber reinforced Polyether-ketone-ketone prepreg tapes (TC1320 AS4D/PEKK). Both tapes contain uni-directional continuous fibers and are developed by TenCate Composites for application in automated tape laying and fiber placement machines. The properties of the materials, as obtained from the material data sheets ([38, 39]) are summarized in table 5.1:

Table 5.1: Global tape properties of as-received tapes

Material	Fiber-volume content (%)	$T_g\ (^oC)^a$	$T_m\ (^oC)\ ^b$	$T_p(^oC)^c$
CF/PEEK	59	143	343	370–400
CF/PEKK	65	159	337	370–400

[a] Glass transition temperature
[b] Melting temperature
[c] Processing temperature

The dimensional properties of the as-received tapes were characterized using methods described in chapter 6 and the obtained values are presented in in the results section.

5.2. Experimental setup

In order to simulate the rapid heating conditions of the LAFP process and create deconsolidated tape specimens with varying process conditions in a controlled manner, an experimental setup was devised. The main components of the setup were a laser heater, an infrared camera for temperature monitoring and tooling to place the prepreg tapes. In order to study the changes of the heated surface profile 'in-situ', a laser line scanner was also installed in the setup. In this section, the experimental heating setup developed for conducting studies on the deconsolidation of thermoplastic tape specimens under rapid heating, is described in detail.

5.2.1. Rapid heating through VCSEL heater

The laser heat source comprised of a Philips vertical cavity surface emitting laser (VCSEL) module, with an output capacity of 2.4kW. The laser contains 12 heating zones which may be independently activated to get a tailored heating profile. The emitted infrared radiation has a wavelength of 120 nm. The independent heating zones of the VCSEL heater were selectively controlled to obtain different heating lengths for the study. Furthermore, since the distance of the tape samples from the heat source was not varied in this study, the laser was mounted in a fixed position above the tool surface for each configuration evaluated. The final configuration used to create deconsolidated samples in this study, did not result in the VCSEL being mounted parallel to the specimen surface and hence a constant working distance was not obtained. This shall be discussed further while describing the final configuration.

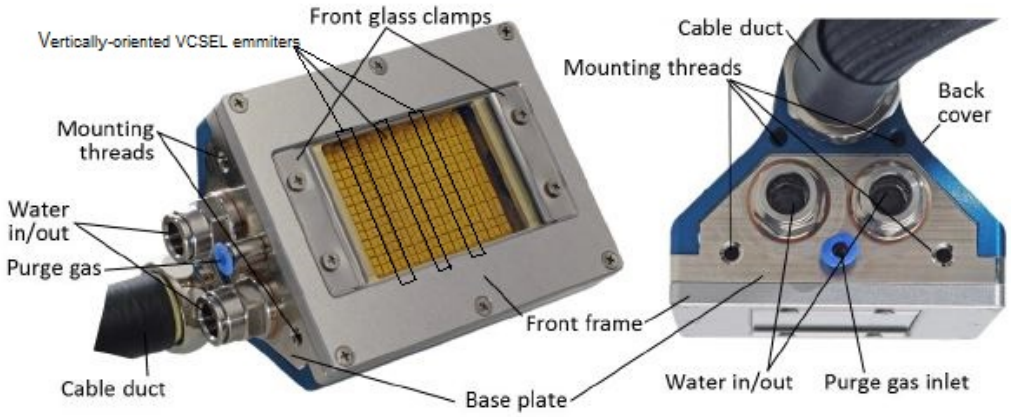

(a) Parts of the VCSEL heater. Modified from [40]

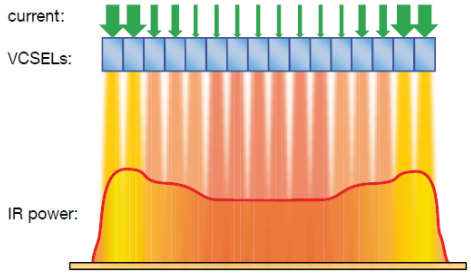

(b) Adjustable heating profile by individual emitter control [41]

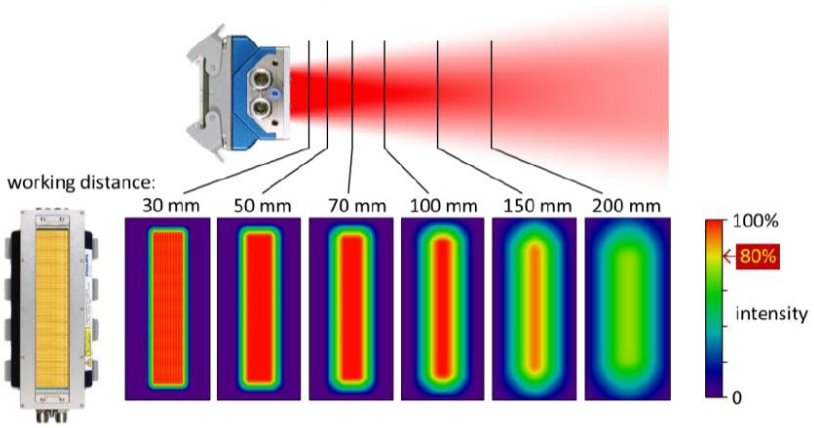

(c) Intensity pattern as a function of distance for the VCSEL laser heater [42]

Figure 5.1: VCSEL laser heater [40–42]

5.2.2. Process temperature measurement

To monitor the temperatures achieved on the tape surface and to identify the power settings required to obtain the desired temperature, a FLIR A655sc high-resolution infrared (IR) camera was used. The IR camera was used to capture thermal images of the specimen at a sampling rate of 25 frames per second, which translates to 1 frame every 40 millisecond.

IR camera calibration

The calibration of the IR camera, depends among other parameters, on the emmissivity of the material, the incidence angle of the IR camera to the surface to be measured and reflections of other surfaces. To experimentally obtain the emmisivity of the prepreg material surface, the variation of the other two parameters was minimized. This was achieved by fixing the camera angle to 55^o inclination to the tape surface and by minimizing the reflections from the tape and tool surface by applying black-matte paint and enclosing the setup in a dark tinted enclosure.

A prepreg tape sample of length 100mm was positioned on the tool surface and fixed with Kapton tape at the edges of the tape (approximately 5mm clamped at both edges). The optical properties of the measured prepreg surface would be affected by a thermocouple attached on the surface and would result in incorrect temperature readings. Hence, a modified procedure based on the ASTM E1933 standard [43] was used to experimentally obtain the apparent emmisivity of the tape surface. The thermocouples were positioned with close contact to the tape surface on a defined region of interest (ROI I) to the left side, as shown in figure 5.2 and secured in position with Kapton tape. The temperature reading from the infrared camera was measured at ROI II on the right. ROI II consisted of 3x3 pixels at the center of the intensity distribution (as seen in figure 5.2), and the measured values from the 9 pixels were averaged to obtain the temperature reading.

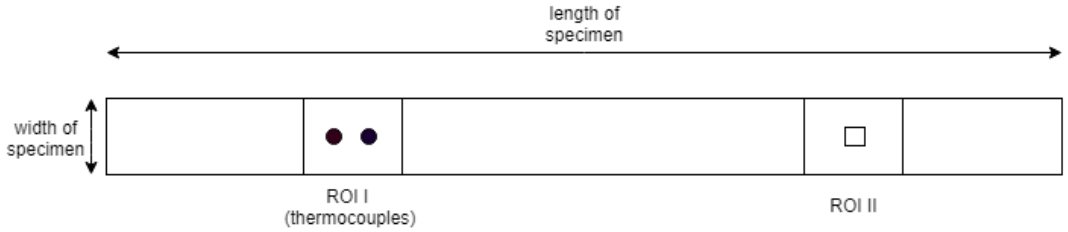

Figure 5.2: Prepreg tape specimen

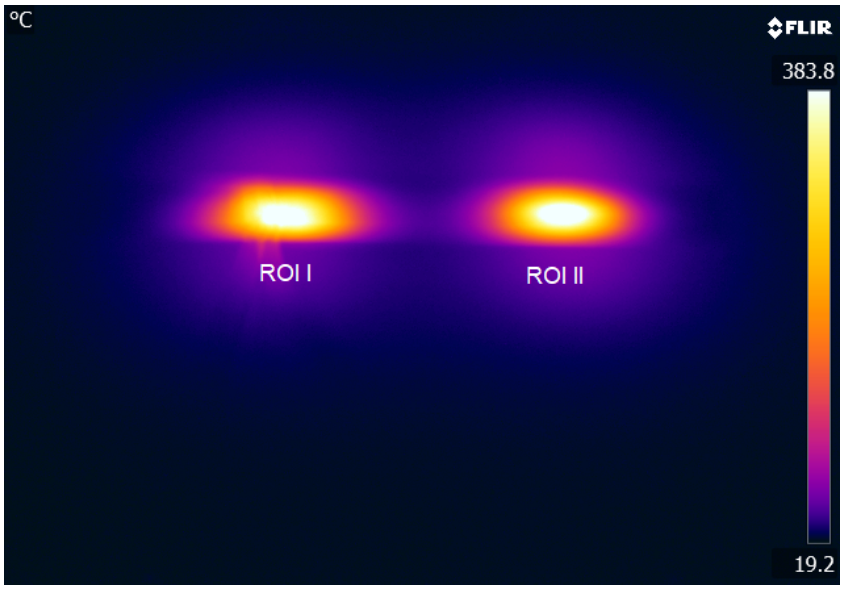

Figure 5.3: Thermal image of calibration experiment

Two zones of the laser were activated with the same power inputs over ROI I and ROI II; as can be seen in the 5.3. The position of the thermocouples was carefully set at the center of the laser intensity distribution, adjacent to each other. The readings from the thermocouples were averaged and compared with the captured thermal image readings at the center of ROI II. The calibration was performed in a temperature range of 360-420^{o}C. Using this technique, the apparent emmissivity was experimentally determined to be 0.84 for CF/PEEK tapes and 0.855 for CF/PEKK material. The calibration data can be found in Appendix A.

5.2.3. In-situ measurements

In order to study the effects of the laser heat on the tape surface morphology during and after completion of the heating phase, a Micro-Epsilon scanCONTROL laser line scanner (LLS) was used. The LLS has a maximum resolution of 2 μm and a sampling rate of up to 20000 Hz.
The operating temperature of the laser line scanner is in the range of 0 to +45^{o}C and hence special care was taken in the experimental setup to not allow reflecting VCSEL heater radiation to heat the device. Furthermore, due to this consideration, the LLS was installed at the maximum possible distance away from the surface of the specimen, while remaining within the measuring range of 53.5 to 78.5mm. Hence, the LLS was installed at a predefined position above the sample and the laser line projected by the sensor was aligned along the width of the sample, to the position where the temperature was calibrated to reach the process temperature. In other words, the scanner was used to obtain the profile variation over time, along the simulated 'nip-point'. The representative location of the simulated nip-point during the heating process, for a 30mm heated spot length, can be seen in an IR camera snapshot during the heating process in figure 5.5.

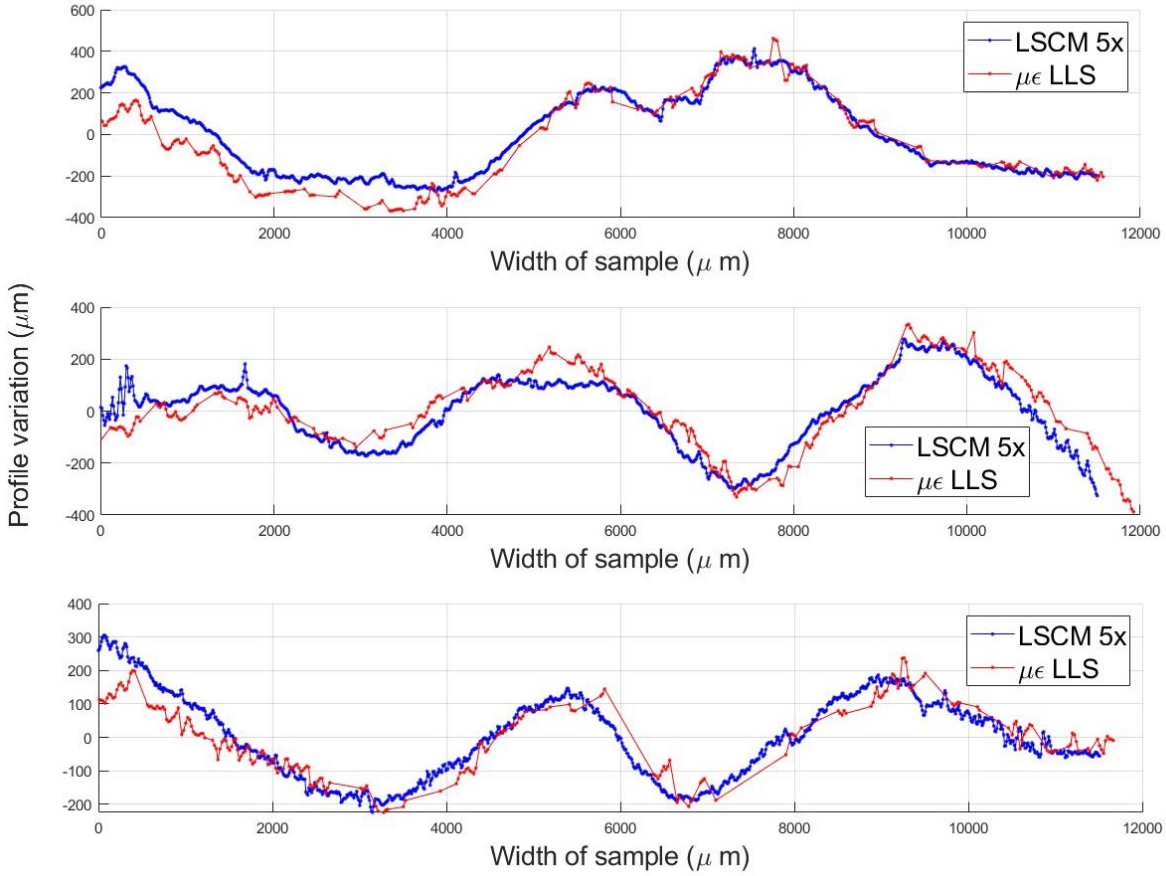

Figure 5.4: Surface profile comparison between LLS and LSCM

The use of the LLS was validated by comparing the obtained profile of the deformed tape after it

cooled down to ambient temperature, with measurements from an Olympus OLS3000 laser scanning confocal microscope (LSCM) of the same tape specimen. A small vertical offset was found between the two profiles, due to the manner in which the tape specimens were fixed onto the confocal microscope stage. However, the profiles obtained by both methods demonstrated the same characteristics. Comparison of profiles from three randomly selected deconsolidated samples can be seen in figure 5.4. Furthermore, the peak-to-valley height of the waviness profile (W_t) was calculated of a representative profile, for a quantitative comparison and the values were found to be just over 2% of each other (650μm and 635μm from the LSCM and LLS respectively).

In order to obtain time-resolved data that could be compared with data obtained through the infrared camera, 100 frames were captured per second of the surface profile of the tape specimens. Hence, one surface profile was captured every 10ms of the heating process and therefore every 4th frame could be compared to the data obtained through the IR camera.

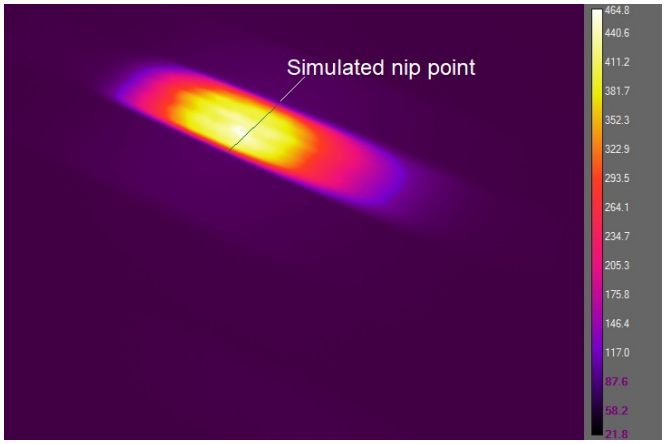

Figure 5.5: Representative IR camera image of simulated nip-point

5.2.4. Final heating setup

The setup went through multiple iterations to arrive at the final configuration. Various different mounting configurations of the laser heater were evaluated. In the initial trials, the laser heater was installed in configuration 1, with the heating modules parallel to the surface of the tape specimen, at a height of 50mm, as seen in figure 5.6(a).
However in such a setup, due to the LLS being mounted at a large angle (45^o), the scanner was not able to obtain enough data points on the surface and hence the resolution of the profile data obtained was not high enough for quantitative analysis. As a result of this, configuration 2 was devised, with the laser heater installed at a 45^o inclination to the tool and tape surface as can be seen in figure 5.6(b). The LLS was mounted perpendicularly above the tape surface in order to obtain enough data points of the tape surface. However, configuration 2 resulted in variable heating temperature along the width of the tape specimen. This was due to the fact that the VCSEL zones are aligned vertically as shown in figure 5.1a and since the heat intensity is directly proportional to the distance of the target from the laser, different locations along the width of the tape exhibited different temperatures.
Hence, to remove this variation of heating intensity along the width of the sample, configuration 3 was designed. The laser was installed at a 45^o inclination, with the individual VCSEL zones aligned along the width direction of the tape. Hence, constant heating intensity was applied along the width. The LLS was installed above the tape surface at a very small angle (4^o) to obtain better resolution data as can been seen in figure 5.6(c). In the figure, the IR camera is not seen, however, the camera was installed at an angle of 55^o from the horizontal tape surface.

Hence, after multiple iterations, it was deemed that configuration 3 was the most suitable for creating deconsolidated tape specimens , with uniform laser intensity application along the width of the specimen at each location along the length. This configuration allowed the LLS to be installed and hence allowed surface profile data to be captured 'in-situ', during the heating phase. Finally, configuration 3 is an interesting configuration to implement, as in the future, the VCSEL heater may be used in a LAFP end-effector, where the laser would have to be installed at an angle similar to this. This would need to

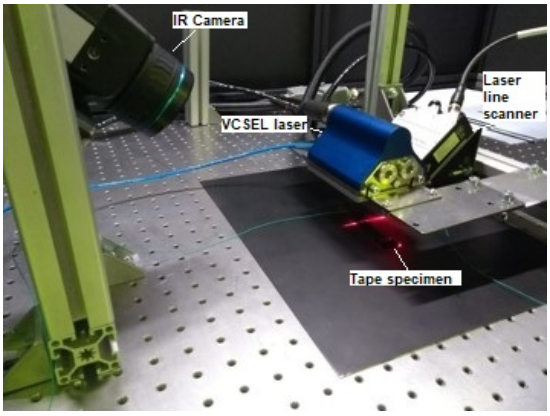

(a) Configuration 1

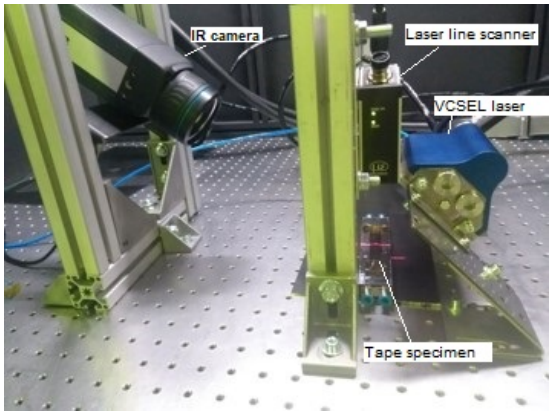

(b) Configuration 2

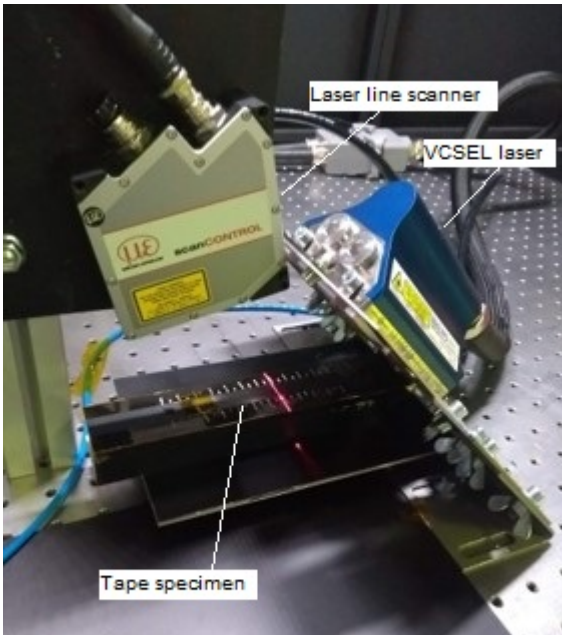

(c) Configuration 3

Figure 5.6: Various configurations of the experimental setup

be done in order to facilitate application of pressure using a roller. Hence, the results obtained through specimens created with configuration 3 shall be also relevant for future work. Therefore, subsequent experiments were conducted using the laser installed as in configuration 3 and the results presented in following chapters are based on the characteristics of the setup.

5.3. Limitations of experimental setup and discussion

With the setup as described above, deconsolidated tape samples could be successfully created with varying process parameters and intensity. However, before reporting results it is important to identify the limitations of the experimental setup in this study, to put the results in context and to draw more relevant conclusions from the obtained data. Some of the perceived limitations of this experimental setup are as follows:

- Due to the design of the VCSEL laser and the absence of a temperature-feedback loop in the setup, it was very difficult to maintain a uniform temperature distribution along the length of the tape specimen (for tape geometry reader can refer to figure 5.2). This was due to the inclination of the laser heater and therefore varying distance between individual laser modules and the tape surface at different locations along the specimen length. An approximately uniform temperature

distribution was obtained while manufacturing specimens, however this was found to be quite difficult to control accurately. Therefore, the temperatures in the range of 360 - 420 were achieved along the heated spot length, with variations typically larger for larger spot lengths, due to more number of individual zones being activated.

- The designed experimental setup simulates the heating of thermoplastic tapes in the configuration of the substrate (placed on a tool), rather than the incoming tape which is fed by a spool with pre-applied tension. Hence, the setup is not accurately representative of the LAFP process, however, this serves the purpose of investigating the effects of rapid laser heating on the material response.
- The heated tape specimens were observed to remain above the T_g and T_m for a maximum time of 4s and 0.45s, respectively. Since, no convection cooling system was incorporated in this experimental setup to freeze the deconsolidated state at the end of the heating process, it is suspected that the microstructure continued to change after the laser heat was switched off. Furthermore, it was observed that the tape continued to warp during the cooling phase. Hence, due to experimental limitation, characterization of the void content and thickness change was done at ambient temperature, after the tape was allowed to deform during the cooling phase. As a consequence, it is important to note that the microstructure may have changed between the nip-point state and the ambient temperature state and hence the thickness and void content information measured may not be accurate. However, in order to understand the underlying mechanisms behind deconsolidation response of the material, this limitation was ignored for the current study.

5.4. Conclusion

In order to experimentally characterize deconsolidation, a robust experimental setup was developed that could be used to prepare deconsolidated tape specimens with varying parameters. The setup consists of a VCSEL laser heater, an IR camera, a laser line scanner, tooling and K-type thermocouples. The setup allows for samples to be created with rapid laser heating of varying heating times and with varying spot lengths. Furthermore, the IR camera and LLS allowed capturing of the temperature profile and surface profile variations along the width in the region of interest, during and after the heating process. After creation of samples, the properties of the deconsolidated tape samples was characterized using various methods, as described in chapter 6.

6

Characterization techniques

After manufacturing deconsolidated tape specimens with varying process parameters, assessment of the severity of thermal deconsolidation, using appropriate characterization techniques was required to be done. In this chapter, the following research questions have been answered: *"How can physical changes due to thermal deconsolidation of prepreg tapes be characterized experimentally?"*, *"How can the deconsolidation phenomenon be studied 'in-situ', during the rapid laser heating phase?"* and *"What previously unreported deconsolidation effects can be observed in prepreg tapes?"*. In order to answer these questions, the choice and relevance of selected characterization techniques is motivated. The phenomenon of thermal deconsolidation in the context of Laser assisted fiber placement is relevant when the deconsolidation state at the end of the heating phase (at the 'nip-point') is captured. Hence, as stated before, the objective of this study was to understand the mechanisms behind the development of deconsolidation effects and therefore, in-situ characterization techniques were focused upon (when feasible) in this study.

6.1. Surface evaluation

To quantitatively and qualitatively study the surface profile of the deconsolidated specimens, two different types of measurement devices with different measurement techniques were mainly used: an Olympus OLS 3100 Laser scanning confocal microscope (LSCM) and the Laser line scanner. Due to the difference in resolution of both measurement techniques, micro-scale surface roughness measurements were performed with the LSCM, while macro-scale surface out-of-plane deformations were studied using profile data obtained from the LLS. Furthermore, for qualitative comparison only, a Keyence 3D Laser scanning confocal microscope VK-X1000 was used due to its capability to scan large surface area. However, this scanner was only used for qualitative comparisons at the the end of the study and not for quantitative analysis of deconsolidation effects. All quantitative surface measurements were performed along a line transverse to the fiber orientation in the UD tape specimens; hence the measurements were done for the surface profile along the width of the specimen.

An important observation that was made in the initial experimental trials was that during the rapid laser heating process, prepreg tapes exhibited warpage along the fiber direction and surface profile waviness in the direction transverse to fibers (along width). This can be observed in figure 6.1 and figure 6.2. In figure 6.1, it can be seen that the deconsolidated specimen (right) exhibits warpage along the fiber direction, whereas the as-received specimen (left) is flat. In figure 6.2, a 2.5mm long section of the tape along the width (only 11.52 mm captured of the 12.62mm total width) is captured using the LSCM at 5x magnification in order to capture the surface profile waviness. The waviness curve along the tape width exhibits peaks and valleys, with the maximum deformation in the z direction being 809.991 μm (orange region) and no deformation in the blue regions. Furthermore, the surface roughness was found to be higher at the peaks of the waviness profile, resulting in a big scatter in roughness values on the surface of the tape along the 'nip-point'. To the author's knowledge, this has not yet been reported in literature and further observations as well as possible causes of such deformation behavior are discussed in following chapters. However, due to the observation of waviness and warpage in the deconsolidated tape specimens, deconsolidation was characterized in terms of the

out-of-plane deformation at the nip-point, in addition to micro-scale surface roughness, to account for the out-of-plane deformation taking place at larger scales.

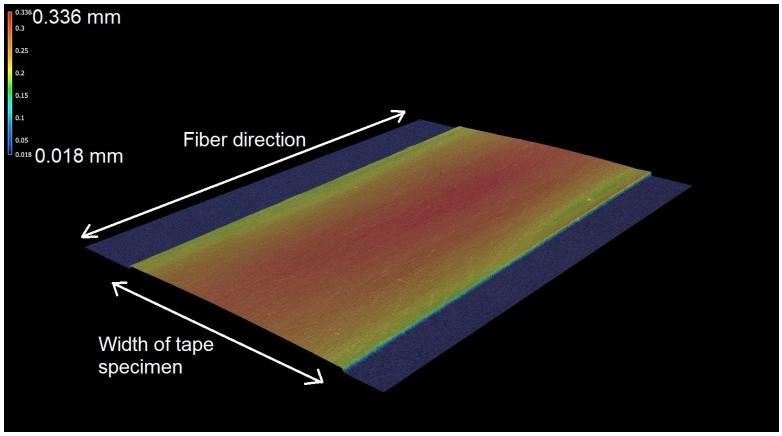

(a) Representative flat surface of as-received tape specimen

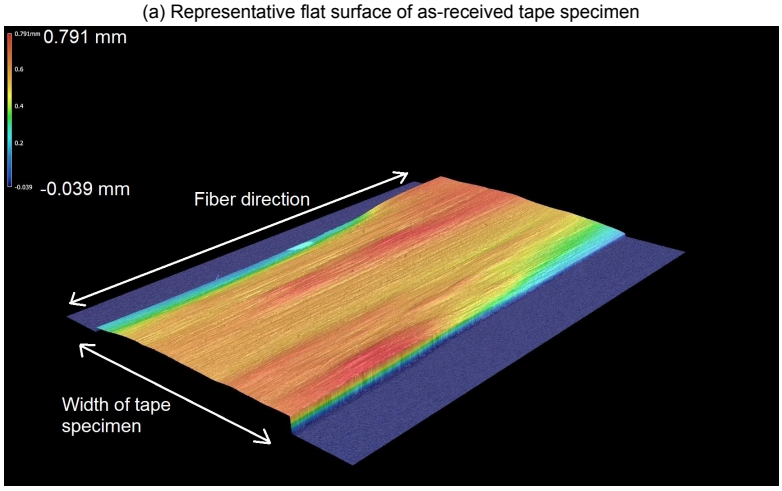

(b) Representative *warped* surface of a deconsolidated tape specimen

Figure 6.1: Comparison of surface profiles obtained from Keyence LSCM wide area scanner

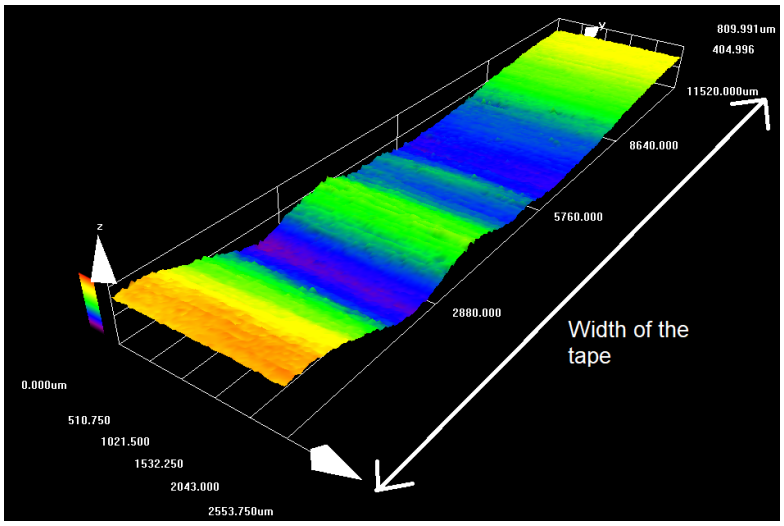

Figure 6.2: Representative waviness in tape specimen along width due to rapid heating; captured using Olympus LSCM at 5x magnification

6.1.1. Surface roughness measurements: cooled state

Surface roughness measurements were made using the LSCM after the tape specimen had cooled down to ambient temperature, after the heating process. All measurements were made at 20x magnification. Each measurement captured an area of 640μm (along fiber direction) x 480 μm (transverse to fiber direction), as can be seen in figure 6.3. In the figure, it can be seen that the fiber direction is along the x-direction and waviness peaks are at higher magnitudes in the z-direction. From these measurements, line surface profiles were extracted along the y-direction. The line profiles were captured at 10 different locations along the fiber direction (x-direction), in order to account for scatter. Following this, a high-pass filter of 96 μm was applied to each primary line profile obtained for an evaluation length of 480μm (transverse to fiber direction), in order to separate roughness profile from the primary profile and remove any global curvature effects. The choice of filter was based on the ISO 4287 - 1997 standard [44], defined for obtaining the roughness profile from a primary surface profile. Finally, the root-mean-square (RMS) roughness was calculated for each of the ten line profiles and the values were averaged.

Due to the waviness in the tape and the resulting higher surface roughness at the peaks of the waviness curve (reason for this observation discussed in subsequent chapters), four measurements were made for each specimen along 20%, 40%, 60% and 80% of the width at nip-point and the maximum RMS roughness.

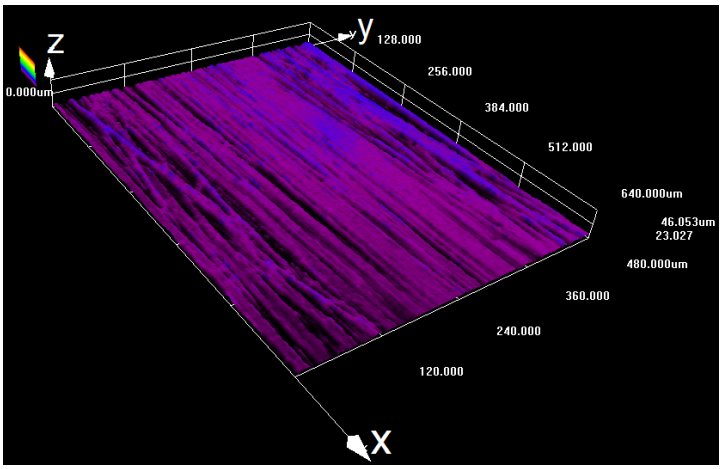

(a) Representative surface roughness of as-received tape specimen

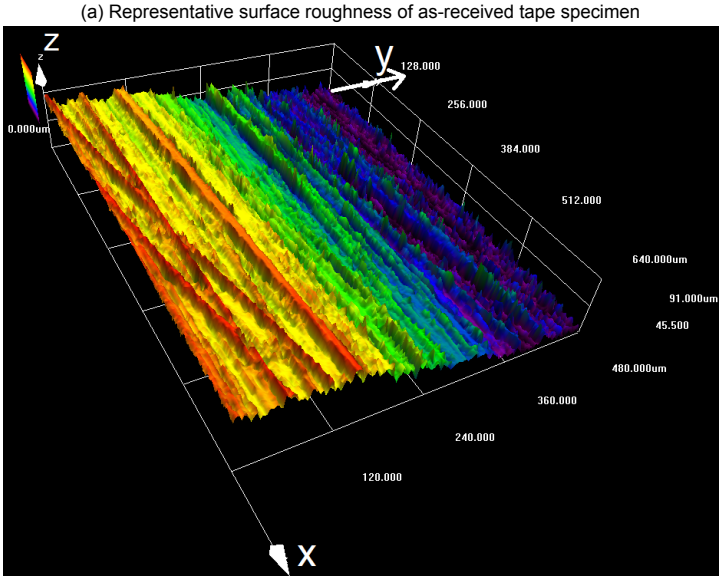

(b) Representative surface roughness of deconsolidated tape specimen

Figure 6.3: Surface roughness measurements from Olympus LSCM

6.1.2. Surface waviness measurements: laser heating phase

As described earlier, the LLS was used to obtain the tape surface profile during the heating phase with a sampling rate of one profile every 10ms. Due to limited resolution of the LLS, the data could not be used to determine the micro-roughness development during the heating phase. However, the profile data could be used to obtain the global deformation of the prepreg surface at the nip-point and provided a lot of information on how the surface deformation occurs during the heating phase, thereby indicating governing mechanisms, that shall be discussed in further chapters.

6.1.3. In-situ surface roughness development

Due to limited resolution of the LLS, it was not deemed possible to monitor the development of surface roughness, during the rapid heating process using the VCSEL laser. However, to study the changes in the prepreg tape surface at various temperature levels, an alternative experiment was performed. This was done by using a hot stage capable of heating the as-received tape specimen up to the required temperatures. The Linkam THMS600 hot stage was placed onto the stage of the Olympus LSCM for capturing surface developments at various temperatures at slower heating rates, as compared to the VCSEL heater.

The as-received tape specimen with a smooth surface was placed on the stage and heated to various temperature to observe the development of surface roughness due to fiber decompaction and to identify the onset of the decompaction effects.

6.2. Cross-sectional microscopy

After surface characterization of the specimens, the effects of thermal deconsolidation in the microstructure at the simulated nip-point were measured by cross-sectional microscopy. Tape specimens were cut, with an offset of 3mm in the length direction from the nip-point, to account for material removal during polishing and grinding. The cut tape specimens were then mounted on plastic thin-sample holders (Struers MultiClips) to keep them oriented vertically and metal clips were attached to add additional weight to the mount, as shown in figure 6.4a. The specimens were then placed in cylindrical moulds and Struers EpoFix resin was poured into the moulds. The specimens were then ground and polished using a Struers Tegramin-201 automatic machine as shown in figure 6.4b.

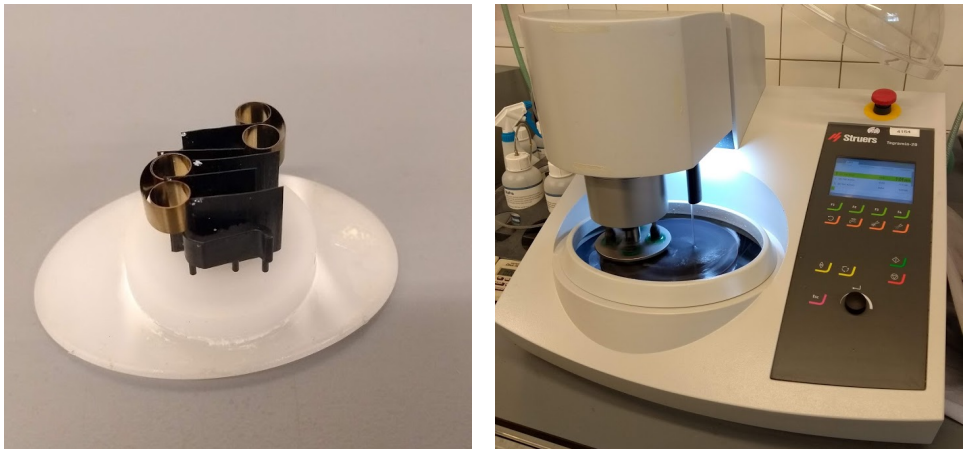

(a) Deconsolidated tape specimens vertically mounted for embedding in epoxy

(b) Struers Tegramin-201 machine used for grinding and polishing

Figure 6.4: Microscopy sample-preparation of deconsolidated tape specimens

6.2.1. Void evaluation

Optical microscopy

The prepared microscopy specimens were studied under a Keyence VHX-2000E digital microscope at 500-600x magnification, to observe the cross-section of the tape specimens, qualitatively and quantitatively. To evaluate the void content over the entire width of the tapes along the nip-point position, the Keyence microscope was used to capture multiple images along the width of the specimen which were

later stitched together to allow digital analysis of global cross-sectional properties.

The quantitative void content analysis of the captured images was done using the image analysis software installed on the microscope work-station. It was observed that void content was locally higher at the locations that corresponded to the peaks of the deformed tape waviness curve. A possible explanation for this non-uniformity of void content in the cross-section of the deconsolidated tape specimens is discussed and motivated in later chapters. However, in order to make comparisons between specimens with different process parameters, the global tape void content along the complete width of the tape was determined and reported.

Scanning electron microscopy
To study void geometry and growth mechanisms in more detail, a scanning electron microscope (SEM) was used to obtain images of the voids formed due to deconsolidation at high-magnification. The measurements were made with a JEOL JSM-840 EDS microscope, which has a magnification in the range of 20 – 300000x with a resolution of up to 3.5 nm. In order to obtain an electrically conductive sample surface, the microscopy epoxy specimens were prepared by sputtering a very thin layer ($\sim 10nm$) of gold particles on the polished surface to be studied.

6.2.2. Thickness evaluation
The change in thickness was characterized by digital analysis of cross-sectional images of the deconsolidated tape specimens using the built-in software of the Keyence digital microscope . Thickness was measured by measuring the perpendicular distance between the two surfaces of the tapes. Due to the warpage and waviness in the tapes, it was also observed that void content and correspondingly thickness at locations along the width corresponding to the peak of the waviness curve of the surface profile was higher than at the tape regions located in the valleys. Hence, the thickness was measured at 20%, 40%, 60% and 80% positions along the width of the tape and the values were averaged. The measurements at each of the locations was made by averaging three observations each.

6.3. Tape deformation
During the thermal deconsolidation of prepreg tapes during rapid laser heating in the LAFP process, it has been suspected by researchers that the tapes undergo deformation in the width direction. Furthermore, as mentioned earlier, it was observed in the initial experimental trials that the specimens warp and hence exhibit an out-of-plane deformation. Hence, in order to characterize these deformations, some techniques were identified, which are described and motivated in this section.

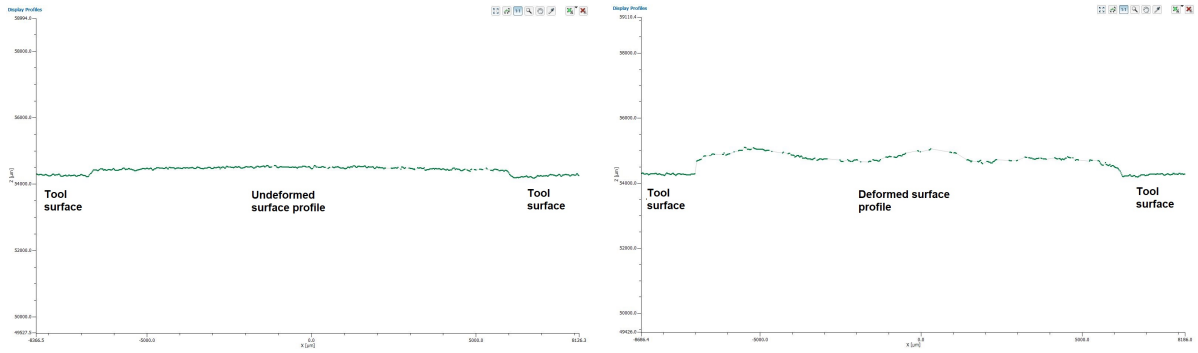

(a) Representative as-received surface profile of CF/PEEK tape (b) Representative deformed surface of deconsolidated CF/PEEK tape

Figure 6.5: Surface profiles obtained using ScanControl software

6.3.1. Width increase at nip-point
The use of the LLS to capture 'in-situ' data on the tape surface allowed capturing of the state of the tape; during the heating phase, at the end of the heating phase as well as after the tape was allowed to cool down. The profile data obtained from the LLS through the ScanControl Configuration Tools software (as seen in figure 6.5) was post-processed in MatLab to obtain the deformations in the width direction of the

tape. It was observed that due to warpage of the tape, the areal measurements in the width direction, were not representative of the actual width of the tape and hence, the captured surface profile was used to obtain the arc-length width of the specimens. Furthermore, in order to avoid inaccuracies in measurement due to a fiber-rich top surface, the waviness profile was extracted from the raw surface profile and the former was used to obtain the width of the tape specimen by arc-length calculation.

6.3.2. Width increase due to CTE

Width increase due to a positive coefficient of thermal expansion (at lower heating rates than the VCSEL heater) was measured by heating the tapes using a hot stage and measurements were made using the LLS as can be seen in figure 6.6. In order to account for variability in the properties of as received tapes, measurements were made using the LLS at ambient temperature as well as at 150^oC. It was observed that at uniform heating of the specimen, with lower heating rates to 150^oC, deconsolidation effects were not observed to the same extent as deconsolidation effects in specimens rapidly heated to 150^oC with the VCSEL heater. Hence, it can be assumed that the width increase captured using the hot stage, was representative of the increase due to CTE.

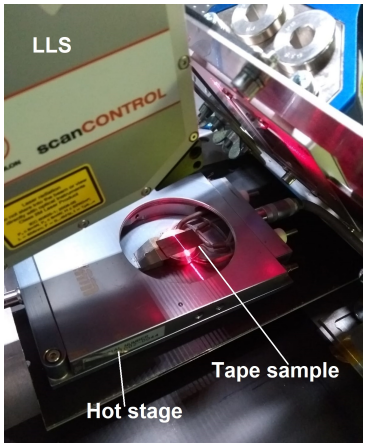

Figure 6.6: Setup for measurement of width increase due to CTE (in-situ)

It is important to not that the width increase results presented in subsequent chapters are a combination of width increase due to CTE and thermal deconsolidation. This was done since it was not possible to determine the amount of width increase due to CTE during the rapid heating process of the laser. However, it was observed that the amount of expansion due to CTE (for slower heating rates) at 150^oC, was small (0.13-0.20 % width increase) and this indicated that in addition to thermal expansion, a major portion of the width increase takes places due to thermal deconsolidation.

6.3.3. In-situ warpape and out-of-plane deformation

The warpage of the tape and the resulting out-of-plane deformation was captured during the heating phase, at the end of the heating phase and during the cooling phase to ambient temperature; from the line profile data at the nip-point obtained through the LLS. The deformations were captured as a function of time and the maximum out-of-plane deformation at the end of the heating phase or at the nip-point was captured and reported. The data was normalized by calculating the deformation from the surface of the as-received tape, in order to account for scatter in thickness properties in the as-received tape samples.

Furthermore, the global deformation in a representative deconsolidated tape specimen was also studied qualitatively using a lab-scale micro computed-tomography (micro-CT) scanner, capable of 180kV/0.5mA. However, due to limited resolution of the device and the small size of samples, only qualitative analysis was possible. Hence, only one sample was scanned at different resolutions ($3.13\mu m$ and $6\mu m$). However, the obtained 3-dimensional images of the specimen provided some valuable information about the deconsolidation phenomenon, as discussed in further chapters.

6.4. Discussion

As described in earlier section, various characterization techniques were identified and adopted in order to characterize the different material responses of thermal deconsolidation due to rapid laser heating with a VCSEL heater, as were reported in literature. in addition to that, during initial trials, observations were made regarding non-uniform material response during deconsolidation, which to the extent of the author's knowledge have not been reported adequately in literature. Hence, some further characterization were devised to obtain a clearer picture of the reasons for the non-linearity and find possible explanation for this new experimental observation. Furthermore, these techniques were also used to characterize 'as-received' tape specimen properties, which were used as baseline properties to evaluate severity of deconsolidation. The measured properties of the tape specimens were determined as presented in table 6.1.

Table 6.1: Measured tape properties of as-received tapes (standard deviation in brackets)

Material	Thickness (μm)	Void-volume content (%)	Width (μm)	RMS Surface Roughness (μm)
CF/PEEK	151.34 (7.7)	0.71 (0.10)	12627 (50)	1.69 (0.39)
CF/PEKK	145.8 (2.55)	0.64 (0.2)	6320 (41)	2.102 (0.32)

6.4.1. Limitations of characterization methods

The characterization techniques as described above were useful in obtaining information about the reasons for deconsolidation and the influence of different process parameters. However, it is also important to identify limitations of the characterization techniques in order to make accurate conclusions based on the results obtained.

- The Keyence digital microscope system available was not able to store the number of images required to stitch the entire width of the CF/PEEK tape at 500x magnification. Hence, during void content analysis, the entire tape width was not evaluated and approximately 0.5 mm width at both edges were not considered in the analysis.
- Due to experimental limitations, the void content and thickness of rapid laser heated tape specimens was measured at the ambient temperature state of the tape after the specimens were allowed to cool down. As explained earlier, it is suspected that the thermal deconsolidation effects continue longer than the heating time. This is due to the fact that the tape remains above the T_g and T_m; with no application of consolidation pressure, even after the heating phase ends. Hence, the void content and thickness obtained through measurements may not be precisely representative of the void content at the nip-point.
- In-situ measurements made by heating the tape specimens using the hot stage have a limitation that the heating rates of the hot stage are not comparable to the rapid heating of the VCSEL laser. This is due to the fact the hot stage was capable of heating at a maximum heating rate of 150^oC per minute, whereas the heating rate of the laser flash was as high as 1600 ^oC per second. Although, one of the main knowledge gaps identified in literature was the lack of knowledge of the effect of rapid heating on deconsolidation effects, this experiment was deemed necessary to understand the underlying mechanisms and in order to test certain hypotheses made in this research.

6.5. Conclusion

Techniques to characterize various material responses due to thermal deconsolidation of thermoplastic prepreg tapes were selected and the choice was motivated in this chapter. In addition to known deconsolidation effects such as increase in void content, increase in thickness and surface roughness development; early experiments indicated that deformation of tape also takes place during thermal deconsolidation during the heating phase with no external pressure applied on the specimens. This deformation was observed in terms of width increase and warpage of the tapes (resulting in out-of-plane deformation in the tape surface profile). Furthermore, it was found that properties such as void

content, surface roughness and thickness had a large scatter, when measured at multiple different locations along the width of the tape. This effect was suspected to be due to higher temperatures observed at the regions at the nip-point, which deform out-of-plane. More discussion on this can be found in following chapters. However, this is an important observation, as to the author's knowledge, this has not yet been reported in literature.

Hence, characterization of the deconsolidated specimens was planned to be done in a way such that different samples could be compared, and hence the effect of process parameters could be studied. Therefore, it was decided to characterize the tape deconsolidation in terms of five responses: surface roughness, maximum out-of-plane deformation, width increase, void content and thickness at the nip- point. Keeping this in mind, an experimental plan was devised which incorporates a Design of Experiments (DoE) approach, to minimize the experimental effort to obtain valuable information about the process. The details of the experimental trials and the obtained results are presented in chapter 7.

7

Empirical results

To identify the influence of the selected factors (reader can refer to research questions in chapter 4) on the deconsolidated state of the tape specimens and to identify key factors that influence the tape properties being measured, a set of experiments were conducted. The research questions addressed in this chapter are as follows: *"What are the qualitative and quantitative relationships between changes in surface roughness, void content development, decompaction and other tape deformation effects of deconsolidated prepreg specimens due to rapid laser heating with varying process parameters*[1] *"* and *"At what temperature does the onset of thermal deconsolidation during LAFP begin?"*

The first two sets of experiments (phase I and II) were performed using Design of Experiments (DoE) approach and analyzed the influence of three of the five factors identified in the research questions (heating time, heated spot length and cooling rate). DoE is a useful experimentation tool, which combines statistical methods to investigate the influence on one or more response variables with a smaller amount of experimental effort than a full experiment with all factors varied. Furthermore, a DoE experimental design can also provide statistical information to determine the repeatability and reliability of the experiments. Instead of varying one factor at a time, a DoE based experimental design can vary factors simultaneously. The different design configurations (different settings for influencing factors) that were generated by the DoE were first created and then characterized to obtain the responses. Finally, conclusions were drawn on the main effects and interactions between factors; based on statistically significant results with the least amount of trials. Following this the influence of different nip-point temperatures (fourth factor - temperature at nip-point) was studied in phase III of experiments. A set of confirmatory experiments were also performed (including the fifth factor - type of polymer matrix), however they are discussed only in chapter 8 in order to verify the trends obtained from the experimental results.

The objective of the first set of experiments was to estimate the key factors influencing the thermal deconsolidation response of CF/PEEK prepreg tapes, in terms of surface roughness, thickness changes, void content, width increase and out-of-plane deformation. For this purpose, a Plackett-Burman (P-B) screening design was selected to study the influence of three of the five factors identified in chapter 4. A P-B design provides the advantage of the ability to study multiple variable more economically than factorial (partial or full) designs and with less negative confounding effects (extraneous influence that may influence results and their relevance). A second set of experiments were done with CF/PEEK tapes to further study the influence of the main factors identified from the first set of experiments, on the response variables. This was done by using a full- factorial three level experimental design for two main factors identified from the first set of experiments. A third set of experiments was performed with CF/PEEK tapes by varying the heating temperature in order to identify the onset of deconsolidation effects as well as study the influence of temperature on the severity of deconsolidation effects. Finally the objective of the final set of experiments with CF/PEKK tapes was to verify whether similar material response could be obtained in other thermoplastic tapes with a different polymer matrix.

[1] Variation of heating time, heated spot length, cooling rate, nip-point temperature and polymer matrix type

7.1. Phase I: P-B Screening design

A Plackett-Burman screening design was used to evaluate the influence of three out of five parameters (called factors in the DoE study) chosen to be studied in the first set of experiments: heating time, cooling rate and heated spot length. This was done due to the fact that all of these factors cannot be varied simultaneously, since they are interdependent. The other factors were studied in subsequent experiments (phase III and IV). Hence in phase I, the heating temperature (average nip-point temperature 360^oC) and polymer matrix type (CF/PEEK) were kept constant. The characterization of thermal deconsolidation was done in terms of surface roughness, void content, thickness increase, width increase and out-of-plane deformation of the tape specimens at the nip-point as explained in chapter 6.

7.1.1. Factors evaluated and test matrix

- Heating time: One of the most important process parameter in LAFP is the material deposition speed or the placement speed. As the placement speed increases, the heating time available before the roller applies pressure on the tape is reduced. To account for this shorter time, higher input power resulting in higher laser intensity, is typically required. Hence, heating time (with varying required power levels) was chosen as a parameter to be included in the experiments, to study the influence of varying heating times and indirectly the influence of placement speed. As the heating time in the LAFP process is dependent on both the heated spot length and the deposition speed, for the purpose of this study, it was required to keep one of the two factors constant. Hence, for the ease of calculations, a 30mm spot length was used to calculate the corresponding placement velocity for each configuration (despite the heated spot length being longer in some configuration). This choice was motivated based on standard heating lengths used in literature [34]. The high and low configuration of the heating time was set to 200 ms and 800 ms, respectively. The lower limit of the heating time was chosen due to the inability of the laser module to heat the tape surface to the desired temperature at shorter heating times, while the upper limit was chosen based on the corresponding placement velocity calculated and verifying if the calculated speed was relevant to be studied in the context of the LAFP process. Due to a combination of varying heating times and a fixed heated spot length, the apparent placement velocities simulated in this study ranged between 150 mm/s (200ms heating time over a 30mm length spot) - 37.5 mm/s (800ms heating time over a 30mm length spot). It is important to note that this is an assumption made to obtain a relevant heating times. However, since the focus of the study was to identify the effects of heating time on the deconsolidation effects, the exact corresponding placement velocity is not calculated in the traditional way of dividing entire heated spot length by heating time. Furthermore, as the reason for varying the heated spot length was to be able to study the influence of boundary conditions to the nip-point (length of melted section of the tape adjacent the nip-point), calculation of placement speeds based on the heating time and the actual heated spot length serves no important purpose.

- Heated spot length: Another setting of the laser heater that can be varied in the LAFP process is the spot size of the laser irradiation. The influence of spot size on the deconsolidation state at the nip-point in the LAFP process is not known and hence this was investigated by varying the spot length, while the spot width remained the same as width of the tape specimens. The relevance of a study on heated spot length is suspected to be very high as this changes the boundary conditions that are applied at the nip-point which is at the center of the spot (in the length direction). As the spot length increases, a larger section of the tape is above melting temperature of the polymer and hence some variation in deconsolidation behavior is expected. This is due to the fact the change in boundary condition (for a larger heated spot size) would result in greater freedom for fiber to de-compact from the tape surface, out-of-plane, in order to reach a lower stress state. As explained in previous chapters, fiber decompaction is suspected to be due to residual stresses in the fibers of the prepreg tape, introduced during the tape manufacturing process. The VCSEL heater was configured to heat the entire heated spot to a temperature above T_m of the tape material (343^oC). The deconsolidated state was characterized along the width at center of the sample, i.e. the intended nip-point. A high configuration of 80mm spot length and a low configuration of 30mm spot length were selected for the experiment. The upper and lower limit were chosen due to the design of the VCSEL heater; the 30mm spot length was achieved by

activating 3 independent zones of the laser, while the 80mm spot length by activating 11 zones out of 12. As the amount of input energy required from the laser to melt the entire heated spot and obtain an average temperature of 360^oC at the nip-point, varied with varying spot lengths; the power levels had to be experimentally determined. Hence, a trial and error method based on engineering intuition was used to determine the required power levels for each configuration before the specimens were manufactured.

- Cooling rate: Since the laser heating process is very rapid, freezing the deconsolidation state without application of external pressure or convection cooling was not found to be possible, due to experimental limitations. In order to study influence of cooling rate on thermal deconsolidation, initially, a tool with cooling water running through was tested. It was found that activating the cooling flow instantaneously after the rapid heating through laser flashes, was not possible. Hence, for a preliminary study on the influence of the cooling rate on the tape deconsolidation, two different tool surfaces (with different surface areas) were used to place the tape specimens, resulting in different cooling rates. The dimensions of the tool and the cooling rates obtained are presented in table 7.1.

Table 7.1: Cooling rates obtained using different aluminum tooling

Tool material	Surface area (m^2)	Obtained cooling rate on tape surface ($^oC/s$)
Aluminum tool I	0.15	121
Aluminum tool II	0.28	184

To evaluate the influence of these three factors on the deconsolidation response of the material, 8 configurations were defined based on a geometric Plackett-Burman design which included replicates for configurations (1.2,1.7,1.8 and 1.10). Hence, 12 specimens were created with configurations as shown in table 7.2. Due to the methodology of the Plackett-Burman design, the test matrix includes some duplicates in order to check repeatability of the experiment and the characterization techniques chosen. This helped the statistical software determine the significance levels of the results and account for experimental scatter. Furthermore, for the configurations which did not have replicates in the design (1.1,1.3,1.4 and 1.5), two samples were manufactured and the values were averaged before inputting in the Minitab software for analysis.

Each configuration was heated to an average nip-point temperature of 360 ^oC while the range of temperatures at the nip-point ranged between 340 ^oC - 400 ^oC due to the observed deformation and local temperature peaks as explained in earlier chapters. In table 7.2, the power levels required for the different configurations, in order to reach an average nip-point temperature of 360 ^oC are presented. These power levels indicate the total power (sum of all individual zones activated), during the heating process. As can be seen, shorter heating time and higher heated spot length, required higher power levels when compared individually. For specimens heated to 30 mm spot length, 3 individual zones of the laser were activated and for specimens heated to 80 mm spot length, 11 individual zones were activated. For more details regarding power levels, reader can refer to table B.1 in appendix B.

Table 7.2: Configuration settings used in the P-B screening design. High levels are indicated by color shaded cells

Parameter	Unit	Symbol	Configuration											
			1.1	1.2	1.3	1.4	1.5	1.6	1.7	1.8	1.9	1.10	1.11	1.12
Heating time	ms	T_h	800	800	200	800	200	800	200	800	200	200	200	800
Cooling rate	$^oC/s$	R_c	184	184	184	121	121	184	184	121	184	121	121	121
Heated spot length	mm	L_s	80	30	30	30	80	30	80	80	80	30	30	80
Power input	W	-	660	222	600	222	1980	222	1980	660	1980	600	600	660

7.1.2. Results of screening design

Rapid heating of the CF/PEEK tape specimens was done using the laser heater, with factors set according to the different configurations as described in table 7.2. During the heating phase, in-situ profile

data was captured using the laser line scanner (LLS). After completion of heating, characterization of the samples was done to study the effect of the different configuration on the response variables. The obtained results from characterization tests are presented in figure 7.1. As discussed earlier, for configurations without any replicates in the design (1.1,1.3,1.4 and 1.5), two samples were created and characterized, and their average value was used as input to Minitab. As can be seen in the results that this was not done for microscopy specimens and hence void content and thickness information from one sample each was taken. Furthermore, the configurations which had replicates in the design (1.2/1.6,1.7/1.9,1.8/1.12 and 1.10/1.11), were each manufactured once and then characterized. The results for similar configurations are plotted overlapping each other as can be seen from the blue and yellow bars, in order to indicate the similarities and scatter in properties of samples created with the same settings. Furthermore, standard deviation in the measured values is presented as error bars in the plots. For measurements made with the LLS (width increase and out-of-plane deformation), error was ±0.1% of the measured range.

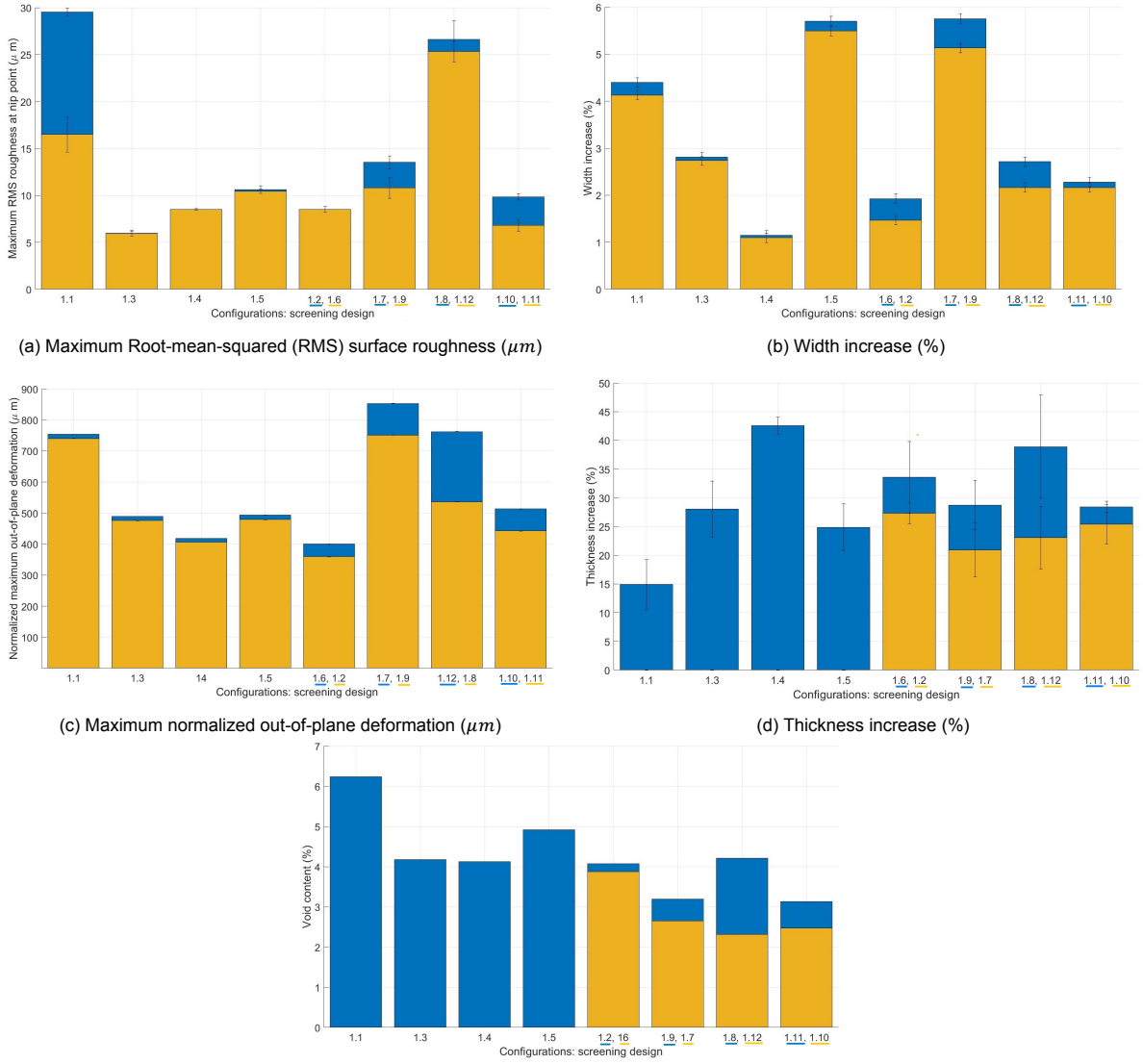

(a) Maximum Root-mean-squared (RMS) surface roughness (μm)

(b) Width increase (%)

(c) Maximum normalized out-of-plane deformation (μm)

(d) Thickness increase (%)

(e) Void content increase (%)

Figure 7.1: Results of screening design

The results of the specimen characterization were processed through the statistical software Minitab in order to obtain statistical information and the relevance of the effect of the factors chosen to be studied. The statistical results are presented in the form of a Pareto chart of the standardized effects

(t-statistics that test the null hypothesis that the influence of the effect is 0) and a main effects plot. The former plot indicates the largest effect to the smallest effect in absolute values of the standardized effects. A reference line is drawn at 2.306 along the horizontal axis in the chart, which can be used to determine whether an effect is statistically significant in the design space or not (effects equal to or higher than the reference line have a significant influence). The reference line is dependent on the confidence level chosen for the analysis (95% for this analysis).

The analysis of variance (ANOVA) data supporting the presented results can be found in Appendix C. It must be noted that the results of the screening design are only used to identify main effects and not used to study interactions. This is due to the fact that in a P-B design, in case an interaction between factors is not negligible, its effect might be confounded with individual factors. This makes it hard to draw conclusions and hence, the first experiment is used only to study the independent influence of the chosen factors on the response variables.

- Surface roughness
  The maximum root-mean-square roughness was determined for each sample by taking roughness measurements at 4 locations along the nip-point at locations corresponding to 20%, 40%, 60% and 80% of the width of the tape, as described in chapter 6. There were large differences in the measured roughness values, due to the waviness of the tape specimens. Hence, the maximum roughness value was obtained from the four measurements, and reported as can be seen in figure 7.1a. The very high scatter in roughness values of configuration 1.1 was attributed to dry fibers poking out of the deconsolidated surface due to the fiber decompaction, resulting in very high local roughness at those locations. Similarly, the high roughness values for both configurations 1.8 and 1.12 can be attributed to dry fibers on the top surface due to the heating process. A representative figure of regions with locally high roughness values due to fibers can be seen in figure 7.2
  In the statistical results, it can be observed from figure 7.3a, that the heated spot length has a significant standardized effect on the roughness values (with a standardized effect of 2.32). Furthermore, heating time is also seen to have a moderate influence (although not found significant in this design space). These observations can be verified by studying the main effects plot (figure 7.3b), where the slopes for the heating time and heated spot length are steeper than for the cooling rate. Although the effect of heating time was not found to be significant in the design space considered in these experiments, it was suspected that heating time may also play a strong role on the roughness development and hence further analysis was required, which was done in phase II of the experiments.

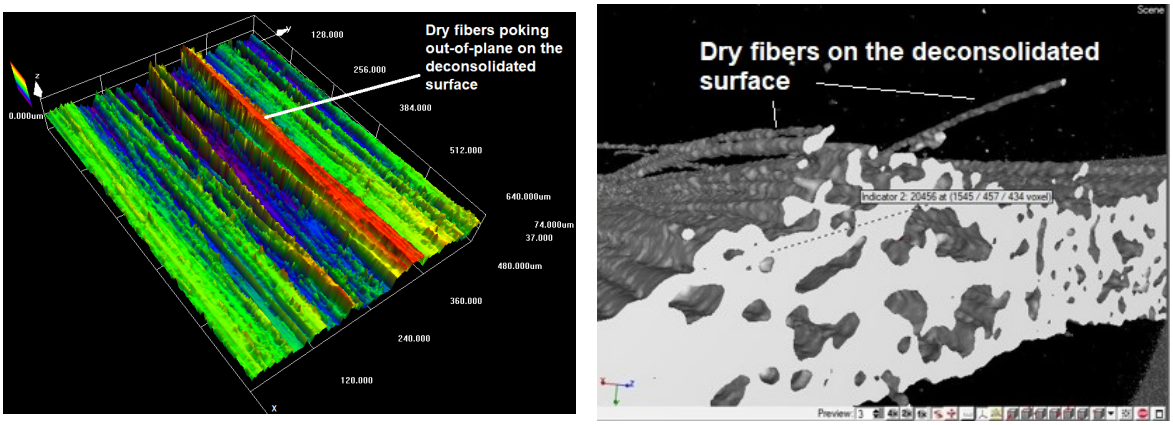

(a) Surface profile of deconsolidated tape specimen through LSCM at 20x magnification

(b) Micro-CT reconstruction of deconsolidated tape specimen at 3.13μm resolution

Figure 7.2: Representative example of high local roughness due to dry fibers

- Width increase
  Width measurements were made using the LLS as described in chapter 6. The width change was measured 'in-situ'. Therefore, the measurements were made to capture the change in width at the the end of the heating phase. In order to account for variability in the width of as-received tapes,

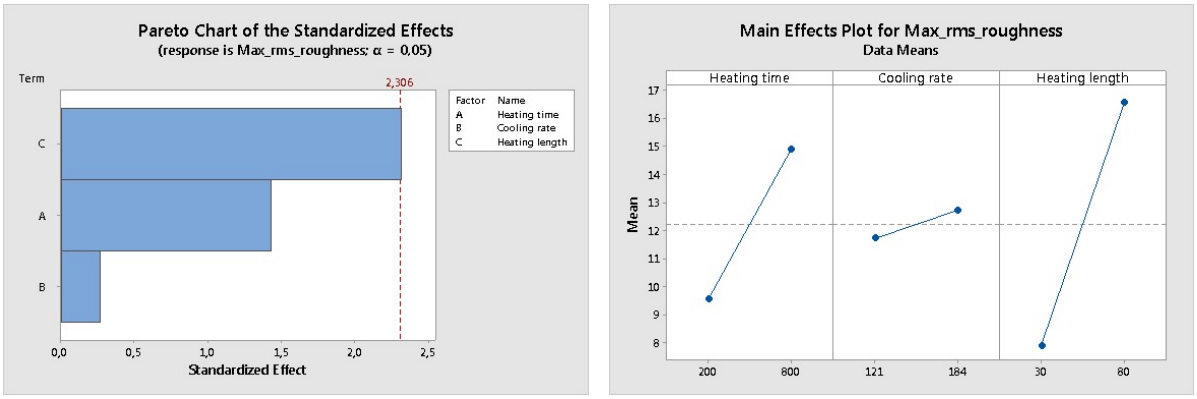

(a) Standardized Pareto plot

(b) Main effects plot

Figure 7.3: Screening design: influence on surface roughness

the increase in width was obtained by subtracting the measured width at the nip-point by the as-received width of the same specimen. Very little scatter was observed in the measurements (seen in figure 7.1b) indicating that the width increase is not strongly affected by the amount of waviness at the nip-point and corresponding temperature peaks, rather is more dependent on the average temperature at the nip-point.

The Pareto plot (figure 7.4) suggest a strong main effect of the heated spot length and a moderate influence of the heating time. This can be verified by studying at the main effects plot where a large difference in mean values of width increase is observed, between the two heated spot lengths of 30mm and 80mm. It was interesting to note that the increase is width was lower for a higher heating time. This aspect was investigated further in phase III of experiments.

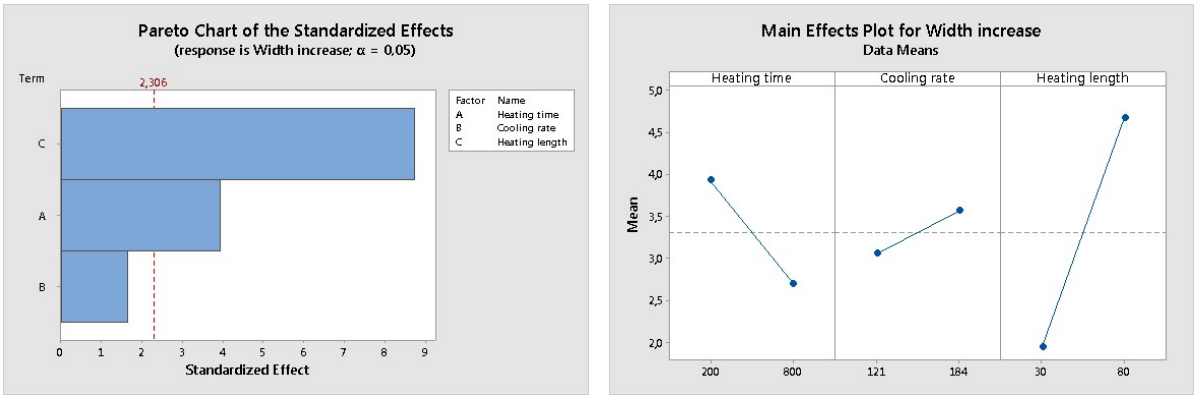

(a) Standardized Pareto plot

(b) Main effects plot

Figure 7.4: Screening design: influence on width increase

- Maximum out-of-plane deformation
  The out-of-plane deformation and the tape waviness, caused by the warpage of tape specimens was characterized for the different configurations. Some scatter is observed in the results obtained (seen in figure 7.1c), especially for configurations 1.7, 1.8 and 1.10 (and their replicates). This scatter was attributed to experimental error. Due to the way the as-received tape material was stored in a spool, it is possible that due to the bending, some specimens were not entirely flat on the tool surface, even when restrained with Kapton tape at the edges. Hence, some slight height variations on the surface of the tape are possible. This is suspected to have influenced the measured results and result in outliers.

  The statistical information as presented in figure 7.5 indicates that the heated spot length had a large standardized effect on the tape warpage and hence the out-of-plane deformation. This observation was in agreement with the observations made for surface roughness.

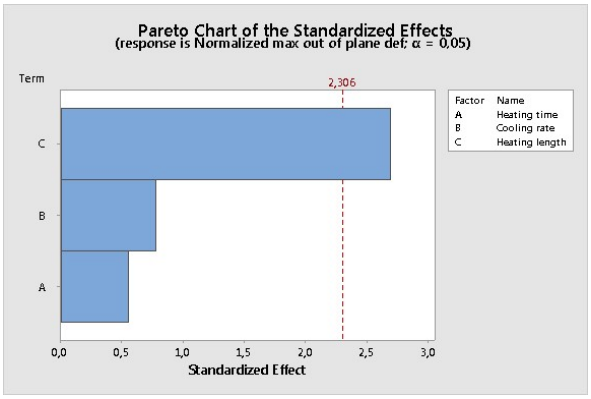

(a) Standardized Pareto plot

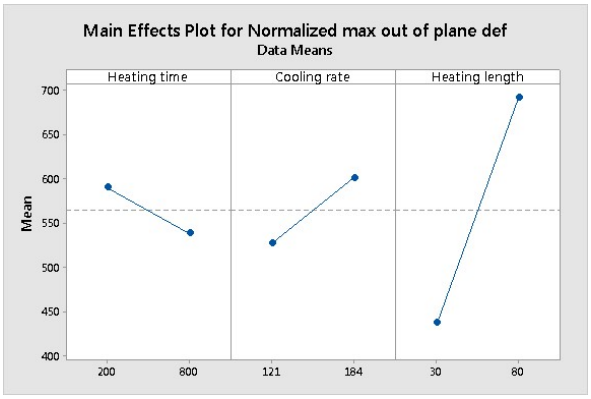

(b) Main effects plot

Figure 7.5: Screening design: influence on out-of-plane deformation

- Global Thickness increase
  The thickness was measured after the tape specimen cooled down to ambient temperature by examining cross-sectional images of the microstructure at the nip-point. The reported values are represented as a percentage increase of the as-received thickness of the prepreg tape specimens. The measurement was performed at 4 locations (20, 40, 60 and 80% of tape width) as described earlier in this section and then averaged to obtain the global thickness increase. Due to the tape waviness, local spots along the nip-point were heated to higher temperatures and higher thickness increase was observed at these local spots. However, due to the chosen method of measuring the average thickness, a large amount of scatter was observed in the results, since the measurements were very sensitive to the location of measurement. The scatter can be seen through the large standard deviation for the reported values in figure 7.1d. A representative cross-sectional micrograph that shows the influence of tape waviness, i.e. higher thickness increase at the peaks of waviness curve, can be seen in figure 7.7. It can be seen that thickness increase is due to the combined effect of voids in the cross-section and movement of dry fiber bundles to the surface. Furthermore, it is interesting to note that at the peaks of the waviness curve correspond to the temperature peaks of the surface temperature distribution, as can be seen in a representative deformed tape profile plotted along with the temperature on the surface at the measured nip-point (figure 7.8).

  The obtained Pareto plot and main effects plot (figure 7.6), indicated that none of the considered factors have a statistically significant effect on the increase of thickness. This is suspected to be due to the large scatter in the measurements, although it might also be due to lower influence of the considered factors on the thickness increase. Since, the data is inconclusive, the influence of the considered factors was further investigated in phase II of the experiments.

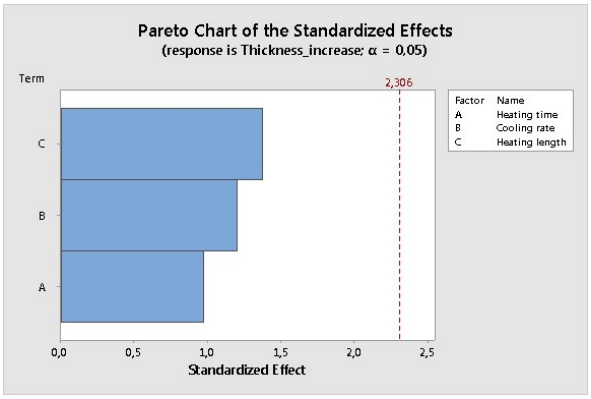

(a) Standardized Pareto plot

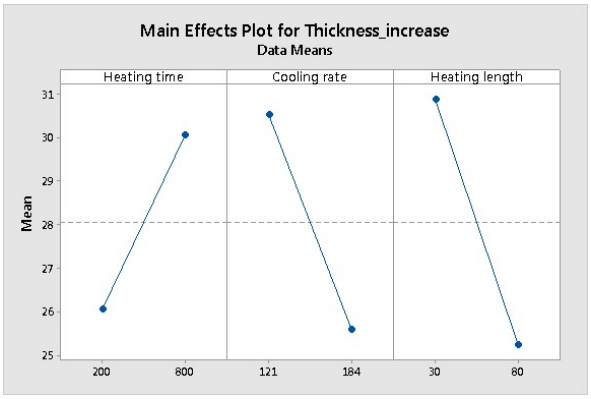

(b) Main effects plot

Figure 7.6: Screening design: influence on thickness increase

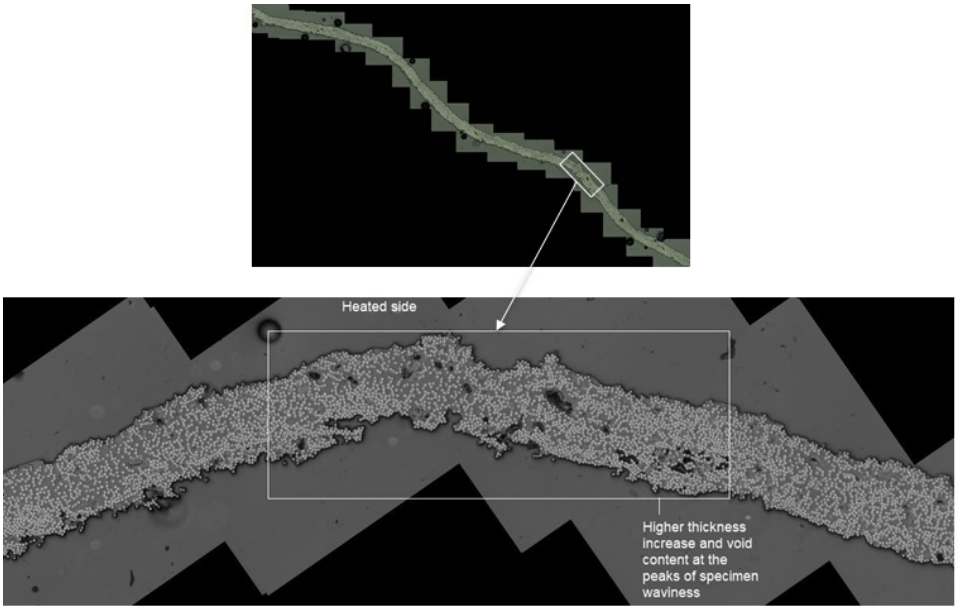

Figure 7.7: Representative cross-sectional image of tape showing higher thickness increase and void content at peaks of tape waviness curve

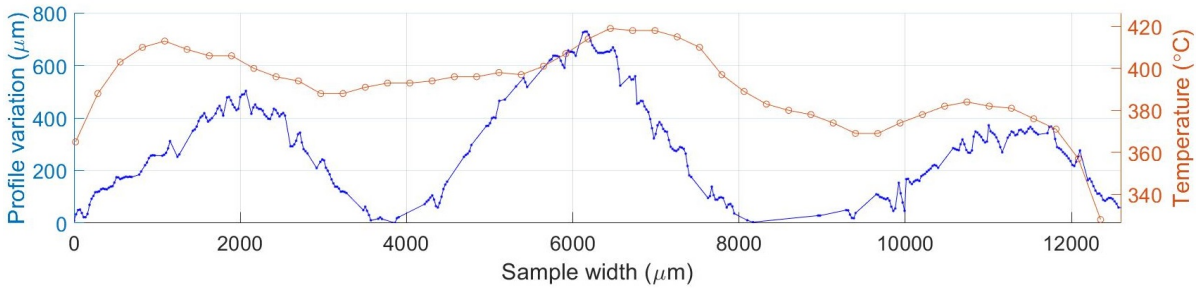

Figure 7.8: Representative temperature variation over the tape surface profile (higher temperatures at peaks of tape waviness)

- Global void content
  Similar to thickness increase, the influence of the considered factors was not found to be statistically significant in the considered design space, on the void content. Although, the global void content was measured at the cross-section of the nip-point, some scatter can be seen in the results for replicated configurations (figure 7.1e). This scatter may be linked to the following limitations of the characterization technique:
  (1) the void content measured through digital analysis of cross-sectional micrographs is highly sensitive to the exact location of the cross-sectional cut along the length of the specimen. Since, the voids were found to be ellipsoidal in nature, the diameter of voids varies at different locations along the fiber direction. This can be seen in figure 7.9. Therefore, the accuracy of results is suspected to be highly influenced by the obtained location of the cross-sectional cut, which is dependent on the accuracy of grinding and polishing process of the samples.
  (2) Errors due to the microscopy sample preparation process are also suspected, wherein the epoxy could have entered into voids and hence the calculated void content from digital microscopy may not be very accurate.

  The obtained standardized Pareto plot indicates that the heating time has relatively stronger influence on void content compared to the other factors, as can be seen in figure 7.10a. The main effects plot (figure 7.10b), indicates that the void content is higher in case of a longer heating; i.e. increase in void content is higher when the heating time is 800ms than at a heating time of 200ms. However, since these results were inconclusive further experimental studies were performed in phase II and phase III, in order to determine the main influential factor and therefore, the driving mechanisms behind void content increase in the microstructure at the nip-point.

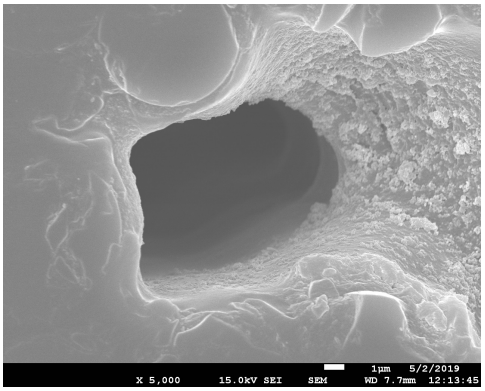

Figure 7.9: Ellipsoidal nature of void seen with varying diameter of voids along the fiber direction (captured at 5000x magnification using SEM)

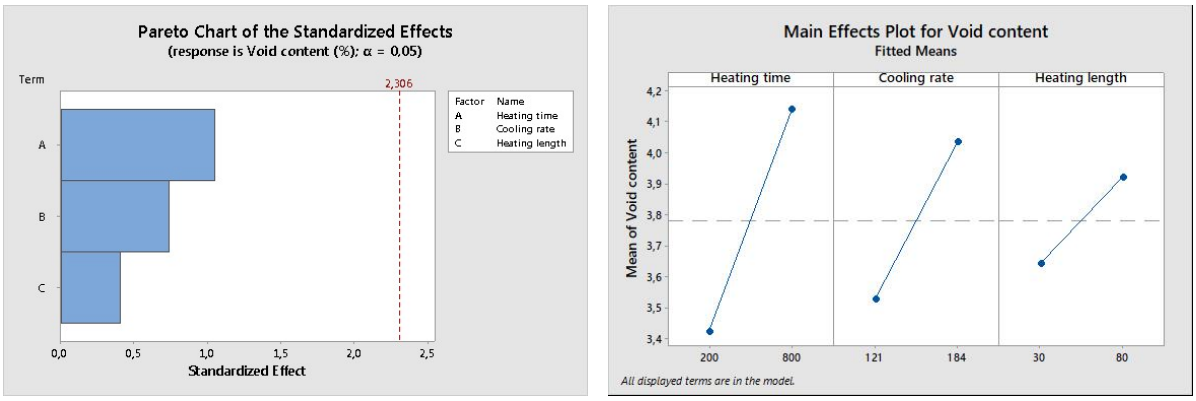

(a) Standardized Pareto plot

(b) Main effects plot

Figure 7.10: Screening design: influence on void content

7.1.3. Discussion

The following main observations were made from the results of phase I of the experiments:

1. It is clear that the studied factors have a different amount of influence on different deconsolidation effects, which also suggests that no common mechanism can describe all of the deconsolidation effects observed in thermoplastic tapes. The information obtained from the screening design was used to identify trends in the material response, however, any non-linearity in the response had to be further investigated, hence the obtained results were used to design further experiments.
2. Based on the observations that tape specimens warp during the heating process (and hence lose contact with the tool surface), as well as the statistically low influence of cooling rate on the material response as observed in this study, it was decided that with the proposed experimental design, the influence of cooling rate could not be objectively studied. Hence, studying the influence of cooling rate through heat conduction through different tool surfaces was not found to be a feasible approach. Therefore, in all further experiments the tool with surface area of 0.28 m^2 was used.
3. Even though all factors show different trends, the influence of heated spot length was found to be the most significantly influencing factor on three of the five response variables considered: surface roughness, width increase and out-of-plane deformation.
4. The relatively equal influence of heated spot length and heating time on thickness increase as can be seen in figure 7.6, suggests that either the considered factors do not have an strong influence on the thickness at all or that thickness increase may be more strongly influenced by a combination of factors (therefore suggesting multiple driving mechanisms). On the contrary, heating time exhibited a stronger influence on the void content increase as compared to other factors. Hence, further analysis on these observation was done in phase II and phase III of experiments.

The obtained results provided some information about the hypotheses being tested, as presented in section 4.2. The preliminary results suggest that fiber decompaction, which is tied to the influence of heated spot length, is indeed important to describe surface roughness. Furthermore, it was found that the influence of fiber decompaction is also significant for out-of-plane deformation and width increase. Hence, the initial hypothesis was expanded to link two of the material responses together (surface roughness and maximum out-of-plane deformation), as it is highly suspected that both are governed by the same mechanism. Further analysis on the factors affecting width increase is required as the results suggest that both heating time and heated spot length have a strong influence.

Based on the observations above, it was concluded that a more in-depth analysis of heated spot length and heating time was required, while keeping the cooling rate constant. Furthermore, non-intuitive observations such as the lower amount of width increase for a longer heating time, needed to be further investigated. Finally, the limitation of the screening design that interactions between factors and their influence on the material response were not obtained, needed to be taken in account. Hence, a more detailed full factorial experimental design was created which tested the material response at three factor levels, in phase II of experiments.

7.2. Phase II: Detailed investigation of influencing factors

7.2.1. Factors evaluated and test matrix

Further analysis on the influence of heated spot length and heating time on the five response variables was done by implementing a 3-level, full factorial design. Such a DoE approach is useful for identifying and investigating quadratic effects as well as interaction effects between different factors. The design matrix is presented in table 7.3. No replicates were made in this study and in each configuration an average nip-point temperature of 360 ^oC was aimed. In order to keep the cooling rate constant, a tool with surface area of 0.28 m^2 was used to place tapes for the laser heating experiment.

Table 7.3: Configuration settings used in the full-factorial design. Intermediate and high levels are indicated by color shaded cells

Parameter	Unit	Symbol	Configuration								
			2.1	2.2	2.3	2.4	2.5	2.6	2.7	2.8	2.9
Heated spot length	mm	L_s	30	30	50	50	80	30	80	80	50
Heating time	ms	T_h	800	500	800	500	800	200	200	500	200
Cooling rate	^oC/s		121								
Power input	W	-	222	420	320	560	660	600	1980	880	880

7.2.2. Results

Specimens were manufactured with specifications as presented and table 7.3 and characterization of the deconsolidated state of the specimens was done. The results of the characterization tests (figure 7.11) were used as input to the Minitab software to obtain statistical information. For each of the measured response, the standardized effects, main effects plot and interaction plots are presented in this section. The Pareto charts and the main effects plot can be interpreted in the same way as the screening design results, whereas the interaction plots can be used to study the variation in material response with both factors (heating time and heated spot length) being varied simultaneously. It is important to note that the reference line drawn in the Pareto charts is not at the same value as that in the screening design (2.776 instead of 2.306). This indicates that since the factors are better defined in the full-factorial design, the significance levels of the influence of the factors on the response changes, as can be expected. Furthermore, due to removal of the cooling rate factor, the amount of scatter introduced by it is reduced, resulting in more statistical significance of the results.

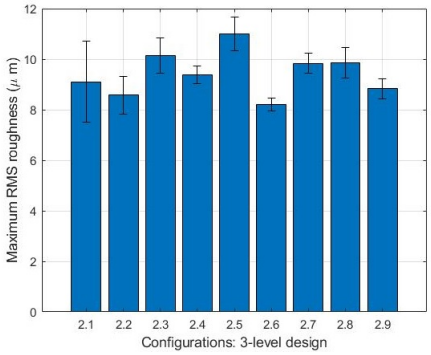

(a) Maximum Root-mean-squared (RMS) surface roughness (μm)

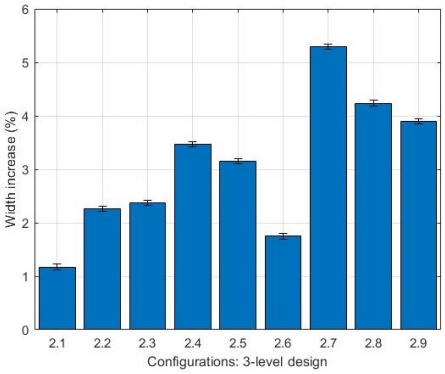

(b) Width increase (%)

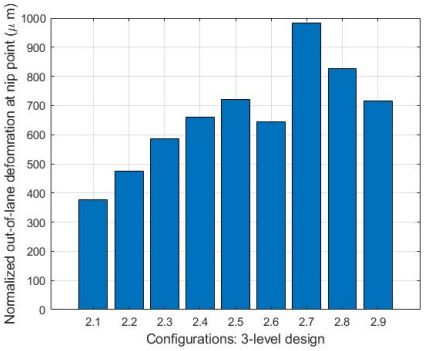

(c) Maximum normalized out-of-plane deformation (μm)

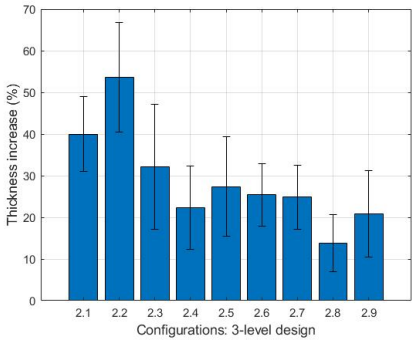

(d) Thickness increase (%)

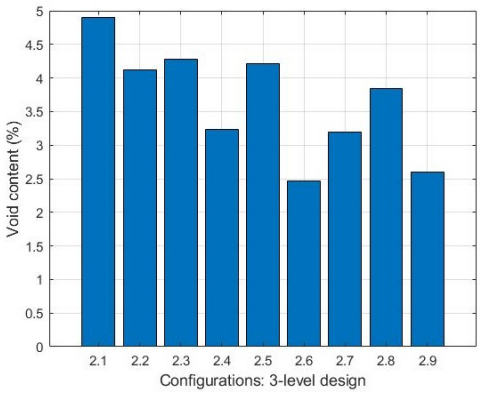

(e) Void content increase (%)

Figure 7.11: Results of three-level full-factorial design

- Surface roughness
  Surface roughness was measured by the same method, as described earlier. Analysis of the maximum surface roughness values (maximum of the 4 measurements done at 20%, 40%, 60% and 80% of the width) at the heated nip-point confirmed the trends obtained in the results of first set of experiments, in terms of the significant influence of heated spot length on the surface roughness. However, with a 3-level setting and a full-factorial design (due to a well-defined design space), the influence of heating time was also found to have a significant influence on the measured maximum RMS roughness value, as can be seen in 7.12. Furthermore, the main effects plot indicated an approximately linear increase in RMS surface roughness with both heating time and heating length in the configuration range considered, as can be studied through the main effects plot presented in figure 7.12b. The deviation seen in the interaction plot 1 (figure 7.12b) for the roughness value of configuration: 80mm heated length and 500ms heating time, is considered to be an outlier which can be ignored due to the method used to obtain the maximum roughness values at the nip-point. The same reason could possibly explain the minor deviation

seen in the interaction plot 2 (figure 7.12d). Hence, in both cases, it is possible that the actual maximum roughness value along the width of the specimen, might not have been measured, since only four measurements were made.

The influence of heating time was found to be significant, although the influence was not found as strong as the influence of heating length. The significance of the heating time indicates that the roughness might be influenced by the amount of time the tape nip-point spends above the T_m. This aspect shall be discussed further in chapter 8. Furthermore, the two factor interaction was found to be negligible as can be seen in the Pareto plot. This indicates that the effect of both factors can be considered relatively independent of the other.

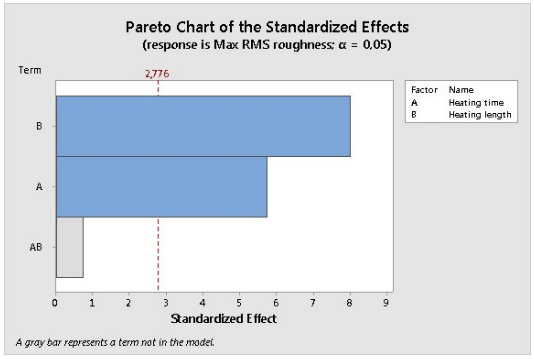

(a) Standardized Pareto plot

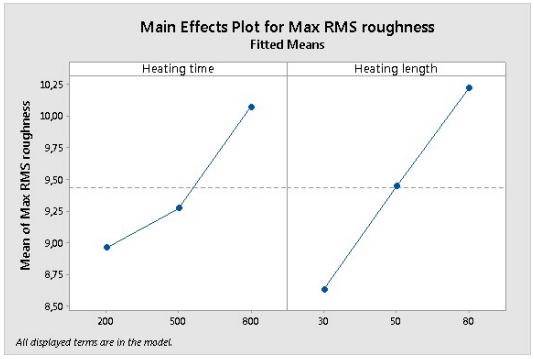

(b) Main effects plot

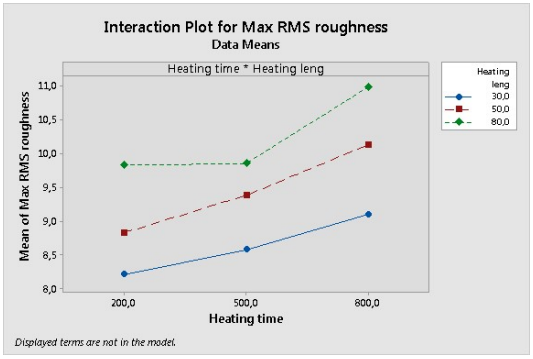

(c) Interaction plot for main effects 1

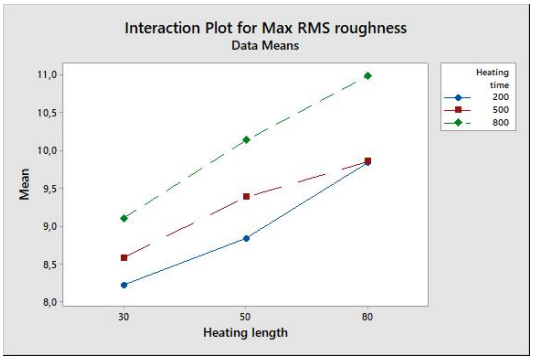

(d) Interaction plot for main effects 2

Figure 7.12: Full-factorial design: influence on surface roughness

- Width increase
  The results for width increase at the end of the laser heating phase agree with results obtained in the screening design as can be seen in figure 7.13. A linear increase in width is seen with increase in heated spot length, indicating a strong influence of boundary conditions applied on the tape nip-point in terms of the distance of the non-melted tape region from the nip-point. Furthermore, it was observed (in agreement with the first set of experiments) that the amount of width increase, is lower for a longer heating time, as seen in the main effects plot. Hence, this non-intuitive observation which was also observed in the screening design was verified and cannot be attributed to experimental error. Further discussion on the possible explanations for this observation is presented in chapter 8. The two factor interaction for width increase was observed to have a negligible effect on the material response. This indicates that the effect of both factors considered is relatively independent of the other.

- Maximum out-of-plane deformation
  The out-of-plane deformation resulting from a combination of fiber decompaction (out-of-plane) and global warpage of the tape at the nip-point was characterized. The obtained results for maximum out-of-plane deformation are presented in figure 7.11c. The statistical results are presented in figure 7.14.

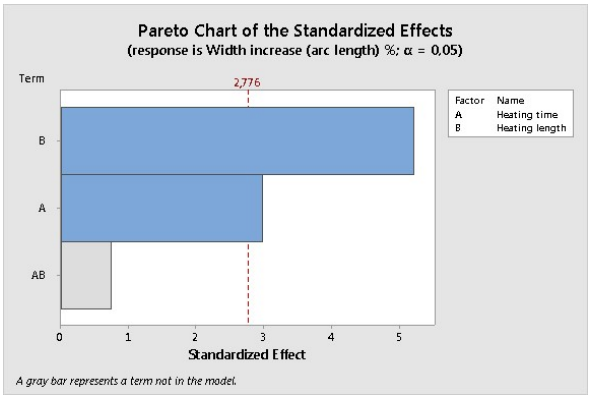

(a) Standardized Pareto plot

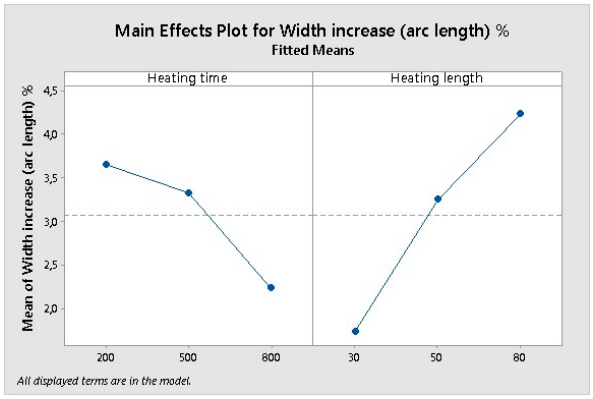

(b) Main effects plot

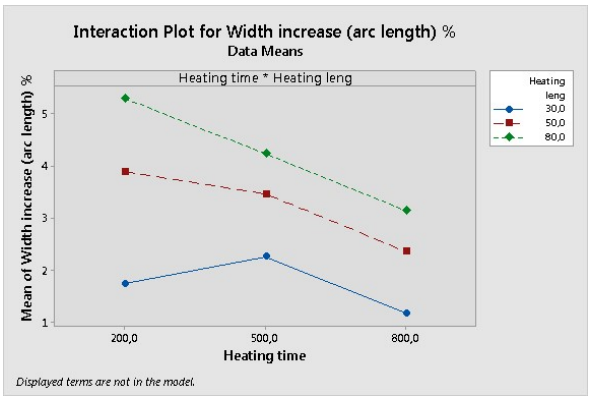

(c) Interaction plot for main effects 1

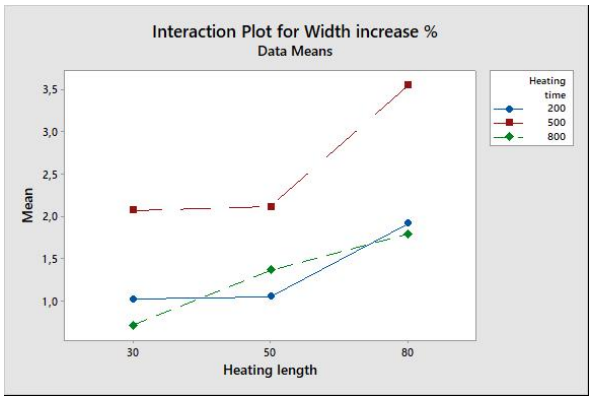

(d) Interaction plot for main effects 2

Figure 7.13: Full-factorial design: influence on width increase

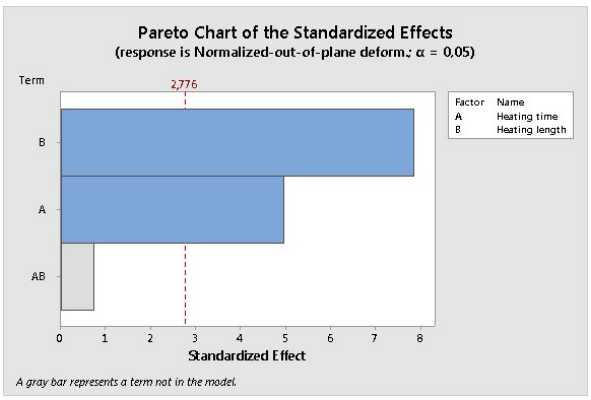

(a) Standardized Pareto plot

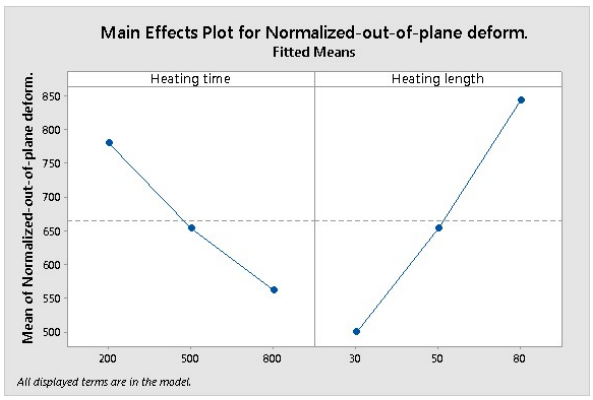

(b) Main effects plot

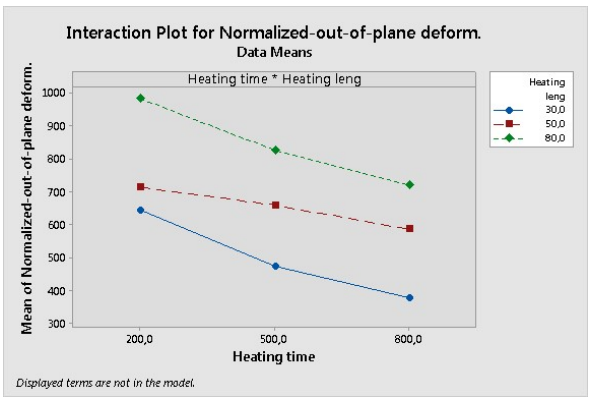

(c) Interaction plot for main effects 1

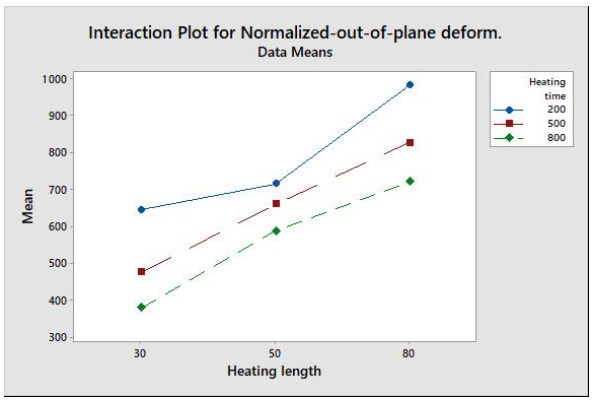

(d) Interaction plot for main effects 2

Figure 7.14: Full-factorial design: influence on out-of-plane deformation

The results confirmed one of the observations made in the screening design, that the out-of-plane deformation is higher for a longer heated spot length, while the final deformation magnitude at the end of the heating phase is lower for a longer heating time (within the configuration range considered). Furthermore, it can be observed from the interaction plots (figure 7.14c and 7.14d) that this behavior is approximately linear when both the factors are varied between the high, mid and low configurations. An interesting observation made was that heating time showed a significant influence on the out-of-plane deformation as can be seen in figure 7.14a, while it did not in the screening design. This difference is suspected to be due to a well-defined design matrix, with the three-level configuration, as this would influence the design space in which the null hypothesis is tested.

It is important to recollect that due to tape deformation, the tape temperature at the peaks in the waviness curve, is locally higher than at the valleys. This was suspected to play a role in the observed influence of the heating time. Further discussion on this aspect is presented in chapter 8. Finally, it was also observed that the two-factor interaction was low and hence it can be assumed that the influence of the two factors on the material response, is relatively independent of each other.

- Global void content
  On analyzing the void content results obtained from deconsolidated specimens, manufactured according to the three-level full-factorial design, it was observed that the heating time has a significant effect on the void content (standardized effect slightly higher than 4), whereas, heating length does not, as can be seen in figure 7.15. The significant influence of heating time was not observed in the results of the screening design. This difference is suspected to be due to the well-defined full factorial design, which alters the design space in which the null hypothesis is tested. A full-factorial design also allows for the effect of factors to be estimated at untested levels, with greater accuracy than with a P-B screening design. Furthermore, the void content was found to increase proportionally with increase in heating time, which indicates that time available for void expansion has a strong influence on the final void content. The trends observed in figure 7.15(b) are not the same for all three heating lengths, as can be seen through the variation between the curves. A possible reason for this is tied to one of the limitations of the characterization technique, i.e. it is very difficult to measure void content exactly at the nip-point. Hence, it is suspected that scatter in observed results could be a result of inaccuracies in the grinding and polishing of microscopy samples, resulting in the void content being measured at a different position of the cross-section than at the nip-point location along the length of the tape. Hence, no conclusive inferences could be made with the obtained results from the three-level design. However, the significant influence of heating time suggested that further experiments were required to understand the reasons for void content increase. Two possible explanations for the significant influence of heating time, based on experimental observations are: i) As seen in the results for out-plane-deformation, at a longer heating time, the magnitude of maximum out-of-plane deformation is lower. Furthermore, it was observed that the temperature distribution became relatively more uniform over the width at longer heating times. This indicates that the void content increase could be linked to a more uniform temperature over the width of the specimen and ii) Higher void content at the peaks of waviness curve of the specimen nip-point (corresponding to the temperature peaks) indicates that temperature at the tape surface of the tape plays an important role in determining the void content. The first observation is further analyzed in chapter 8, whereas the second observation was studied further in phase III of experiments.

  Finally, the two-factor interaction is found to be low as compared to the effect of heating time on the void content. However, the approximately equal effects of the heated spot length and the two-factor interaction, indicates that the factor B (heated spot length) was heavily confounded (both effects combined), indicating that the effect of factor B could not be observed separately.

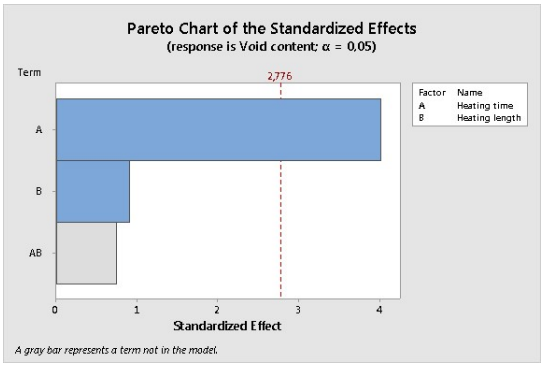

(a) Standardized Pareto plot

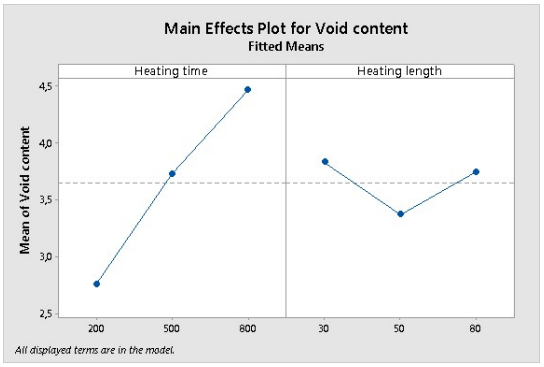

(b) Main effects plot

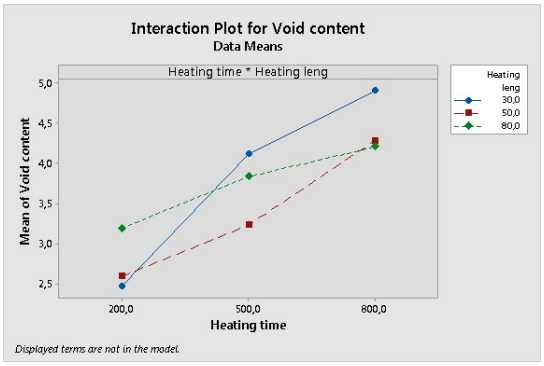

(c) Interaction plot for main effects 1

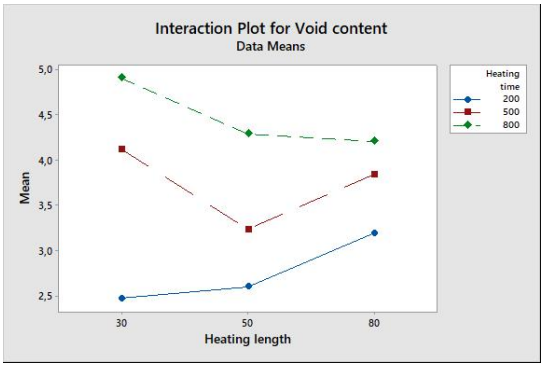

(d) Interaction plot for main effects 2

Figure 7.15: Full-factorial design: influence on void content

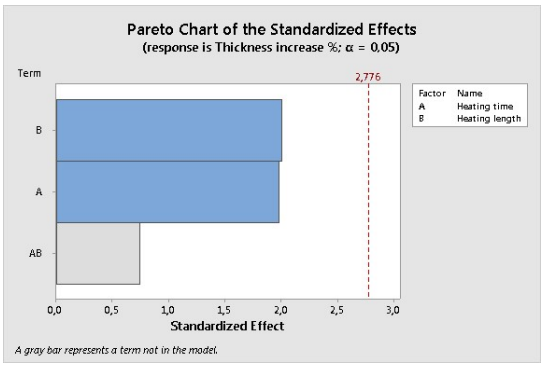

(a) Standardized Pareto plot

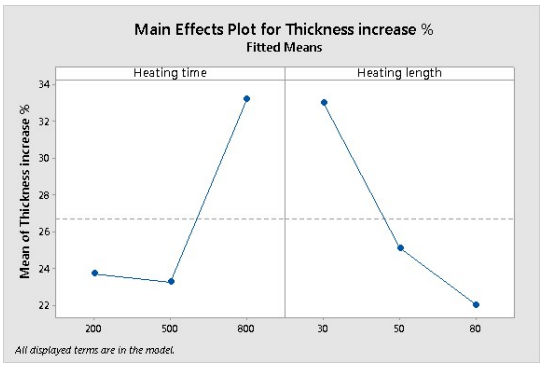

(b) Main effects plot

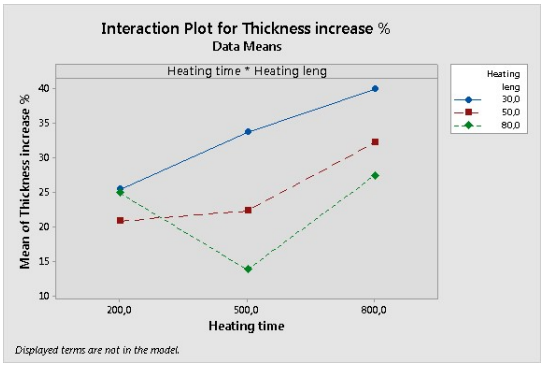

(c) Interaction plot for main effects 1

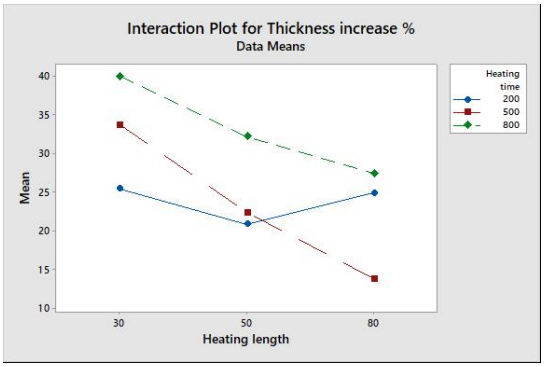

(d) Interaction plot for main effects 2

Figure 7.16: Full-factorial design: influence on global thickness increase

- Global thickness increase

  The thickness increase was characterized using the same method as explained in earlier sections. The scatter of the data as seen in figure 7.11d, is suspected to be due to the method chosen to obtain the global thickness increase, wherein four measurements were made along the width at the nip-point location and the average thickness increase was determined. Hence, due to the big variation in thickness values over the width of the tape at the nip-point, it is important to acknowledge that these results may be inconclusive. The statistical results presented in figure 7.16 indicates that similar to earlier results obtained in the screening design, the two factors do not have a significant influence.

  However, it is interesting to note that the material response for both sets of results suggest that both factors have an approximately equal effect. Furthermore, the data suggests that for a shorter heated spot lengths, the global width increase is higher as compared to that for longer heated spot length. This is found to be counter-intuitive as the a longer heated spot length was expected to increase the amount of out-of-plane fiber decompaction on the heated surface of the tape. Another interesting observation made in the main effects plot (figure 7.16a that with a longer heating time, the amount of thickness increase is higher as compared to shorter heating times. This confirmed the previous observation that void content increase (and hence thickness increase) is influenced by the amount of time the tape undergoes heating and remains above the T_m of the polymer. Hence a clear indication between thickness increase and void content increase could be observed. Further analysis of these observations is done in later sections.

  Finally, the low effect of the two-factor interaction suggests that the response of both effects was relatively independent of each other.

7.2.3. Discussion

Due to the higher resolution of the full-factorial design and three-level configuration settings, a lot of information was gained over phase I of the experiments. From the obtained results, verification of trends observed in the screening design was done, linearity of the measured response variables as a function of the factors was studied and two-factor interaction were considered in the design.

The following main observations were made in phase II of experiments that are useful in understanding the deconsolidation phenomenon:

1. The roughness development results confirmed that the heated spot length at the nip-point greatly influences the final roughness after deconsolidation. This was interpreted as an indication that the boundary conditions applied on the nip-point (in terms of the length of melted tape section adjacent to the nip-point) highly influences the amount of fiber decompaction. This further influences the surface roughness due to the resultant fiber-rich top surface.
2. The observation that amount of increase in width, is higher for a shorter heating time as compared to longer heating time, was found to be counter-intuitive. It is important to acknowledge that the reported width increase is due to a combination of thermal expansion in the direction transverse to the fibers as well as thermal deconsolidation effects in the microstructure of the tape specimens. Further analysis of width increase by taking into account the other factor chosen to be studied (temperature variation) is required before drawing conclusions.
3. The relatively low 2-factor interaction effect for all of the characterized responses, suggests that the influence of both heating time and heated spot length is relatively independent and very minor confounding of the effects takes place. This is a important result as it verifies the trends observed in the screening design, where interaction effects could not be studied due to lower design resolution. The almost equal effects of heated spot length and two-factor interaction in the response for void content, indicates that the influence of heated spot length is heavily confounded in the results and the individual influence on the spot length cannot be isolated from the obtained results. This could be due to scatter in results because of experimental limitation or could be due to heated spot length indeed not having a strong influence on the void content. However, further analysis of the material response in terms of void content and thickness increase is required to make further conclusions.
4. Additional information was gained about the linearity of the measured material responses by implementing a 3-level design. It can be seen that for surface roughness increase, width increase

and out-of-plane deformation, the influence of both considered parameters (heated spot length and heating time) is approximately linear (some minor deviations were observed due to unequal intervals for heated spot length). Scatter due to possible experimental error may be the reason for inconclusive results for void content increase and thickness increase. This aspect needed to be further evaluated after reviewing information obtained from phase III of experiments.

5. The observation that increase in specimen thickness is higher at longer heating times indicates that through-the-thickness void content may have a stronger influence than previously suspected. Furthermore, the inversely proportional effect of heating length on the thickness increase indicates that the influence of fiber decompaction may not be the primary driving force behind thickness increase. Hence, this directly contradicts the hypothesis made in chapter 4, that fiber decompaction out-of-plane is the primary driving force for observed thickness increase. Investigation to verify this effect was done in further experiments.

Based on the observed results of the detailed design, no common influencing factor could be identified for all of the response variables characterized in this study. It could be concluded that heated spot length and heating time both have significant influence on the deconsolidation response of the CF/PEEK tape material, in terms of surface roughness, out-of-plane deformation as well as width increase at the end of the heating phase. While, the considered factors also influence the void content and thickness of the tape specimens, their effect was not found to be statistically significant.

7.3. Phase III: Temperature variation experiments

In the first two phases of experiments, the influence of three of the five parameters to be evaluated in this study was considered i.e. heated spot length, heating time and cooling rate. Based on the results obtained from the two DoE runs, some mechanisms influencing deconsolidation in terms of surface roughness development, out-of-plane deformation and width increase could be identified which shall be discussed further in chapter 8. However, the performed experimental trials did not indicate a significant influential factor for void content increase and thickness increase. While, thickness increase is influenced by out-of-plane fiber decompaction, the influence of heated spot length (which directly influences out-of-plane decompaction of fibers) was found to be statistically insignificant. Hence, based on literature, it is suspected that void growth in the cross-section due to thermal expansion could be an explanation for void content increase. Furthermore, this idea was reinforced by the observation that in the deformed tapes, at the peaks of the waviness curve (and corresponding high temperature regions), higher void content and thickness was observed, as was seen in figure 7.7 and 7.8. This indicated that temperatures at the surface of the tape, locally influenced the amount of void content and thickness increase.

Based on this information, a set of experiments was conducted with different average temperatures at the nip-point (ranging between 150^oC and 400^oC) between different samples, in order to study the influence of temperature on the resultant thermal expansion of voids. Furthermore, the influence of different temperatures at the nip-point was also studied on the width increase, roughness development and out-of-plane deformation, in order to gain more information about the possible mechanisms that explain the results obtained in phase I and II of the experiments. in addition to gaining more information about mechanisms that govern the deconsolidation responses characterized in previous experiments, this section aims to answer the research question: *"At what temperature does the onset of thermal deconsolidation during LAFP begin?"*.

7.3.1. Test matrix

The test matrix used to manufacture specimens with deconsolidated regions is presented in table 7.4.

7.3.2. Results

The results obtained after characterization of the manufactured specimens with the different configurations as described in table 7.4 are presented in figures 7.17-7.21.

Global void content

The results for void content as a function of average nip-point temperature can be found in figure 7.17. Data for the specimen heated to 200^oC was not recorded due to sample damage during the preparation for microscopy. The void content can be seen to increase with increasing nip-point temperature,

Table 7.4: Test matrix for nip-point temperature-variation experiments

Specimen	Heated spot length (mm)	Heating time (ms)	Average nip-point temperature (^oC)
1			150
2			200
3			250
4	50	500	300
5			320
6			350
7			400

approximately linearly. It is suspected that possible reasons for the lower void content measured for the specimen heated to 250^oC could be (1) scatter in initial void content of as-received tapes or/and (2) choice of wrong cross-section along the tape length which might not have corresponded to the nip-point of interest. It is important to note that although the temperature distribution over the nip-point of the tape remains relatively constant for specimens heated to 150 ^oC (indicating that no a low amount of waviness and warpage takes place); at higher heating temperature, out-of-plane deformation of fibers takes place and the temperature distribution over the nip-point is not uniform. At higher average nip-point temperatures, this effect is exacerbated, as can be seen in the figure. Hence, the characterization was done by considering the average temperature over the width direction, while the error bars indicate the range of surface temperatures that were observed at the nip-point.

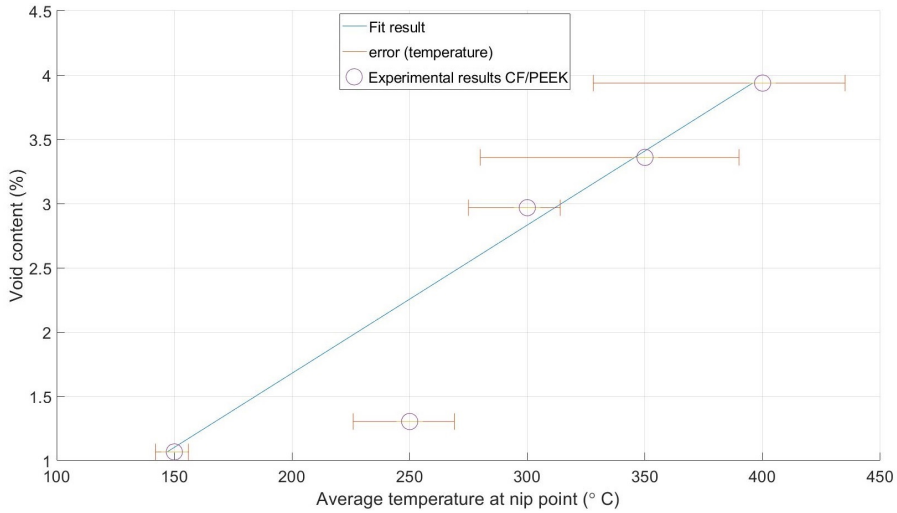

Figure 7.17: Void content as a function of varying nip-point temperatures

Global thickness increase

The results obtained from global thickness increase show that thickness shows an approximately exponential growth, with an increase in average temperature at the nip-point, as can be seen in figure 7.18. This indicates that thickness increase may be influenced by another mechanism, in addition to out-of-plane fiber decompaction, as stated in the initial hypothesis. On studying cross-sectional micrographs, such as the one presented in figure 7.7, it can be identified that the increase in thickness is due to both fiber decompaction and void content in the cross-section. It is interesting to note that the rate of thickness increase rises sharply in samples heated to temperatures above an average nip-point temperature of 300^oC. As can be seen in the sample heated to 300^oC (average), the actual range of temperatures at the nip-point does not exceed the T_m of PEEK (343^oC). Hence, although due to lack of experimental data, the exact temperature at which rapid increase in thickness takes place is not identifiable, the results indicate that this exists in the range between 300-350 ^oC. This indicates that at a nip-point temperature range above T_m, a rapid increase in thickness can be observed. The suspected reason for this behavior shall be further discussed in chapter 8.

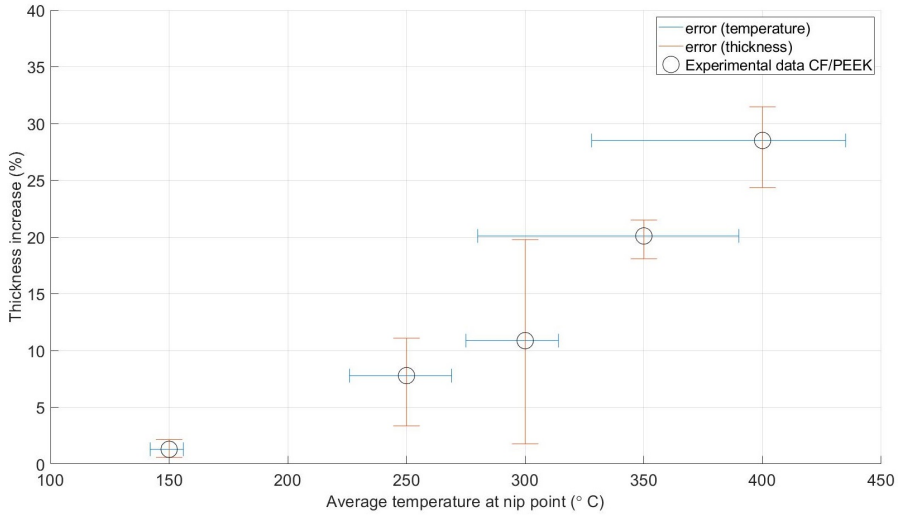

Figure 7.18: Thickness increase as a function of varying nip-point temperatures

Surface roughness

The maximum roughness on the tape surface exhibited an increase with increasing temperatures at the measured spot. It must be noted that the results reported for surface roughness values are plotted against the corresponding temperature at the location of measurement along the nip-point. Hence, the data is not plotted against the average nip-point temperature. The experimental data suggests that this increase is not linear (as can be seen in figure 7.19) and the increase in roughness values takes place at a relatively lower rate till a point in the 250-300 ^oC range, followed by a rapid increase in roughness values. Due to lack of experimental data, it cannot be clearly identified at which exact temperature the increase takes place rapidly, however, it can be deduced based on the obtained data, that it exists in the range between 250 -300^oC. A possible explanation for this may be that although some decompaction starts to occur at temperatures above the polymer T_g, a minimum temperature may be required for the polymer viscosity to reduce below a critical value which allows for rapid decompaction and hence higher surface roughness.

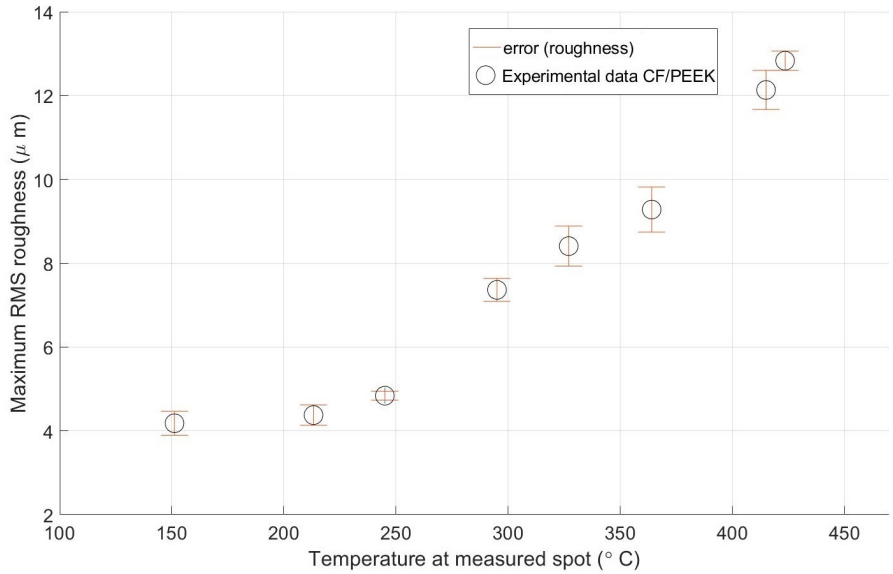

Figure 7.19: Increase in maximum RMS roughness as a function of actual temperature at the measured spot

Width increase

The width increase at the nip-point, as a function of average nip-point temperature was characterized, as can be seen in figure 7.20. It can be observed that the tape width increases approximately linearly with increase in the nip-point temperature. These results agree well with the observations made by Kok [25] that tape width increases linearly as a function of temperature. However, a major difference between the two studies is that the author measured the tape width increase after placement of the tape (post consolidation by roller) and not at the end of the heating phase (before consolidation), as done in this study. The relevance of this difference is discussed in subsequent chapters.

It was initially suspected that due to a high polymer viscosity below the melting temperature T_m, increase in width at temperatures between T_g and T_m could be dominated by the positive coefficient of thermal expansion of CF/PEEK prepreg material, in transverse direction. In order to check the validity of this theory, measurements were made with the LLS, of the tape width increase by heating tape specimens to 150^oC using the hot stage at lower heating rates than with the VCSEL laser. The measured width indicated that an increase in the range of 0.13-0.20 % increase of the tape width could be expected due to thermal expansion. However, vales obtained from the laser heating experiments suggest that the actual width increase is much higher and hence it can be deduced that thermal deconsolidation has a strong influence on the observed width increase phenomenon. Hence, these experiments provided further information about the deconsolidation response on the material, which can be used to identify the possible dominant mechanism that explain width increase due to thermal deconsolidation. However, it is important to note that the presented results indicate the total width increase (due to thermal CTE as well as thermal deconsolidation), since it was impossible to distinguish between the two during rapid laser heating. A discussion on the proposed mechanisms can be found in chapter 8.

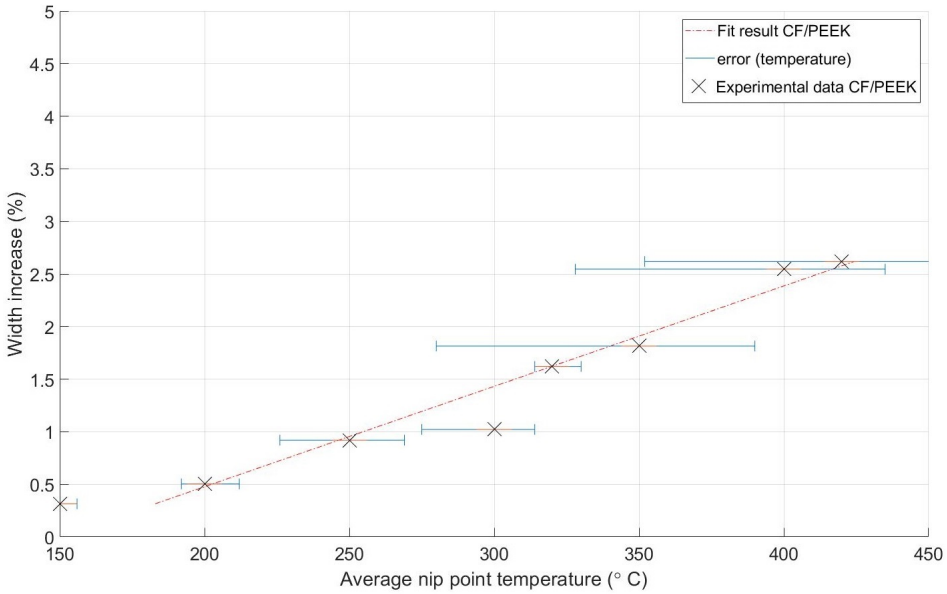

Figure 7.20: Width increase as a function of average nip-point temperature

Out-of-plane deformation

The maximum out-of-plane deformation on the tape surface was characterized for each of the specimens and the results can be seen in figure 7.21. It can be observed that the magnitude of out-of-plane deformation increases at a low rate till an average nip-point temperature in the range of 300-350^oC. Beyond this average nip-point temperature, the magnitude of deformation increases very rapidly. This is an interesting observation as it indicates that the amount of deformation is temperature dependent but it shows a non-linear response to increase in temperature. Further discussion on the relevance of these results is presented in subsequent chapters.

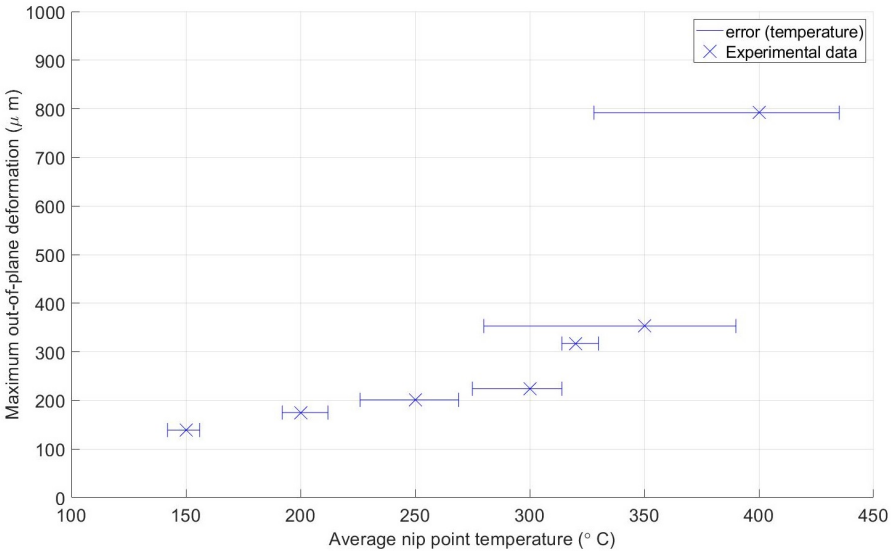

Figure 7.21: Out-of-plane deformation as a function of average nip-point temperature

7.4. Discussion and conclusion

The obtained experimental results indicate that the thermal deconsolidation response of thermoplastic prepreg tapes does not have one primary driving mechanisms and is a result of multiple mechanisms, acting simultaneously. It was identified from the DoE trials that the heated spot length and heating time have a strong influence on the fiber decompaction behavior in the out-of-plane direction, resulting in a rougher surface as well as higher out-of-plane deformation. Furthermore, an influence of varying nip-point temperature on void content, thickness increase, surface roughness, width increase and out-of-plane deformation was identified in phase III of the experiments.

It was apparent from the obtained results that the surface roughness and out-of-plane deformation of the tape heated surface are interlinked to a great degree. This is due to the fact that decompaction of fiber in the out-of-plane direction was found to influence both the properties to a large extent. This conclusion is based on the strong influence of the heated spot length on the response of the materials in terms of these effects. However, it is important to note that warpage of the tape also influences the measured out-of-plane deformation and hence the effect cannot be explained purely due to fiber decompaction. Furthermore, it was identified that the response of thickness increase of the tape material is influenced by the amount of void content in the cross-section as well as the decompacted dry fibers on the heated surface.

The higher void content in the microstructure, at regions along the tape width with higher local temperatures due to the tape waviness (as explained in previous sections), was an interesting observation made in the initial experiments. Further analysis of the effect of average nip-point temperature on the void content, confirmed that the void content is directly proportional to the temperature on the surface of the tape. This indicates that an increase in void content could be due to thermal expansion of pre-existing voids in the microstructure, in addition to the voids created due to movement of fibers.

An interesting observation made as an outcome of the experimental trials was that the width of tape specimens increase during the rapid heating phase of the LAFP process, when no external pressure is applied. This contradicts models found in literature, which explain width increase of placed tapes during LAFP, as a result of squeeze flow of melted tape matrix material due to the consolidation pressure and subsequent fiber spreading. Furthermore, the increase in width as a function of the heated spot length, heating time and heating temperature was also studied and the obtained results were used to identify possible mechanisms and changes in the tape cross section which may explain the observed results.

Experiments performed with varying nip-point temperatures indicate that at temperature just higher than the T_g, i.e. at 150^oC, some effects of thermal deconsolidation can already be seen, albeit the magnitude of these effects is very low. The increase in void content, thickness and width is particularly low, whereas a relatively large increase in surface roughness can be seen. Hence, it can be concluded that the onset of deconsolidation begins at temperatures above the glass-transition temperature, how-

ever, only the increase in surface roughness is large, probably due to slight decompaction of fibers in the out-of-plane direction. On the other hand, void increase through-the-thickness and width increase is negligible. Further discussion about all of the observations made in this chapter, can be found in chapter 8 and confirmatory experiments performed to verify the obtained results are also presented.

8

Mechanisms governing thermal deconsolidation during LAFP

In the previous chapters, the experimental approach, the characterization techniques and the obtained results were presented and the choices motivated. In this chapter, a discussion on possible governing mechanisms that explain the observed material response to rapid laser heating is provided and some hypotheses are tested. This chapter aims to answer the main research question: *"What are the main physical mechanisms that influence thermal deconsolidation in thermoplastic prepreg material?"* and all sub-questions, as proposed in chapter 4.

8.1. Main mechanisms identified

As described in previous chapters, the main material responses due to thermal deconsolidation in CF/PEEK prepreg tapes can be classified into five distinct categories. These include width increase, surface roughness increase, tape deformation (out-of-plane), void content increase as well as thickness increase. No common dominant mechanism was identified for all of these responses and hence each mechanism is discussed individually in this section. The proposed mechanisms are then justified with experimental evidence obtained during this study.

8.1.1. Decompaction of fiber-bed

1. **Initial hypothesis:** Fiber decompaction in the out-of-plane direction (possibly due to residual stresses introduced in the tape during tape manufacturing), is the main mechanism behind surface roughness development
   Further proposition: Fiber decompaction has a strong influence on out-of-plane deformation in addition to surface roughness.

   The statistically significant influence of the heated spot length on the deconsolidation response in terms of surface roughness, out-of-plane deformation, width increase as well as void content, indicates very strongly that fiber decompaction is one of the main mechanisms that influences deconsolidation in prepreg tapes during laser assisted fiber placement. This is due to the fact that a change in heated spot length, changes the boundary condition applied at the nip-point, in terms of the length of tape region that is above T_m. Furthermore, the distance of the heated section to the clamped part, where the tape specimen is restrained to the tape surface is also an important aspect, which is experimentally confirmed in section 8.2.3.

   Fiber decompaction as explained earlier is believed to occur due to release of residual fiber stresses within the tape material, which are frozen when the polymer is below glass-transition temperature (T_g). When the tape is heated to temperatures above the T_g, the fiber stresses work against the polymer viscosity in order to decompact and hence reach a lower stress state. As can be observed in the plot of surface roughness as a function of temperature (figure 7.19); as the temperature increases and polymer viscosity decreases, the fibers encounter less resistance to decompact and hence increase the surface roughness of the tape. Therefore, due to a longer

section of tape above T_m, a higher amount of fiber decompaction can be expected, as the fibers try to achieve a lower stress state. Furthermore, the experimental data suggested that the time spent by the tape above T_m had a direct influence on the RMS roughness values as observed in figure 8.1. The roughness values increase with a higher time specnt above T_m for different spot lengths.

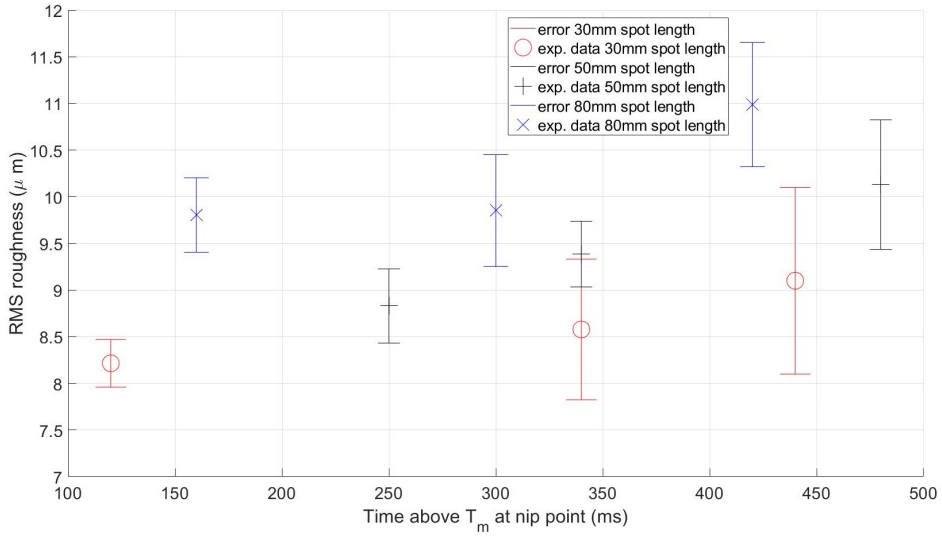

Figure 8.1: Time above T_m at tape nip-point vs RMS roughness values obtained; for different heating lengths (30mm, 50mm and 80mm)

It is also suspected that fiber decompaction is a reason for warpage in the tape and both of these physical phenomena result in out-of-plane deformation in the tape. This shall be discussed more in further sections. Hence, it can be concluded that the proposed initial hypothesis is true and it can be further extended to state that *Fiber decompaction in the out-of-plane direction, is the main driving mechanism explaining surface roughness of the deconsolidated sample and it strongly influences the magnitude of out-of-plane deformation*.

2. **Initial hypothesis:** Fiber decompaction results in void formation near the heated surface (in the microstructure)
   Further proposition: Fiber decompaction is a minor contributor to void content increase during the heating phase.
   In figure 8.2, a comparison of cross-sectional micrographs of the deconsolidated specimens heated to different average nip-point temperatures for the same heating time of 500ms is presented. In subfigures b-e, the lower surface was the one heated by the VCSEL heater. It can be seen that at nip-point temperatures lower than $T_m = 343^oC$, the dominant cause of voids in the microstructure is fiber decompaction. This can be seen as the density of voids near the heated surface are higher than in the mid-section through the thickness (indicated within white boxes). Furthermore, the average diameters of the voids near the heated surface are either close to the fiber diameter or the combined diameter of a fiber bundle adjacent to it. This indicates that when the fibers decompact, they create voids in their original position due to *traction and subsequent cavitation* in the polymer matrix. As the temperature increases and gets close to the T_m, the voids in the cross-section begin to grow and hence voids due to cavitation are no longer dominant. This can be seen in subfigures d-e where an increase in the void content is seen through-the-thickness mid section, which is clearly higher than the void content at the edges of the tape.
   The cross-sectional micrographs (figure 8.2), suggest that at nip-point temperature higher than the T_g but lower than the T_m of the polymer, void content due to fiber decompaction is dominant. However at nip-point temperatures higher than the T_m, another mechanism (thermal void growth) may play a stronger role, which shall be discussed in section 8.1.2. It is important to note that for longer heating time (800ms), the amount of voids in the middle of the through-the-thickness cross-section, as compared to the voids at the surface increase rapidly and the onset of change in

dominant mechanism is at a temperature lower than T_m, suggesting that these mechanisms are very dependent on the temperature dissipation through-the-thickness (more uniform for longer heating times). At higher nip-point temperatures, it is suspected that a higher amount of heat is dissipated through-the-thickness, resulting in growth of voids due to thermal expansion. At lower nip-point temperatures, as the heating time remains the same, lower amount of heat is dissipated through-the-thickness and hence void content is mostly located near the heated surface due to fiber decompaction. A similar phenomenon was seen to occur in specimens heated for a longer heating time, as it allows for more time for the tape to achieve more uniform through-the-thickness temperature. Hence in specimens heated for a longer time, the proportion of voids in the middle of the cross-section were found to be higher than at the surface. Furthermore, voids due to fiber decompaction resulting in traction and cavitation can be seen in more detail in figure 8.3. It is important to note that the voids due to cavitation are not clearly seen in figure 8.2 (not a sharp contrast), due to the embedding process for microscopy, wherein the resin entered the gaps between fiber bundles as well as some open voids on the viewing surface. However, the visible gaps in between decompacted fiber bundles and the tape cross-section can be considered as voids for the purpose of this study.

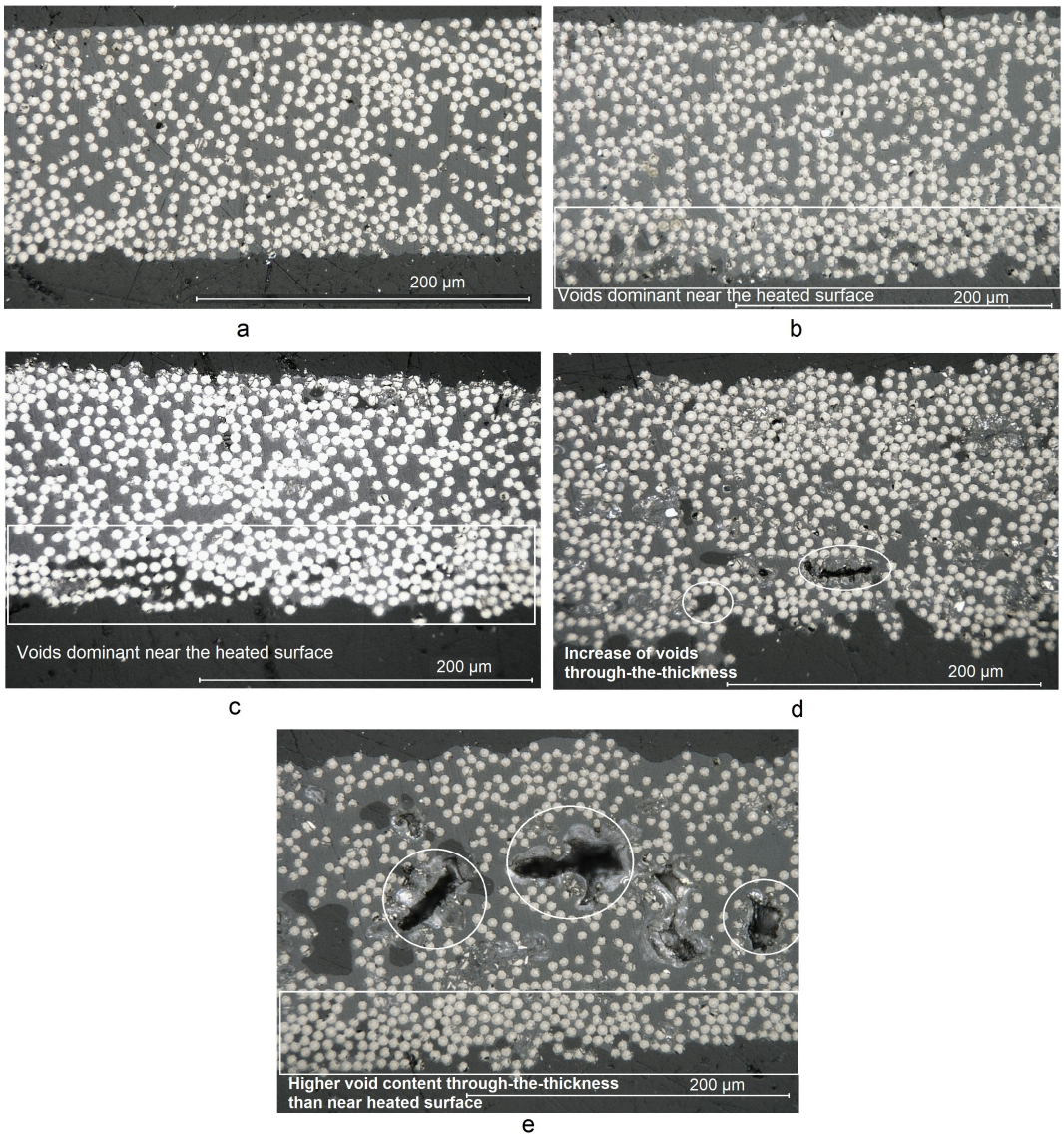

Figure 8.2: Comparison of cross-sectional micrographs of deconsolidated specimens at varying nip-point temperatures: a) ambient temperature, b) 150^oC, c) 250^oC, d) 300^oC and e) 350^oC ; heated for 500ms. The bottom surface in the subfigures b-e is the surface heated by laser

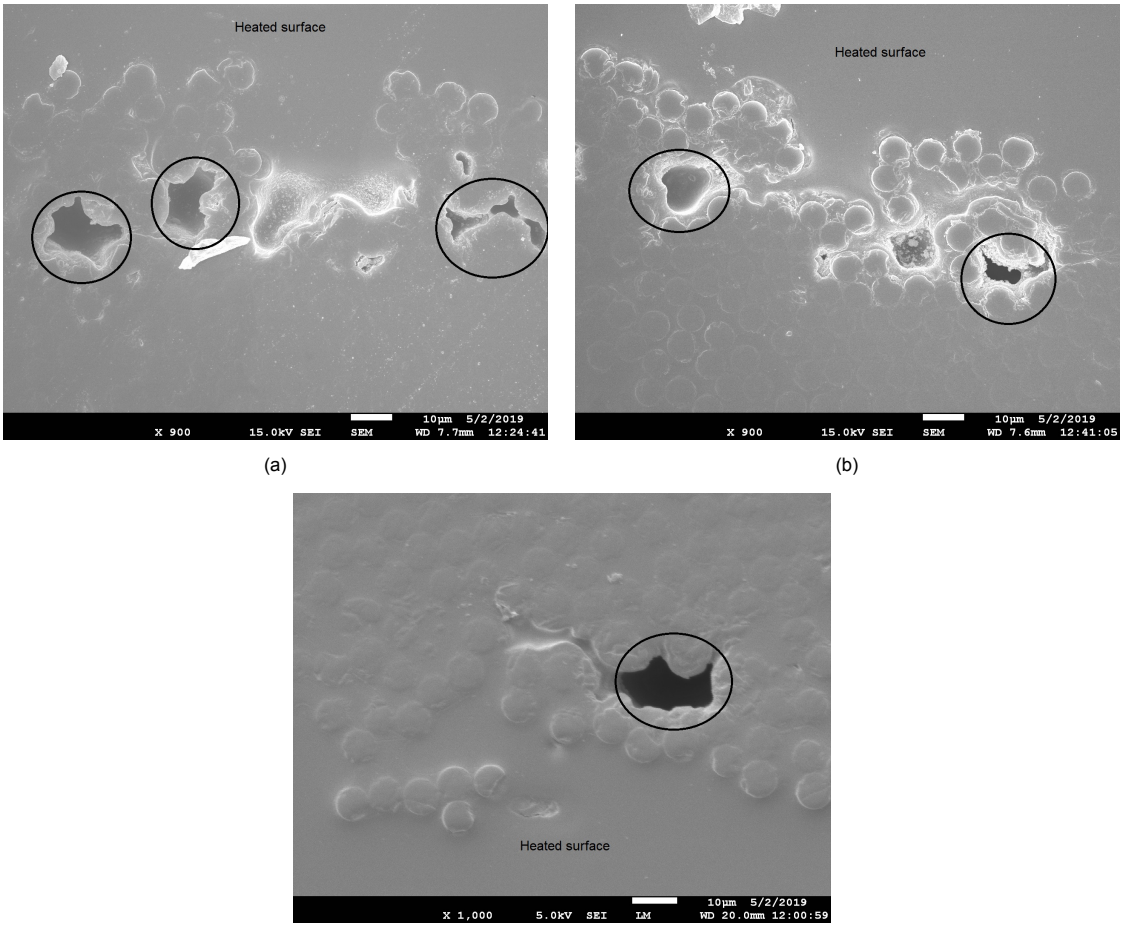

Figure 8.3: Voids due to traction and cavitation after fiber decompaction

Hence, based on the information reviewed, it can be concluded that the initial hypothesis proposed: *"Fiber decompaction results in void formation near the heated surface"* is true, however, the experimental data also indicates that the influence of fiber decompaction on the void content increase is minor at processing temperature (above T_m), while another mechanism has a stronger influence on the final void content.

8.1.2. Void thermal growth

Proposition: Increase in void content at processing temperature (above T_m and within the range of 370^oC to 400^oC) is primarily due to thermal void growth in the cross-section of the prepreg.

As explained in previous sections, the results obtained from experimental trials suggest that the void content majorly influenced by fiber decompaction at temperatures between the T_g to T_m. Due to the increase in void content, an increase in thickness is also seen. However, as the nip-point temperature approaches T_m, it was observed that there was an increase in void content (and thickness) in the middle of the cross-section. This is suspected to be due to thermal expansion of voids already present in the as-received tape, based on the observation that samples heated to higher temperature exhibited higher void content in the middle of the through-the-thickness cross-section, as compared to near the heated surface. This can be seen in figure 8.2.

The influence of heating time on the void content, as seen in chapter 7 clearly indicates that the void content is sensitive to the time the tape nip-point spends above the melting temperature T_m of the polymer (reader can refer to figure 8.4 for verification). This can be further verified by studying cross-sectional micro-graphs of specimens heated at heating time of 200ms and 800ms, as seen in figure 8.5. Furthermore, the average temperature at the nip-point also influence the void content as was observed in figure 7.17.

The reason for these observations can be attributed to the fact that since the laser heats up fibers at the tape surface (discussed in more detail in section 8.1.4), heat needs to dissipate through-the-thickness for any void growth. When the tape specimens are heated to different temperatures at the same heating time, the specimens heated to a higher temperature dissipate more heat through-the-thickness as compared to specimens heated at a lower temperature. Furthermore, with an increase in heating time, with the same average nip-point temperature, the temperature dissipation over the tape microstructure becomes more uniform, resulting in more voids due to thermal expansion.

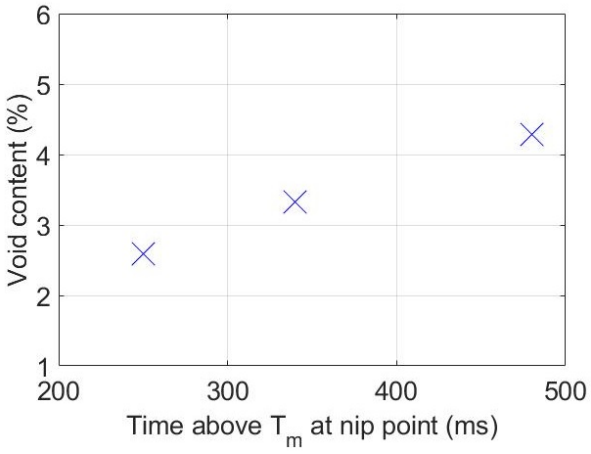

Figure 8.4: Void content at the nip-point as a function of time spent above melting temperature ($T_m = 343^oC$) for 50mm heated spot length

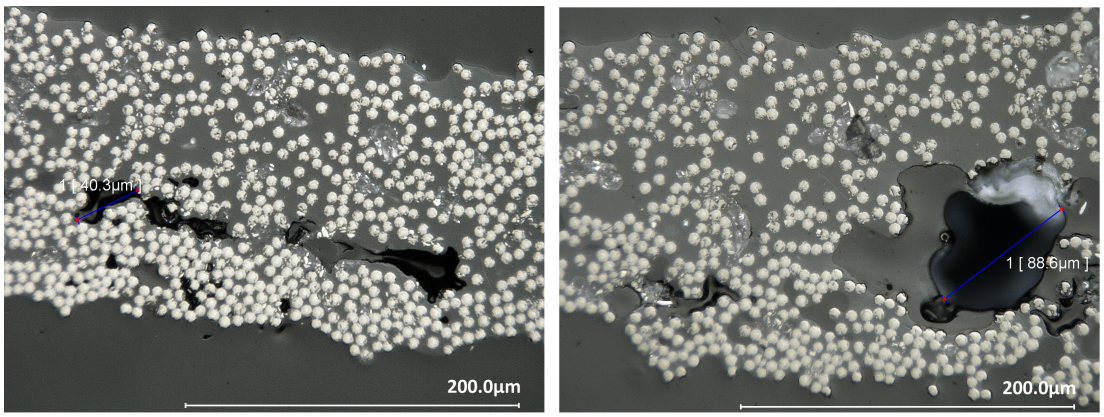

Figure 8.5: Influence of heating time on the void content. Left: smaller size voids at shorter heating time and right: larger voids at longer heating time. Suspected due to larger thermal expansion

8.1.3. Polymer matrix chain movement in melt phase and void coalescence

Since, width increase has not been reported due to thermal deconsolidation in the heating phase (before roller pressure is applied), no initial hypothesis was framed. However, based on the observed experimental results, the following explanation for width increase during rapid laser heating is proposed:

Proposition: Width increase during the heating phase occurs primarily due to polymer movement in its melt phase and is also influenced by void coalescence and fiber rearrangement (due to relaxation of tape out-of-plane deformation) during deconsolidation.

It was experimentally observed that the increase in width (% of as-received width), rises with an increase in average nip-point temperature in prepreg tape specimens, when the heated spot length and heating time remains constant. This is indicated by the plot of temperature versus width increase, as can be seen in figure 7.20. While, it must be acknowledged that a portion of width increase is due to

the positive coefficient of thermal expansion (CTE) of PEEK tapes in the direction transverse to fibers, on further analysis of this observation, it was concluded that the CTE only accounts for a minor portion of the total width increase observed. Therefore, it can be concluded that a major portion of the width increase is due to thermal deconsolidation in the prepreg tape specimens.

Zero shear viscosity of CF/PEEK and its dependence on the temperature can be used as an indication that the polymer matrix chain movement or 'flow', may be the primary driving force behind increase in width during the heating phase. It is suspected that since the tape specimens were restrained in the length direction during the heating trials, the polymer movement is seen predominantly in the width direction. The zero shear viscosity is measured at very low shear rates and indicates the viscosity of a material at rest. The zero shear viscosity and the Newtonian viscosity of PEEK and CF/PEEK composites has been found to decrease with an increase in temperature ([12, 42]), as can be seen in figures 8.6a and 8.6b, respectively. Although, the boundary conditions applied on the tape specimens in the laser heating experiments, may not the same as zero shear test conditions, the observed trend of viscosity decrease with an increase in temperature, can be used as an indication that polymer movement in the melt phase may explain the measured width increase.

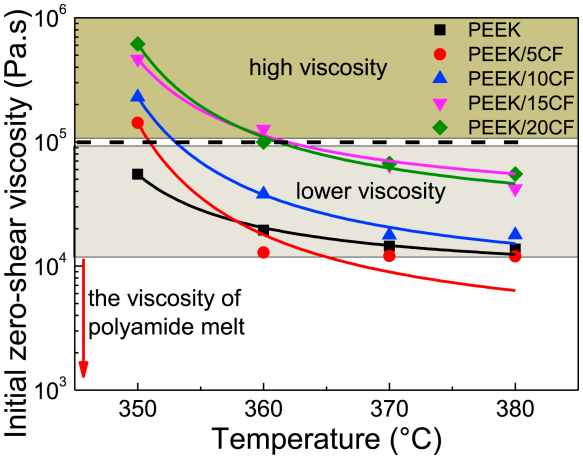

(a) Zero shear viscosity of PEEK and CF/PEEK composites vs temperature as proposed by [42]

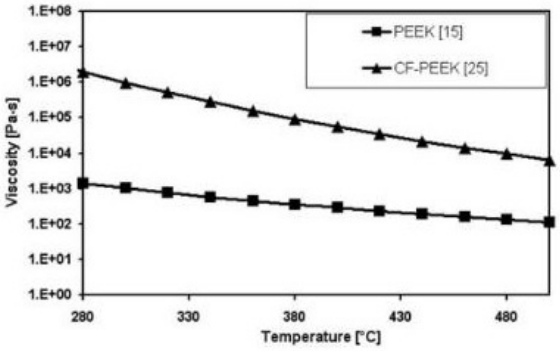

(b) Newtonian viscosity of PEEK and CF/PEEK composites vs temperature as proposed by [12]

Figure 8.6: Temperature vs viscosity for PEEK and CF/PEEK

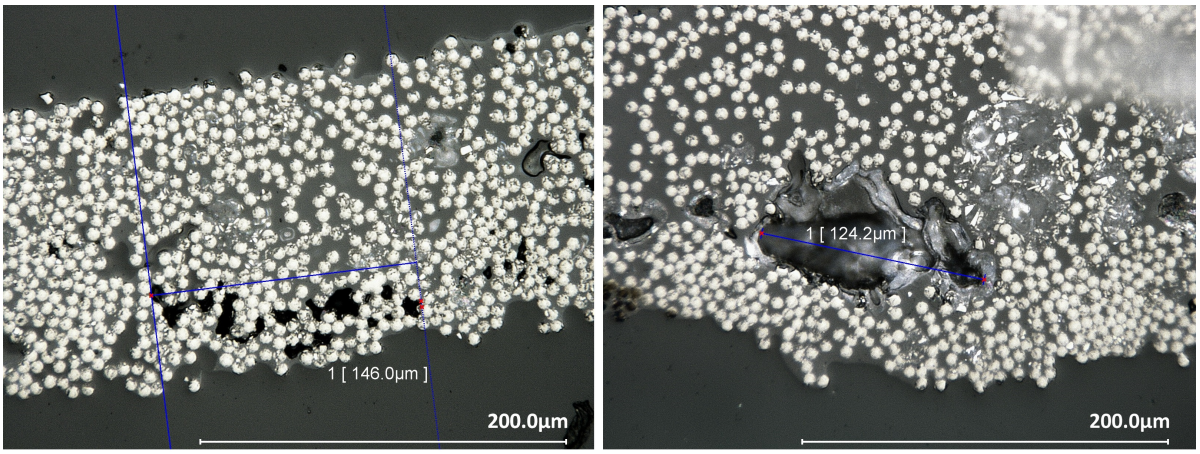

Figure 8.7: Influence of heating time on width increase: Left- multiple small voids (heating time 200ms) typically seen at shorter heating times contributing to larger width increase and Right - coalesced voids (heating time 800 ms), typically seen at higher heating times, contributing to lower overall width increase

Furthermore, while the primary mechanism describing width increase may be linked to viscosity variation and matrix movement or 'flow', some secondary forces contribute towards the observations

made regarding the width increase, in the experimental results. As pointed out in chapter 7, an interesting observation was made that the increase in width for longer heating times of the laser, resulted in lower amount of width increase as compared to specimens heated for shorter time. This can be seen in figure 7.13b. Based on this two mechanisms are suspected that may explain this observation:

- Due to the tape specimens remaining at temperature above T_m for longer heating times, small voids in the cross-section (which were identified in specimens heated for shorter heating times), coalesce together, resulting in less displacement of the tape constituents in the width direction and therefore contributing to the lower observed width increase. This phenomenon can be seen in figure 8.7. In part (a) the sample heated for 200ms exhibits more number of voids clustered together, whereas (b) exhibits typically coalesced voids in specimens with 800ms heating time.
- The magnitude of out-of-plane deformation was observed to be lower for longer heating times, as observed in chapter 7. The reason for this is discussed in the following section. However, the waviness of the tape specimen along the width (due to fiber decompaction), resulted in extension of the tape along the width. Since, the viscosity is lower at the processing temperature, less resistance to width change is posed by the polymer matrix. As the width increase was characterized as the arc length of the waviness curve of the deformed tape specimen along the width, this change in width was captured. Hence, this is suspected to be a reason why the increase in width was observed to be larger at shorter heating times. A visual representation of an un-deformed tape vs a deformed tape with a longer width can be seen in figure 8.8.

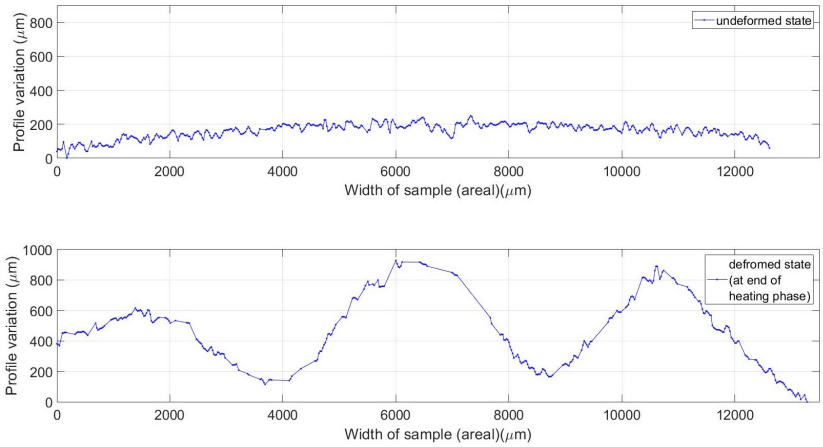

Figure 8.8: Increase in width observed in the same specimen, before and after deconsolidation (heating time 200ms - heated spot length 80mm) - captured with the LLS. Note: the observed width is the areal width and not the arc-length calculated from the waviness profile (which would be higher)

Since, the changes in the microstructure could not be monitored in-situ, due to experimental limitations, the proposition holds true for the results obtained in this study. However, it must be acknowledged that the proposed mechanism are what the experimental results indicate.

8.1.4. Warpage of tape

The deformations observed in the tape in the out-of-plane direction can be categorized into two distinct types and each takes place in two different axes: (1) waviness of the tape surface along the direction transverse to the fibers and (2) warpage of the tape surface along the length of the specimen (parallel to fiber direction). Waviness as explained earlier is caused due to fiber decompaction on the heated surface. Due to different regions of the tape along the width showing different out-of-plane deformation, the surface profile exhibits waviness. Minor variation in temperature along the length of the tape specimen (due to the variable intensity distribution of the inclined VCSEL laser) as well as variation in surface quality of the tape is identified as the reason that the waviness of surface profile along the width was different at different locations (along the length). Due to this, the tape exhibits warpage along the length during and after the heating process.

Experimental observation of waviness along the tape width (nip-point) confirms the observations in literature such as by Slange et al. [45]. According to the author ”deconsolidated AFP specimens

showed significant out-of-plane waviness". These observations by the author specifically pertained to individual fibers/fiber bundles "popping out-of-plane", hence resulting in rough and fiber-rich surfaces.

In order to investigate the source of the warpage and how it influences the temperature distribution on the surface of the tape at end of the heating phase; the temperature distribution and the surface profile was compared for all specimens during the heating phase 'in-situ'. Since, the LLS captured a lot of noise during the laser heating phase (due to reflections), the deformed state was characterized at the end of the heating phase (which also represents the nip-point state). The deformation vs temperature plot (figure 8.10), indicates that the temperature peaks corresponded exactly with the peaks of the waviness profile for all specimens. Furthermore, it was found that at the peaks of the profile waviness curve, there was a local increase in void content, surface roughness and thickness. Data for more samples can be found in appendix B for reference.

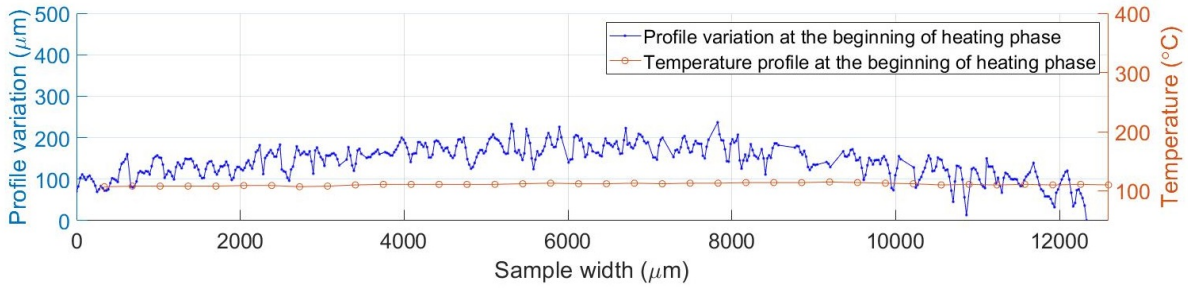

Figure 8.9: Representative comparison between surface profile and temperature distribution at the beginning of laser heating phase

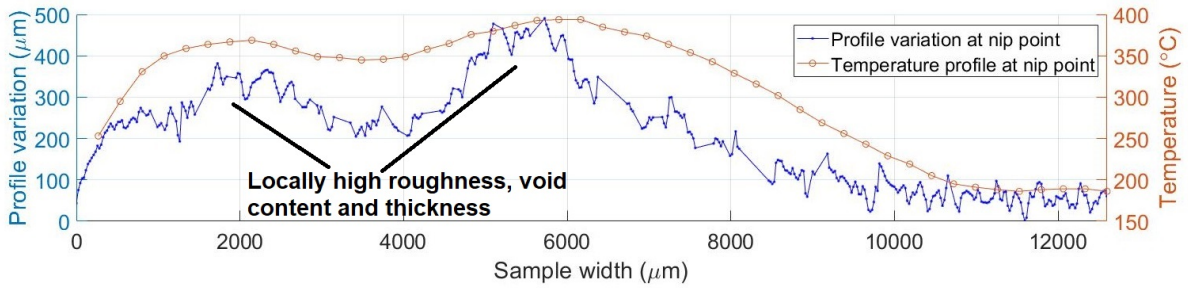

Figure 8.10: Representative comparison between surface profile and temperature distribution over nip-point of a specimen

This typical plot of deconsolidated tape surface and corresponding temperature distribution over width, indicates that the incident laser energy absorption is primarily done by the fibers, which then heat up the matrix through dissipated heat. According to Beer-Lambert's law [47], the absorption characteristics of laser irradiation in a composite material is a function of the incident laser intensity, surface reflectivity, absorption coefficient and the penetration depth. In the case of laser heating of unidirectional composite materials, the heat transfer process is mainly determined by the physical properties of the matrix and fibers. This agrees with the simulative study done by Yan et al. [46] which indicates that due to higher absorbance of fibers as compared to polymer matrix material, a temperature profile variation can be expected on the surface heated by a laser source. These results can be seen in figure 8.11. In the figure, a geometrical representation of the modeled CFRP is presented in subfigure (a), the surface temperature field distribution over the unidirectional CFRP sample is presented in subfigure (b) and the cross-sectional temperature distribution in the thickness direction is presented in subfigure (c). It is interesting to note that the temperature variation seen over the surface is much lesser than the variation observed in this study. A possible explanation for this observation is presented below.

Since, the absorption rates of fibers is higher than the matrix material [46], the incident energy is deposited on the surface of the fibers. As the fibers decompact OoP from the tape surface and move closer to the laser source, they absorb more laser energy. Furthermore, due to the decompacted fiber bundles being resin-poor, the local temperature at these location remains higher as compared to other

regions along the surface profile. Hence, it can be expected (and seen in experimental results) that as the fibers decompact during the heating process, the temperature at the peaks of the waviness curve increases higher than the other regions and this effect is exacerbated during the heating process.

It is interesting to note that in the beginning of the heating process, the temperature variation along the width of tape specimens created in this study had a small variation of 0.8% (close to the simulated variation of 0.5% reported in [46]), however, as the heating process progresses, temperature variation of up to 50% is observed along the width (figure 8.10), with a uniform laser intensity. This is very different from what is reported in [46]. The reason for this is suspected to be the rapid decompaction of fibers, exacerbating the non-uniformity of temperature field. This is not seen in the results of literature, since the authors have assumed a constant surface profile. In figure 8.11(a), it can be seen that the authors do not account for out-of-plane decompaction of fibers from the unidirectional CFRP and the model geometry stays the same during the heating process. Hence, the variation in temperature seen in figure 8.11 (b) and (c), does not show as large a variation of temperatures over the surface, as observed in this study.

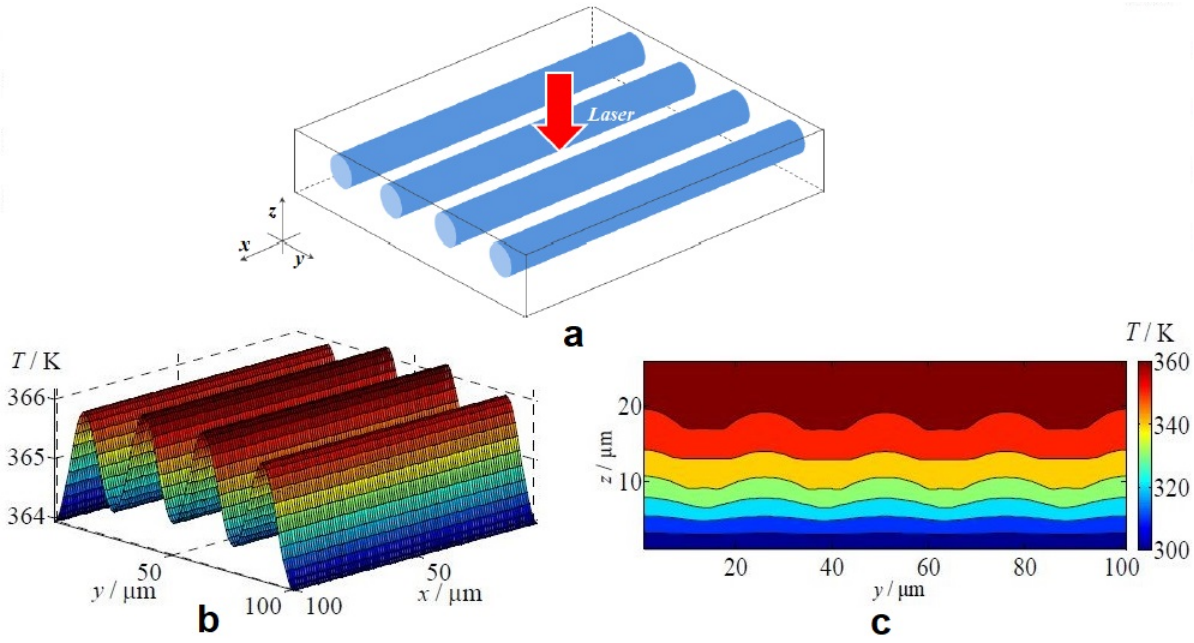

Figure 8.11: Temperature field distribution in a uni-directional CFRP composite with laser intensity of $200W/cm^2$ on the surface along the width of the sample. Modified from [46]

Proposition: The main mechanism identified and proposed, based by the experimental results is that the tape deformation in the out-of-plane direction takes place in the following order of events:

1. Heating up of fibers on the surface of the as-received tape. The fibers/fiber bundles in the regions with a locally higher roughness (due to fibers not well impregnated in matrix material), absorb more laser energy than the surrounding matrix as well as adjacent fiber bundles which are well-impregnated in matrix (less rough regions) and heat up to higher temperatures.
2. As some regions of the specimen heats up to higher temperature, the matrix material surrounding the heated fibers is heated locally through heat dissipation. This results in the onset of fiber decompaction (out-of-plane), due to release of residual stresses and lower resistance from the less-viscous polymer matrix around the fibers. Hence, some regions rise higher than others as can be seen in figure 8.10.
3. Due to the fiber decompaction: 1) the locally decompacted fibers move closer to the laser heat source and absorb relatively more energy, 2) exhibit higher temperatures due to lack of surrounding matrix material where heat may dissipate and 3) reflect away some laser irradiation from the tape surface regions present in the valley of waviness curve. Hence, the temperature peaks are seen at the peaks of the waviness curve and this further exacerbates the non-uniformity in temperature along the nip-point.

4. Due to the inclined orientation of the laser and varying distance of spots along the length of the tape to the laser source, different locations along the length have a different laser intensity applied. Hence, the waviness at different regions along the length of the tape is different (also depends on the as-received tape uniformity). Therefore, the tape exhibits warpage along the length of the fibers and a waviness in the direction transverse to the fibers. The combined effect of these mechanisms results in the tape deformation as seen in figure 6.1b and 8.22b.

Time dependent deformation: Influence of input energy

The time-resolved data of maximum out-of-plane deformation (captured using the LLS) obtained for 80mm of heated spot length and different heating times is presented in figure 8.12. All specimens were heated to a maximum temperature in the range of 400-420 ^{o}C. In the presented results, the region of the tape specimen (along the width) that exhibits the maximum deformation at the end of the heating phase was considered by averaging the data for 30 data points (in order to avoid noise in the measurement due to the LLS laser reflection). This data was plotted against temperature at the considered spot of the tape during the heating process, corresponding to the time-resolved deformation. The plot suggests that a few aspects govern the maximum deformation (averaged value of 30 data points) at the end of the heating phase in the tape specimens. The observations made based on figure 8.12 and verified with data from other specimens with the same configuration, as shown in figure B.3, are as follows:

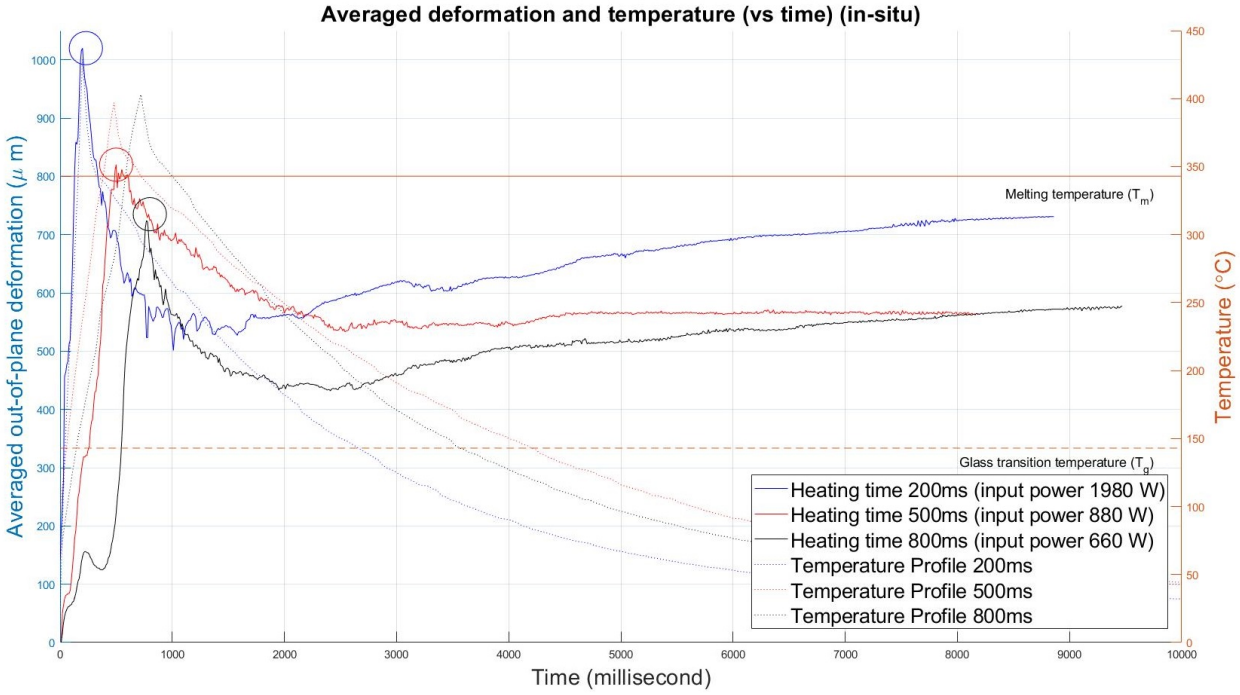

Figure 8.12: Representative time vs average deformation plot at the end of heating phase for different heating times. O marks the maximum out-of-plane deformation observed as well as the end of the heating phase (time) for each specimen

- For shorter heating times, a larger amount of input energy, results in a higher local out-of-plane deformation of the tape as well as a steeper increase in deformation with respect to time. The incident laser radiation generates heat when the energy of photons is absorbed by fibers on the tape surface. At rapid heating (200 ms) with higher input energy (1980 W) (as compared to longer heating time - 800ms, at lower input energy of 660 W), local spots in the tape are instantaneously heated to higher temperatures, whereas for lower heating times, the rate of temperature increase is lower. Hence, the magnitude of out-of-plane deformation at the nip-point and the rate of deformation is directly proportional to the amount of input energy.
- The second main observation made is the varying amounts of deformation obtained at the different heating times. The lower amount of deformation during longer heating time is suspected to be due to the fact that during a longer heating time, the input laser intensity is lower and the time available for heat dissipation from the fibers to the matrix and to the surrounding regions along

the tape width is higher. This results in a relatively more uniform temperature distribution at the end of the heating phase and hence the magnitude of deformation at the particular spot at the tape is lower.

- The steep drop in deformation corresponding to a steep drop in temperature at the end of the heating phase, indicates that the out-of-plane deformation (as captured in this study), is influenced not only by out-of-plane fiber decompaction but also the global warpage of the tape. After the heating stage ends, no further out-of-plane deformation of fibers would take place as the polymer matrix surrounding the continuous UD fibers, starts cooling down, providing higher resistance to any further movement of fibers. Furthermore, on reviewing the time resolved variations over the entire tape surface (as captured by the LLS), it can be concluded that a major contribution to the observed relaxation in figure 8.12 (for all three specimens), is due a change in warpage of the tape. As different sections of the tape cool with different cooling rates (due to some sections remaining in contact with the tool as well as variable heating along the length), the surface profile along the width continues to warp and this accounts for the drop in the measured deformation at a section of the tape width. However, due to limitations of the in-situ data from the LLS, it is difficult to conclusively state the exact reason for the observed observations, with regards to the out-of-plane deformation after the heating phase ends.
- Through-the-thickness temperature distribution is also an important aspect to consider. It is expected that the tape temperature through-the-thickness becomes more uniform with time, after the heating phase ends. As the surface temperatures remain high (above T_g) for a few seconds after the heating ends, it is suspected that further increase in thickness of the tape continues. Another aspect to consider is the changes in the tape warpage during the cooling of the tape. The combined effect of these factors is suspected to be the reasons that the tape deformation continues to rebound after the initial drop. Therefore, a combination of non-uniform temperature distribution over the length of the tape and through-the-thickness directions causes further tape deformation, after the heating phase ends, as can be seen in figure 8.12. The lower amount of rebound for the specimen heated for 500ms may be the linked to the limitation of the approach, where the section of the tape where deformation was measured, not exhibiting a thickness increase during the cooling phase.

Hence, due to a complicated test setup and measurement technique, this information must be evaluated critically and should only be used as an indication towards the reasons for the observed response of the material. Despite the experimental limitation, it is important to realize that for the LAFP process, only the deformation at the end of heating phase is relevant, since the deconsolidation state would be rapidly cooled and compacted by the roller, as soon as the heating phase ends.

8.2. Confirmatory experiments

8.2.1. Influence of polymer matrix type on deconsolidation effects

This goal of this part of the research activities, was to answer the research question: *"What is the effect of changing prepreg tape polymer type on the observed deconsolidation effects?"*

To ascertain whether similar material response to what has been observed and reported in previous chapters can be expected from carbon fiber reinforced tapes with a different polymer matrix, some confirmatory experiments were performed with CF/PEKK tapes, with as-received properties as given in tables 5.1 and 6.1. Specimens were manufactured with different average nip-point temperatures while keeping the heating time and heated spot length constant (500 ms and 50mm, respectively). The specimens were then characterized and the results compared to the results obtained for CF/PEEK tapes.

In figure 8.13, the maximum RMS surface roughness values obtained for the different tape specimens can be seen. The roughness values are plotted against the temperature at the same spot where the roughness was measured, using the IR camera data. The results show a similar behavior of both materials, suggesting that fiber decompaction is opposed by the viscous matrix, till the tape reaches a temperature in the range of 250-300 ^oC. After this critical temperature, the viscosity of the matrix is suspected to drop to sufficient levels for rapid out-of-plane movement of fiber bundles [12, 42] (proposed variation in viscosity with temperature can be seen in figures 8.6a - 8.6b). This trend can be seen for both the materials although CF/PEEK shows a steeper increase in roughness values. This difference could be attributed to variation in the polymer melt kinetics of the PEEK and PEKK material.

Furthermore, the experimental data for CF/PEKK suggests a slight shift to the right (rapid increase after a higher temperature). This could be due to higher T_g of PEKK as compared to PEEK (PEEK - $T_g = 143^oC$ and PEKK - $T_g = 159^oC$), which may delay the onset of rapid fiber decompaction.

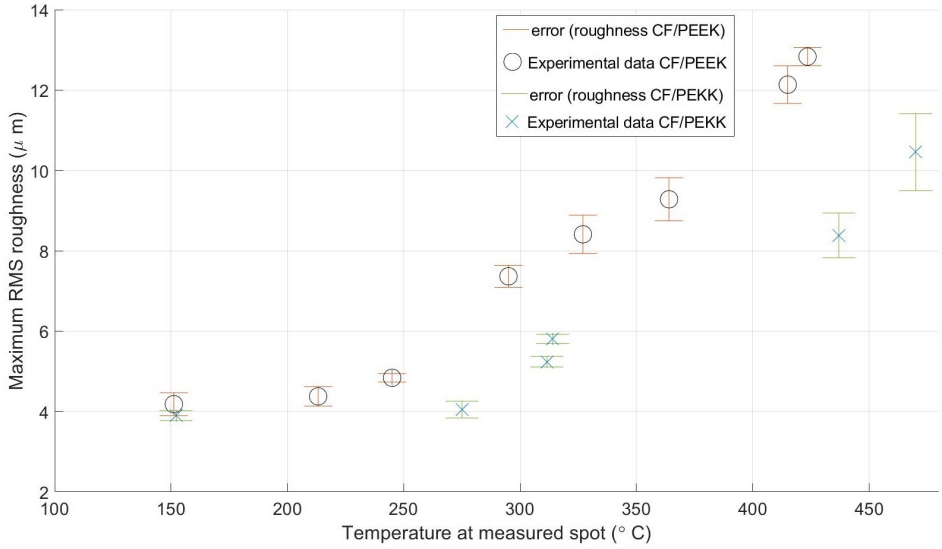

Figure 8.13: Comparison of roughness development as a function of measured temperature for different thermoplastic materials

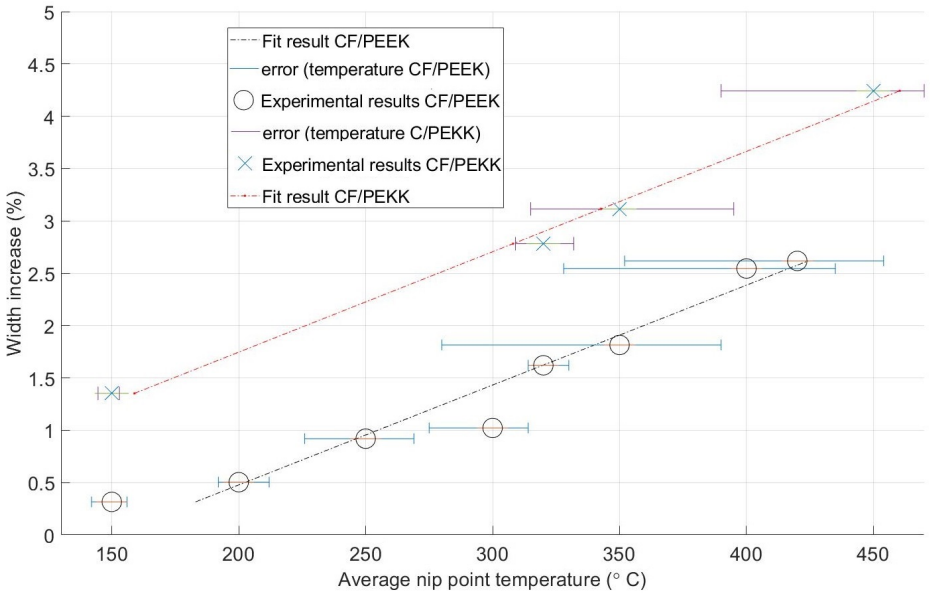

Figure 8.14: Comparison of width increase as a function of nip-point temperature for different thermoplastic materials

In figure 8.14, the experimental results for width increase of CF/PEKK and CF/PEEK tapes are plotted for comparison. It can be seen that both materials exhibit an approximately linear increase in width with an increase in temperature. As explained in earlier sections, a small ratio of the width increase takes place due to the positive coefficient of thermal expansion of the prepreg tapes in the transverse direction, while the majority of the width increase is due to thermal deconsolidation during the laser heating process. A higher width increase of 0.31% was observed due to CTE in CF/PEKK tapes (as compared to 0.12-0.2% for CF/PEEK), when they were heated to 150^oC. The variation in the percentage of width increase observed for both the materials could be due to the difference in width of the as-received tape material (12.6 mm wide CF/PEEK tapes and 6.3 mm wide CF/PEKK tapes), different as-received void content (0.71% and 0.64% for CF/PEEK and CF/PEKK respectively) as well as the

difference in amount of thermal expansion.

Similar to the width increase observed for CF/PEEK, a proportional increase in void content and thickness increase was observed for CF/PEKK tape specimens heated to different nip-point temperatures, as seen in the plots presented in figure 8.15 and 8.17. This can be also be qualitatively observed in the cross-sectional micrographs of the specimens, as can be seen in figure 8.16

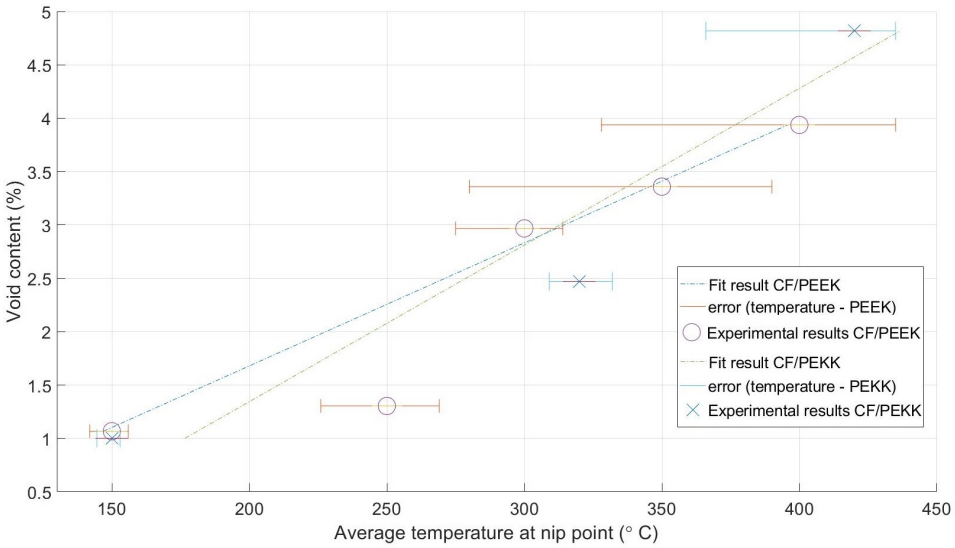

Figure 8.15: Comparison of void content as a function of temperature for different thermoplastic materials

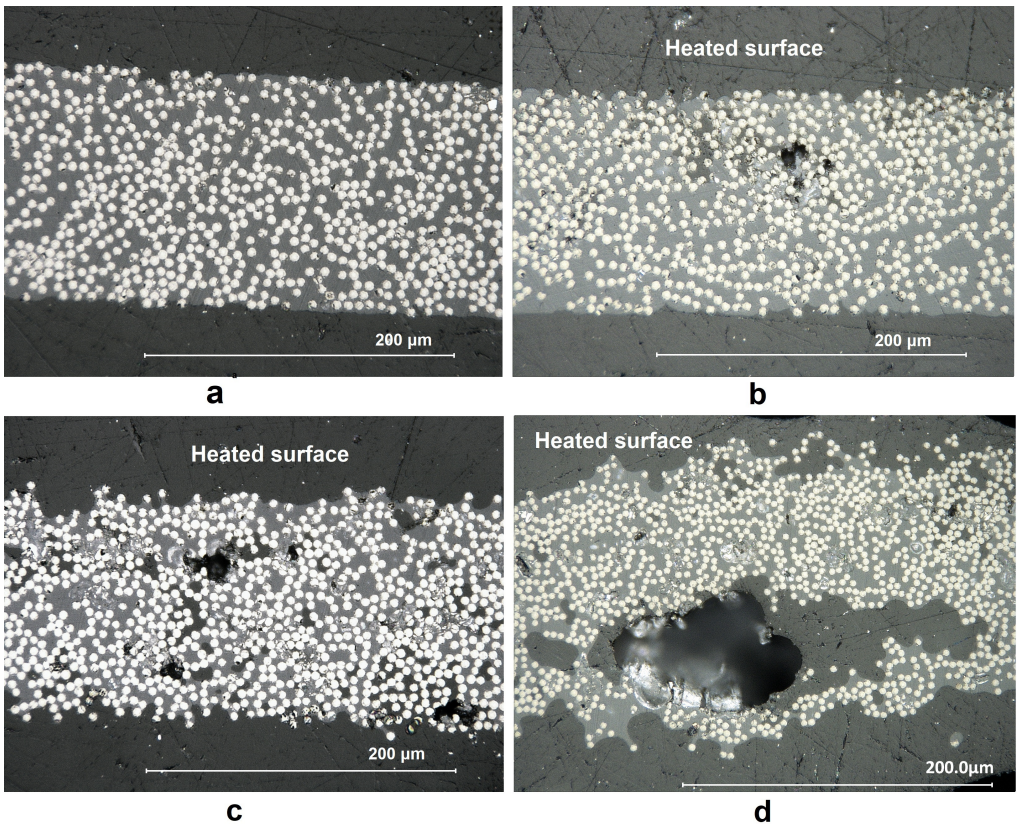

Figure 8.16: Void content at different average nip-point temperatures for CF/PEKK tapes: a - specimen at ambient temperature (as-received), b - specimen heated to $150^{o}C$, c - specimen heated to $320^{o}C$ and d - specimen heated to $420^{o}C$

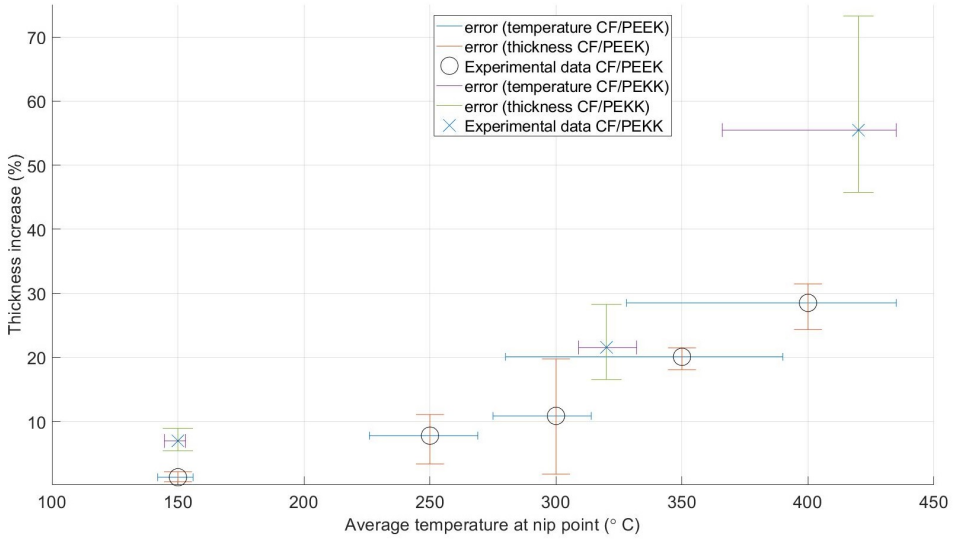

Figure 8.17: Comparison of thickness increase as a function of temperature for different thermoplastic materials

The out-of-plane deformation was also compared for both materials, as a function of temperature. Due to few data point, the temperature beyond which the increase in deformation for CF/PEKK becomes rapid, could not be identified. However, the measured material response of CF/PEKK showed a similar trend as that for CF/PEEK. Hence, it can be concluded that the rapid rise in out-of-plane deformation is linked to an increase in viscosity of the polymer matrix in the range of temperature around T_m.

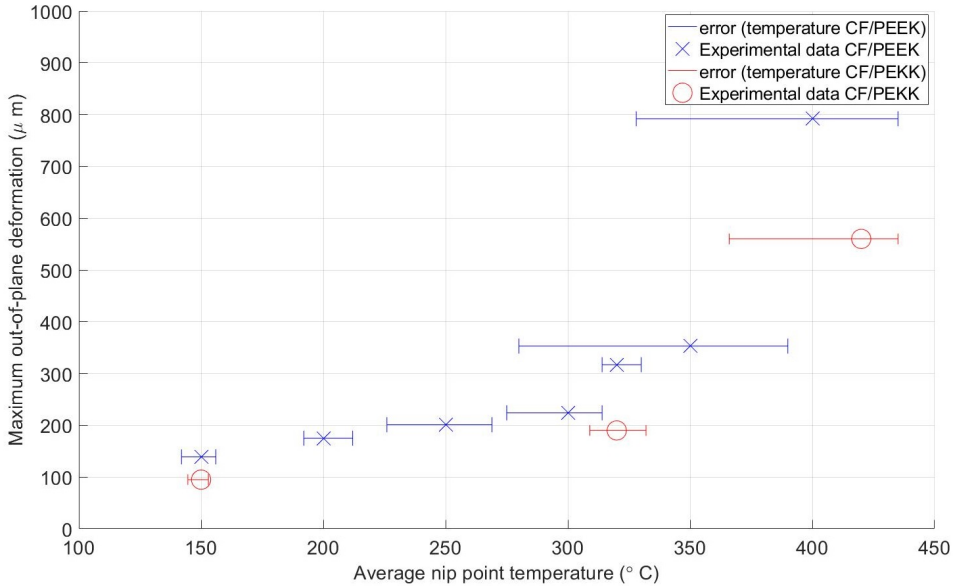

Figure 8.18: Comparison of out-of-plane deformation as a function of temperature for different thermoplastic materials

8.2.2. Influence of heating rates on fiber decompaction

The amount of fiber decompaction observed for tapes heated with rapid laser heating ($1200^oC/s$) as compared to a heating through the hot stage at considerable lower heating rates ($130^oC/min$), was much higher. Both samples were heated to a temperature of 400 ^oC and the roughness characterization was done using the LSCM. The tape warpage and waviness were qualitatively studied.

On characterizing the tape surface with the LSCM, it was observed that although the tape surface deforms due to the different CTE of prepreg material in the transverse and longitudinal directions to the fibers, almost no global waviness in the surface profile (along the width) as well as no warpage of the tape was observed. Further the roughness values obtained for both specimens indicated that

roughness is higher in the case of rapid laser heating as compared to relatively slower heating through the hot stage. The results of roughness measurements can be found in table 8.1 and figure 8.19.

The results indicate that fiber decompaction is exacerbated in the case of rapid laser heating due to the nature of energy absorption on the tape surface. Since the incident energy is mostly absorbed by the fibers on the top surface of the prepreg tapes, non uniformity in the temperature field occurs. This results in fibers to decompact in some regions of the tape, while some regions remain flat. On the other hand due to a relatively more uniform heating of the tape specimens through the hot stage, local fiber decompaction is not observed to be as exacerbated. Furthermore, while roughness values do increase, no waviness and resulting warpage is observed. Hence, this provides a possible reason why fiber decompaction is not found to be as exacerbated as what can be observed with rapid laser heating. This observation confirms findings by Slange et al. [45], that after deconsolidation of blanks through LAFP, some out-of-plane waviness was observed at the ply interfaces. The authors also reported that after deconsolidation of blanks through oven heating (at lower heating rates), a more intact ply interface was observed, which indicates that the heating rate and the mechanisms of energy absorption during the heating process, influences the amount of out-of-plane fiber decompaction.

Table 8.1: Comparison of RMS surface roughness for CF/PEEK tape specimens heated at different heating rates

Sample	As-received RMS roughness (μm)	Deconsolidated RMS roughness (μm)
Heated by hot stage	2.43 (0.26)	4.51 (0.39)
Heated by laser	2.17 (0.14)	11.21 (0.6)

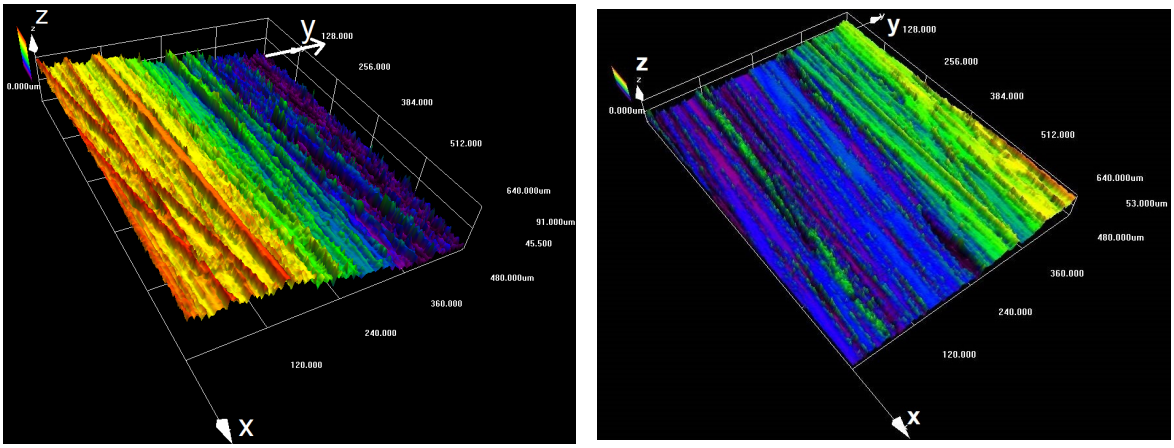

(a) Deconsolidated tape surface due to laser heating. Maximum z-axis measurement - $91\mu m$

(b) Deconsolidated tape surface due to hot stage heating. Maximum z-axis measurement - $53\mu m$

Figure 8.19: Comparison of surface roughness for CF/PEEK tape specimens heated at different heating rates

8.2.3. Influence of boundary conditions on the tape

To study the effect of tape tension and boundary conditions on the out-of-plane deformation and to verify whether warpage of the tape can be observed even in tensioned tapes in the context of LAFP, an experiment was performed. Specimens restrained to the tool surface, with only the heated region left unrestrained were created and compared with tape specimens restrained at the edges only; as can be seen in figure 8.20. The same parameters were used for both specimens; 50 mm heated spot length, 500 ms heating time and 560 W input power to achieve an average nip-point temperature of 400 ^{o}C. The specimens were then characterized to study the material response in terms of out-of-plane deformation and surface roughness. The results can be seen in figure 8.21 and table 8.2.

As can be seen in figure 8.21, the amount of warpage of tape is relatively less in the case of the more restrained tape specimen, whereas the edge-restrained specimen exhibits waviness and warpage over the heated spot. By a qualitative analysis, it can be seen that due to the restraint, fibers are not allowed to decompact out-of-plane to the same degree as in the case of restraints at the edges. The data presented in table 8.2 suggests that although the magnitude of out-of-plane deformation is almost the

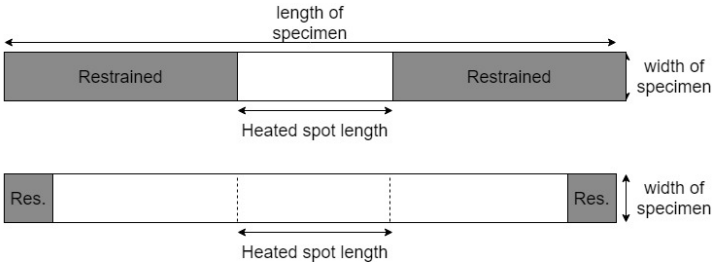

Figure 8.20: Heating setup for simulating different boundary conditions on the heated tape specimen

same for both cases, on studying the surface scans of the obtained surface profile, it can be observed that the out-of-plane deformation is mainly at the free edge of the tape. Fiber decompaction in the center of the tape surface is not prominent and the variations in the temperature profile at the nip-point were found to be much lower. Furthermore, a smaller width increase can be observed for the restrained specimen. This agrees with the proposition presented earlier, that width increase in influenced by the amount of out-of-plane fiber decompaction and the resulting fiber re-arrangement. Hence, it can be concluded that tape tension during the heating process, has an influence on the amount of surface roughness development observed as well as the width increase, since it inhibits fiber decompaction in the out-of-plane direction.

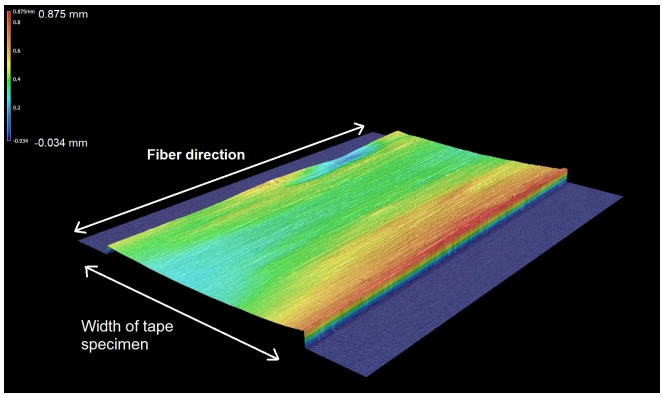

(a) Deconsolidated region restrained specimen

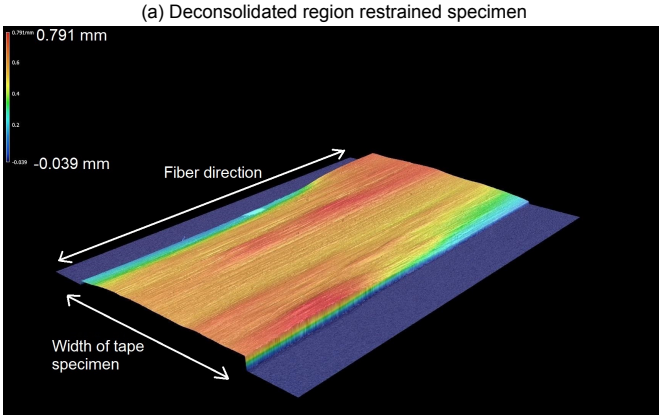

(b) Deconsolidated region edge-restrained specimen

Figure 8.21: Effect of tape boundary conditions on deconsolidation state

8.3. Discussion and Conclusion

Based on the results obtained through experimental phases I-III, as presented in chapter 7, multiple mechanisms were proposed that explain the various deconsolidation effects seen in carbon fiber reinforced thermoplastic prepreg tapes. Experimental evidence was presented to substantiate the propositions made in this chapter. These mechanisms can be classified into four main categories:

Table 8.2: Deconsolidated state characterization of restrained and un-restrained specimens

Specimen	Maximum Peak-to-valley height: waviness $W_t(\mu m)$	Maximum RMS roughness $R_q\ (\mu m)$	Width increase (%)
Restrained CF/PEEK tape	636.8	8.423 (0.4)	2.506
Edge restrained CF/PEEK tape	631.98	11.214 (0.6)	3.4679

1. Fiber decompaction in the out-of-plane direction.
   It is proposed that fiber decompaction takes place in the out-of-plane direction due to residual stresses introduced during tape manufacturing. Release of these stresses during the heating process results in a rougher surface and more out-of-plane deformation of the fibers. This indirectly causes warpage of the tape specimen and creates voids near the heated surface due to traction and cavitation due to fiber/fiber bundle movement.
2. Void thermal growth
   It is proposed that at processing temperature of the polymer (370-400 ^oC for PEEK and PEKK), the growth of voids through-the-thickness of the specimen, is primarily due to thermal expansion of air and volatile. This proposition was substantiated qualitatively and quantitatively by studying cross-sectional micrographs of the tape specimens created at different configurations. Furthermore, void growth is also suspected to contribute to thickness increase during the heating process.
3. Polymer matrix movement in the melt phase which results in width increase of the tape specimens.
   The increase in width of the prepreg tape specimens is suspected to take place primarily due to movement of polymer chains in the melt phase, during the rapid heating. Due to the boundary conditions applied on the tape (restrained in the fiber direction), the movement of polymer chains was found to be in the transverse direction resulting in width increase.
4. Warpage of the tape
   Non-uniform temperatures were observed in the direction transverse to fiber direction (along the width) as well as the along the fiber direction. The former was caused by out-of-plane fiber decompaction while the latter due to setup of the VCSEL heater. As a result, different amounts of tape waviness were observed at different locations along the fiber direction, which resulted in warpage of the tape.

In order to verify the observed material response, some confirmatory experiments were performed. The results of the confirmatory experiments are summarized as below:

1. Influence of polymer type on the observed trends
   Heating trials were conducted with CF/PEKK material in order to verify whether similar material response to thermal deconsolidation can be expected, as was observed in CF/PEKK tape specimens. The results indicate that similar trends were exhibited by deconsolidated CF/PEKK specimens, which strengthen the proposed mechanisms that provide possible explanations for the deconsolidated state of thermoplastic prepreg tapes under rapid laser heating.
2. Influence of heating rate
   It was found that the amount of fiber decompaction observed in specimens heated uniformly at lower heating rates was much less than specimens heated with rapid laser heating. Hence, it was concluded that both the rapid heating rate as well as the laser energy absorption mechanism of carbon-fiber reinforced thermoplastic tapes has a strong influence on the deconsolidation effects observed.
3. Influence of tape tension
   By performing an experiment it was identified that on tensioning tape specimens by restraining the specimen onto the tool surface, fiber decompaction in the out-of-plane direction, amount of warpage as well as the width increase observed in the tapes was much lower than specimens which were less restrained. This confirmed the proposition that decompaction of fibers is dependent on the boundary conditions applied at the nip-point. Furthermore, this indicated that the effects of thermal deconsolidation may be reduced by applying a minimum critical tension on the tapes. To determine the tension required to minimize fiber decompaction in the out-of-plane direction, further research is required.

Hence, based on the experimental investigation conducted on the phenomenon of thermal deconsolidation, information was gained on the degree to which the studied parameters influence the material response. This information was further used to identify, propose and verify possible underlying mechanisms that explain the deconsolidation process. The obtained results are significant as they helped identify the key mechanisms that take place during the rapid heating process and explain the obtained deconsolidated state. Various aspects of the tape deformation due to deconsolidation were identified, which were unreported in previous work on prepreg deconsolidation under rapid laser heating, such as the work by Kok et al. [13], Kok [25] and Slange et al. [45]. Furthermore, some of the observations made in literature, regarding the thermal deconsolidation of pre-consolidated laminates (at lower heating rates), do not hold true for deconsolidation of prepreg tapes at rapid heating rates. The main inconsistency is due to the fact that in literature it has been identified that thermal expansion of voids only accounts for a small portion of the total void increase [35], whereas in this study, it was concluded that thermal expansion plays a major role in determining the void content in the deconsolidated tape specimens.

The observed deformations and change in quality of the prepreg tapes due to rapid laser heating, makes the phenomenon very important to be taken into account when developing predictive models, as the final part quality is dependent on the state of the material before it is consolidated by a compaction roller. The non-uniformity in the temperature profile at the nip-point due to deconsolidation effects, is also a cause for concern, as it may influence the quality of interlaminar bonds during placement. Further analysis of the relevance of the obtained results is presented in chapter 9 and recommendations for further research are provided in chapter 10.

III

Conclusion and Recommendations

9

Research conclusion

In this chapter, a summary of research conclusions made, based on the information presented in the previous chapters is summarized. The influence of various process parameters was studied on the deconsolidated state of prepreg tapes and based on the obtained results, possible governing mechanisms were proposed and substantiated. Although, it has been stated in literature [45], that at rapid heating rates and at deposition speeds characteristic of LAFP process, thermal deconsolidation due to fiber decompaction may not be possible; it has been proven otherwise in this study. Even at heating times as low as 200ms, effects of fiber decompaction as well as thermal void growth were seen.

In order to create deconsolidated tape specimens with rapid laser heating, an experimental setup with the VCSEL heater was designed and implemented. Various characterization methods were identified to study the influence of varying parameters on the deconsolidated state of the material. The material characterization was done in terms of expected material responses, based on literature, as well as some previously unreported material responses, that were exhibited by deconsolidated prepreg tape specimens. Hence, five properties were characterized for each specimen: surface roughness, maximum out-of-plane deformation, width increase, void content increase and thickness increase.

Influence of studied factors on thermal deconsolidation response of material

The factors selected in the beginning of the study, whose influence was studied on the deconsolidated state of the tape specimens were: heated spot length, cooling rate, heating time, nip-point temperature and the polymer matrix type. It was found that the influence of the studied parameters varied, based on the response variable measured. From the design of experiments approach (experimental phase I and II), it was identified that the heated spot length and heating time have a strong influence on the fiber decompaction behavior in the out-of-plane direction, resulting in a rougher surface as well as a higher magnitude of out-of-plane deformation. Furthermore, an influence of varying nip-point temperature on void content, thickness increase, surface roughness, width increase and maximum out-of-plane deformation was identified.

It could be concluded from the experimental observations that surface roughness and out-of-plane deformation on the heated tape surface are interlinked and are governed by the same primary mechanism: fiber decompaction in the out-of-plane direction, due to release of residual stresses. This conclusion is based on the strong influence of heated spot length on the deconsolidation response of the material, in terms of roughness and out-of-plane deformation. As explained in previous chapters, the heated spot length influences the boundary condition applied at the nip-point, since, a larger heated spot length would increase the length of melted tape section adjacent to the nip-point. Furthermore, the response of thickness increase of the tape material is influenced by the amount of void content increase in the cross-section due to internal void pressure (due to thermal expansion), as well as due to decompacted dry fibers or fiber bundles on the heated surface.

Main mechanisms identified

The main mechanisms that describe the observed effects of thermal deconsolidation, as identified in chapter 8, are recapitulated here:

1. Fiber decompaction in the out-of-plane direction.
   It is proposed that fiber decompaction takes place in the out-of-plane direction due to residual stresses introduced during tape manufacturing. Release of these stresses during the heating process results in a rougher surface and more out-of-plane deformation of the fibers. This indirectly causes warpage of the tape specimen and creates voids near the heated surface, due to traction and cavitation of the decompacted fibers/fiber bundle.

2. Void thermal growth
   It is proposed that at processing temperatures (above the T_m of the matrix material), the growth of voids due to internal void pressure, is primarily responsible for the high void content through-the-thickness. This proposition was substantiated qualitatively and quantitatively by studying cross-sectional micrographs of the tape specimens created with different configurations. Furthermore, higher void content is also suspected to contribute towards increase in width of the tape during the heating process. Here, it is important to acknowledge that the deconsolidated state at the end of the heating phase could not be captured and the void content was characterized only after the tape cooled down to ambient temperature. However, for specimens heated for 200ms (with 30mm heated spot length), the tape remained above T_m for as little as 250ms (reader can refer figure to 8.4) and yet an increase in void content was observed. This indicates that thermal expansion of voids does take place even at very short time spent by the tape surface, above T_m.

3. Thickness increase. A hypothesis was proposed in the beginning of the study stating that: *"Fiber decompaction is the main contributor to increase in thickness of the tape specimen, at rapid heating rates, since, very less time is available for thermal expansion of voids through-the-thickness of the specimen"*. However, on reviewing the experimental data, it was identified that although the out-of-plane fiber decompaction does contribute to thickness increase, a more significant contribution is due to increase in void content after deconsolidation. Despite the short heating times, a large increase in void content was observed, contributing majorly to the observed thickness increase of the tape cross-section. This observation can be verified from qualitative analysis of cross-sectional micrographs as well as the obtained trends of the influence of heating time and heated spot length on thickness increase, as discussed in chapter 7.

4. Polymer matrix movement in the melt phase results in width increase of the tape specimens.
   The increase in width of the prepreg tape specimens is suspected to take place primarily due to movement of polymer chains in the melt phase, during the rapid heating. Due to the boundary conditions applied on the tape (restrained in the fiber direction), the movement of polymer chains was found to be in the transverse direction resulting in width increase. Furthermore, some contribution of void content in the microstructure is also expected towards width increase. It was observed that for longer heating time, void coalescence takes place which results in a lesser width increase as compared to shorter heating time.

5. Warpage of the tape
   Non-uniform temperature distribution was observed along the fiber direction as well as transverse to fiber direction. The former was caused by the setup of the VCSEL heater, while the latter due to out-of-plane fiber decompaction (and higher laser energy absorption by the decompacted fibers). Due to this, different tape waviness was observed at varying locations along the fiber direction, which resulted in warpage of the tape.

Relevance of obtained results for LAFP process

This section answers the research question: *"What is the relevance of this work in the context of the LAFP process and prepreg tape material development activities?"*. This section also evaluates the validity of the proposed hypothesis: *"The deconsolidation effect is less pronounced for shorter heating times with higher heat intensity"*.

1. The observation that width increase takes place during the rapid laser heating phase in this study, was found to be an important result for the LAFP process, as it indicates that the width increase can be expected even when no compaction pressure is applied on the tapes. A maximum width increase up to 5% of the initial tape width (0.66mm increase in width) was observed for one of the specimens at the end of the heating phase. Contrary to this, the generally reported width increase

in literature (not considering deformation due to thermal deconsolidation) after tape placement is in the range of 5-10% (approximately 1mm for a 12.5mm width tape) [28].

This is a significant observation, as it indicates that the available models that describe width increase as squeeze flow of molten matrix under consolidation pressure and the subsequent fiber spreading, are based on an inaccurate approach. Hence, they do not accurately predict deformation, as has been reported in literature. This observation about width increase during the heating phase, with no external pressure applied, has not been experimentally observed in literature and is an important aspect to consider for better process understanding.
The significance of an unaccounted-for increase in width for the placed tape was identified by Schledjewski and Schlarb [28]. The authors suggest that when tapes with drastic width fluctuations are used during ATP, gaps and overlaps may occur, which result in poor (non-uniform) pressure application on the placed tapes and eventually cavities trapped in the microstructure.

2. Due to out-of-plane fiber decompaction and the resultant waviness of the surface profile of the nip-point, it was observed that the temperature distribution at the nip-point was not uniform and a large variation in the temperature range was observed ($\pm 100^{o}C$). This is a significant observation for the LAFP process, since such temperature variations may results in some parts of the tape being at a temperature lower than the T_m or T_p, which in turn may result in poorer interply bonding.

3. The amount of fiber decompaction is related to the amount of residual fiber stresses in the microstructure and purely depends on the manufacturing process adopted by the tape manufacturer. To this end, techniques such as annealing to relieve these stresses in tapes developed for LAFP would be helpful.

4. The as-received tape roughness (due to fibers on the heated surface), influences the amount of fiber decompaction and hence the amount of tape warpage as explained in chapter 8. To avoid or to minimize warpage of the tape, two parameters that can be varied are the applied tension on the tape and the thickness of resin-rich layer on both surfaces of the tape. This forms an important aspect to be investigated further.

5. Choice of prepreg, in terms of the manufacturer (and manufacturing process), has been proven in literature to be have an influence on the observed deconsolidated state of the tape. Quality criteria for placement-grade tapes have also been defined, which produce better results ([28]). As similar trends were observed from the CF/PEEK and CF/PEKK tapes in this study, it is suspected that one possible reason for this observation, is that both tapes were made by the same manufacturer. In the work of Kok [25], it has been observed that tapes from different manufacturers show different deconsolidated state (with the same input parameters) and hence further investigation with prepreg tapes from different manufacturers, is required to verify whether the proposed mechanisms hold true in all cases. However, the presence of warpage due to fiber decompaction and subsequent non-uniform heating, is a strong indication of the fact that a tape with a different fiber matrix ratio or less fiber density at the heated surface (resin rich surface) would deform in a different fashion.

6. It was found that shorter heating time with a higher laser input intensity, resulted in lower amount of increase in surface roughness, void content and thickness at the nip-point. However, the out-of-plane deformation and the width increase were observed to be higher. Hence, the proposed hypothesis that *"the extent of thermal deconsolidation is lesser for shorter heating time (with higher input laser intensity)"*, as stated in chapter 4, cannot be objectively tested to be true or false.

7. It is not known to what extent the out-of-plane deformation of fibers during the heating process, influences the intimate contact development, since the decompacted fibers as well as the overall tape warpage would get flattened by the compaction roller. However, it is suspected that due to a rough fiber rich surface and waviness of the tape surface, full intimate contact development will be prohibited. Therefore, the obtained results indicate that deconsolidation effects might have adverse effects on the interlaminar bond development. Further experimental analysis is required to assess the influence of the different deconsolidated tape states (due to the varying parameters as investigated in this study), on intimate contact between two prepreg tapes.

10

Recommendations

The focus of this work was to investigate the phenomenon of thermal deconsolidation on thermoplastic prepreg tapes and to identify the main influencing factors. Based on this information, possible governing mechanisms were proposed. A major conclusion of this research is that the deconsolidated state of prepreg tapes due to rapid laser heating has different characteristics than the deconsolidated state of laminates due to thermal treatment at slower heating rates. Despite this observation, some common mechanisms that describe the deconsolidated state for both, were identified. This work provides an understanding of the influential factors and mechanisms that govern the material response of prepreg tapes during deconsolidation, due to rapid laser heating and can be used as a starting point for developing predictive process models.

The following main recommendations that require attention in future work, to improve the current process knowledge on thermal deconsolidation during LAFP, are proposed:

1. The influence of a heated tool surface is known to influence the quality of placed tapes in LAFP. However to the author's knowledge, a study on the influence of tool temperature, on thermal deconsolidation during LAFP, has not been conducted. Hence, an investigation on this aspect would add to the current understanding of deconsolidation effects and possible ways to minimize the effects during LAFP.

2. The characterization of microstructural changes was done after the tape specimens were heated and then allowed to cool down to ambient temperature, without the use of a rapid cooling mechanism. It was identified in this work that the tape surface may remain above T_m of the polymer for as long as 480 ms and above the T_g for as long as 3000ms, after the heating phase ends. It is suspected that during this time the tape continues to deform. Due to this limitation, it was impossible to capture the exact deconsolidated state (in terms of microstructural information) that could be expected at the nip-point of the LAFP heating phase. Hence, it is recommended that in further work on this topic, a freezing mechanism using rapid convection cooling be implemented.

3. The observed fiber decompaction in the out-of-plane direction and the resulting non-uniformity of temperature on the tape surface is a big concern for the LAFP process. This is because it was observed that in some cases the temperature variation may result in some sections along the nip-point to be below T_g of the polymer while other sections remain above the T_m (more than $\pm 100^o C$ variation). To this end, as-received tapes with thicker neat matrix layers on both surfaces, might result in lower fiber-rich top surface and hence higher interlaminar bond quality.

4. The experimental setup designed for this work, does not simulate the exact conditions that are present during LAFP. This is due to the fact that in the LAFP process, the incoming tapes are fed in by an overhead spool and the tape is heated by the laser on the lower surface. The substrate on the other hand is already consolidated in the previous run of the machine, and hence the consolidation state is different than the as-received prepreg. To verify whether similar material response can be expected from the incoming tape configuration, a modified experimental setup is required to simulate that boundary condition.

5. In this work, the 2D spatial distribution of prepreg constituents (fibers, voids and matrix) was studied qualitatively and quantitatively. Furthermore, some micro-CT scans were obtained of the deconsolidated tape section, to study the 3D spatial distribution of the tape constituents. However, the study was limited to a qualitative analysis, due to insufficient resolution capability of the available equipment. A 3D reconstruction of voids in the deconsolidated section of the specimens would provide a lot of information on the void formation mechanisms. Another important reason for obtaining 3D reconstructions to study void content is linked to the limitations of the specimen preparation method for 2D optical microscopy, wherein, due to the embedding and polishing process, it is suspected that a lot of information is lost (such as voids getting filled with resin). Hence, it is recommended that qualitative and quantitative studies of void geometry and spatial distribution be done in future work, using high-resolution micro-CT reconstructions.

6. Confirmatory experiments with CF/PEKK tapes showed similar material response to deconsolidation, as CF/PEEK tapes. However, it is suspected that the deconsolidation response of thermoplastic tapes during LAFP is sensitive to the manufacturing method adopted for the as-received prepreg, the initial quality as well as the constituent properties (such as geometry, energy absorption, viscosity etc.). A similar trend of the effects of deconsolidation on the material response was observed, due to the fact that both the materials which were tested were made by the same manufacturer. To this end, it is recommended that further investigation be conducted on the influence of a variation in tapes of different manufacturers. This in turn will help verify whether the proposed mechanisms are material specific or can be expected from all types of thermoplastic composite tapes.

7. A large scatter in void content, thickness and roughness properties was observed during this work, due to the tape deforming out-of-plane during the heating process. This made it difficult to identify trends and draw conclusions. Hence, the characterization techniques must be adapted to obtain more accurate properties of the deconsolidated sample. This recommendation is also linked to the experimental limitations of the available characterization equipment.

8. It was observed that tensioning the tape by completely restraining the non-heated section to the tool surface with Kapton tape, as explained in figure 8.20 resulted in lower amounts of fiber decompaction in the out-of-plane direction and hence lower surface roughness values. Furthermore, due to lower tape waviness at the nip-point the temperature distribution on the tape surface was found to be more uniform. This indicates that tape tensioning may be be used to minimize the degree of deconsolidation and further investigation on the optimum pre-tension force is required.

IV

Appendices

Appendix A: Infrared camera calibration

The data obtained from the calibration experiments is provided in this appendix. The calibration process was based on a modification of the ASTM E1933 standard [43], as was explained in chapter 5. In order to calibrate the IR camera for the rapid heating cycles, the emmissivity of the prepreg tape material was determined experimentally. The aim of the calibration experiment was to achieve comparable results between the thermocouple readings and the temperature readings from the infrared camera in the range of 350 - 450 ^{o}C. The tapes were heated for 500ms with the VCSEL heater.

It must be acknowledged that since the emmissivity varies as a function of temperature on the surface of the tapes (and hence the changing reflectivity), the comparison was approximate. Furthermore, it is also important to acknowledge that since the tapes deform during the heating process, some error due to changing reflectivity due to surface deformation was present. The average of the measurements from the two thermocouples was compared to the measurement of the IR camera and the experiments were repeatedthree times each. In order to match the temperature profile in the temperature range of interest, the emmissivity was varied from the default emmissivity of 0.95.

In figure A.1 and A.2, the representative calibration data for CF/PEEK and CF/PEKK tape specimens is provided.

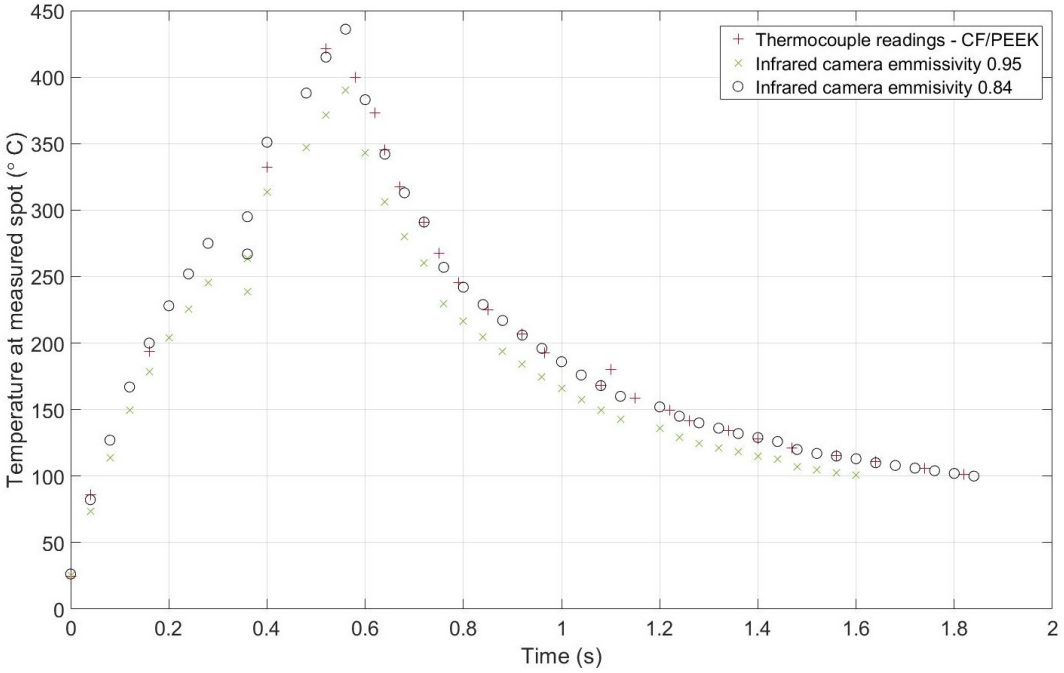

Figure A.1: Representative calibration for CF/PEEK tapes - Comparison of thermocouple readings to calibrated and un-calibrated infrared camera readings during laser heating. Camera inclination 55^{o}

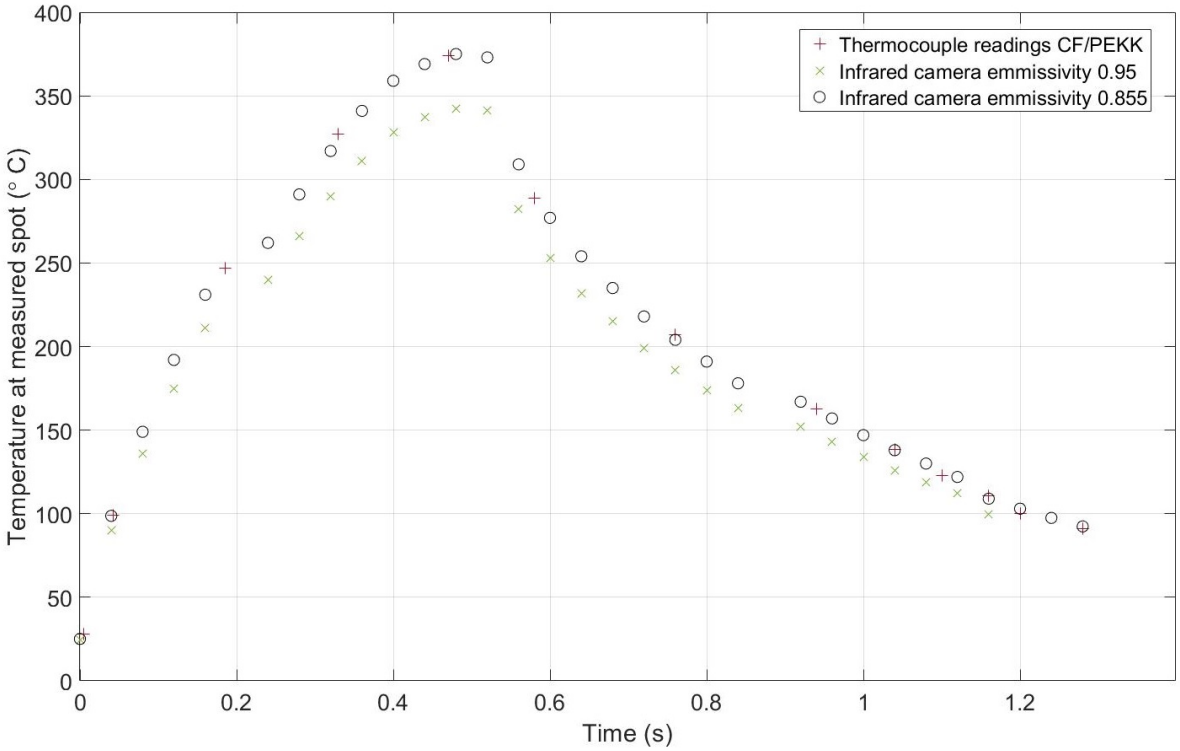

Figure A.2: Representative calibration for CF/PEKK tapes - Comparison of thermocouple readings to calibrated and un-calibrated infrared camera readings during laser heating. Camera inclination 55^o

A deviation of approximately 5^oC was observed between the calibrated IR camera readings and the thermocouple readings. This deviation is suspected to be due to two main reasons:

- The response rate of thermocouples is much lower than the IR camera measurements. Hence, the rate of change of recorded temperatures by the thermocouples was not entirely accurate. Furthermore, the sampling rate of the data acquisition system for the thermocouples did not provide data at equal intervals, as can be seen in the plots.
- Due to out-of-plane deformation during the heating phase, some error due to varying reflectivity of the tape surface was present.

However, these possible errors were acknowledged while evaluating the obtained results in this study.

B

Appendix B: DoE specimen results

Power levels for DoE specimens

Table B.1: Power levels of individual zones of VCSEL heater for DoE I

Configuration	VCSEL zones activated	Power in each zone (%)	Total input power (W)
1.1	1 - 11	30	660
1.2	7 - 9	37	222
1.3	7 - 9	100	600
1.4	7 - 9	37	222
1.5	1 - 11	90	1980
1.6	7 - 9	37	222
1.7	1 - 11	90	1980
1.8	1 - 11	30	660
1.9	1 - 11	90	1980
1.10	7 - 9	100	600
1.11	7 - 9	100	600
1.12	1 - 11	30	660

Table B.2: Power levels of individual zones of VCSEL heater for DoE II

Configuration	VCSEL zones activated	Power in each zone (%)	Total input power (W)
2.1	7 - 9	30	222
2.2	7 - 9	70	420
2.3	6 - 11	32	320
2.4	6 - 11	56	560
2.5	1 - 11	30	660
2.6	7 - 9	100	600
2.7	1 - 11	90	1980
2.8	1 - 11	40	880
2.9	6 - 11	88	880

Surface profile vs temperature at nip point: Verification data

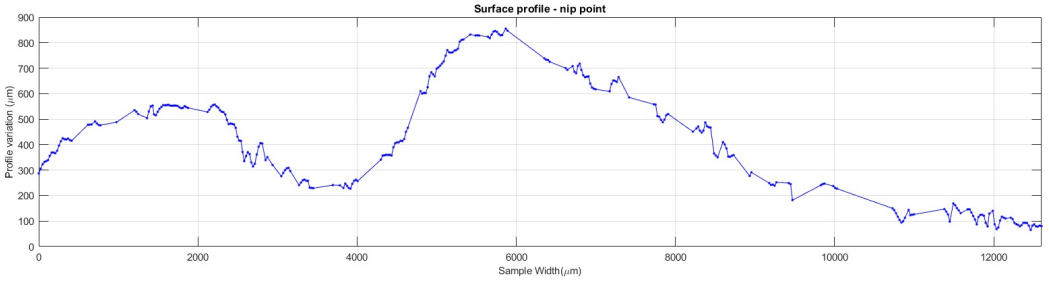

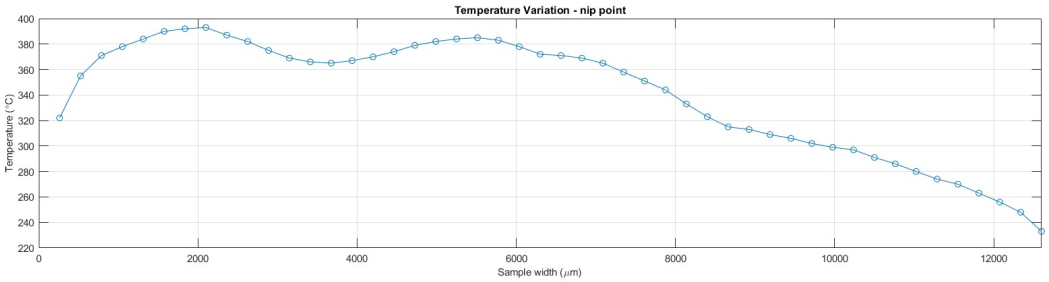

(a) Sample 1

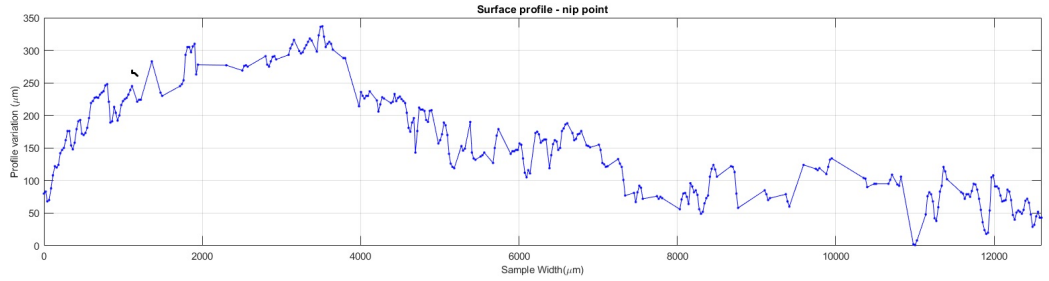

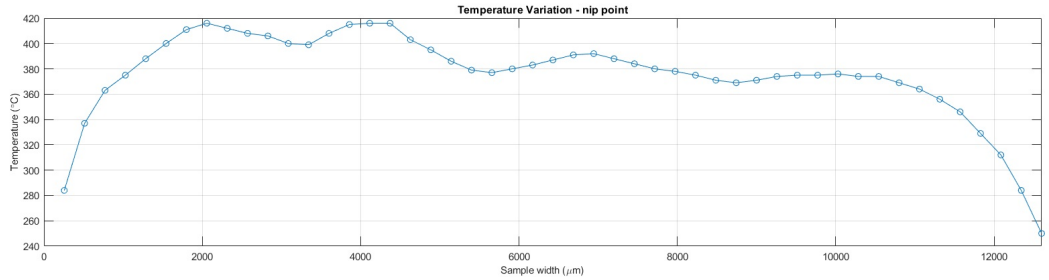

(b) Sample 2

Figure B.1: Comparision of surface profile and temperature distribution at nip point of heated tape: Verification - I

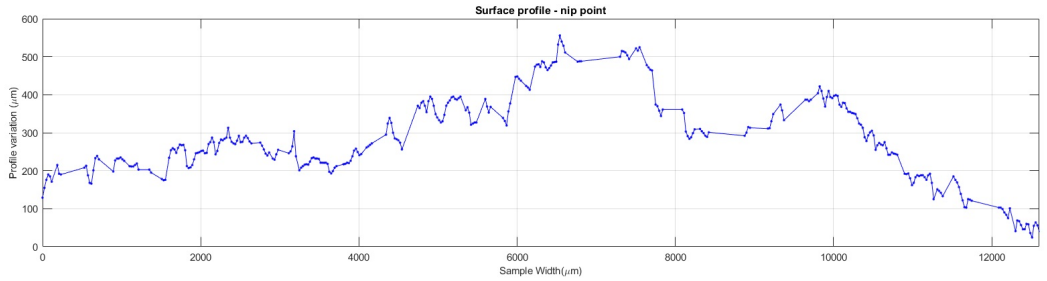

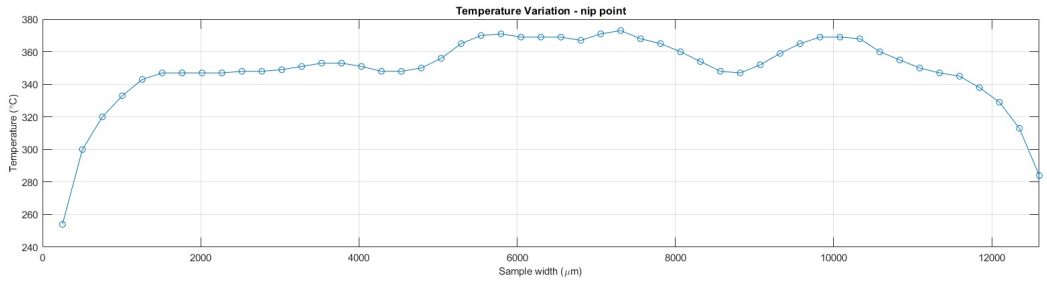

(a) Sample 3

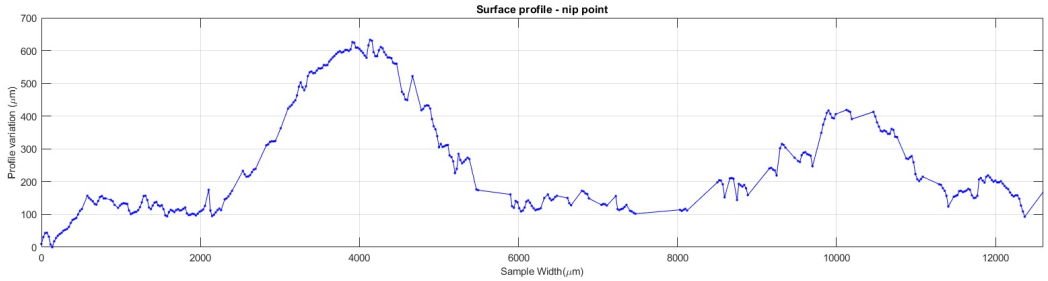

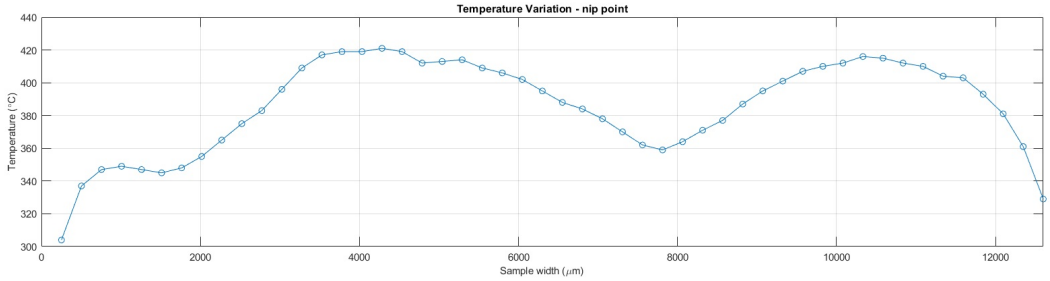

(b) Sample 4

Figure B.2: Comparision of surface profile and temperature distribution at nip point of heated tape: Verification - II

Average deformation vs time during heating phase: verification

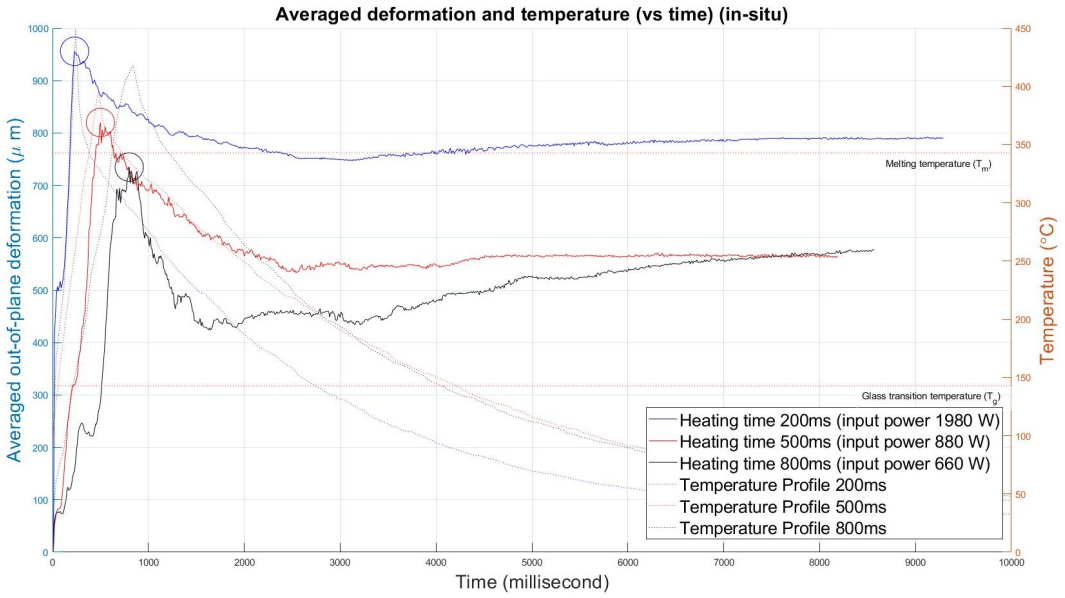

Figure B.3: Average tape out-of-plane deformation during the heating phase: verification

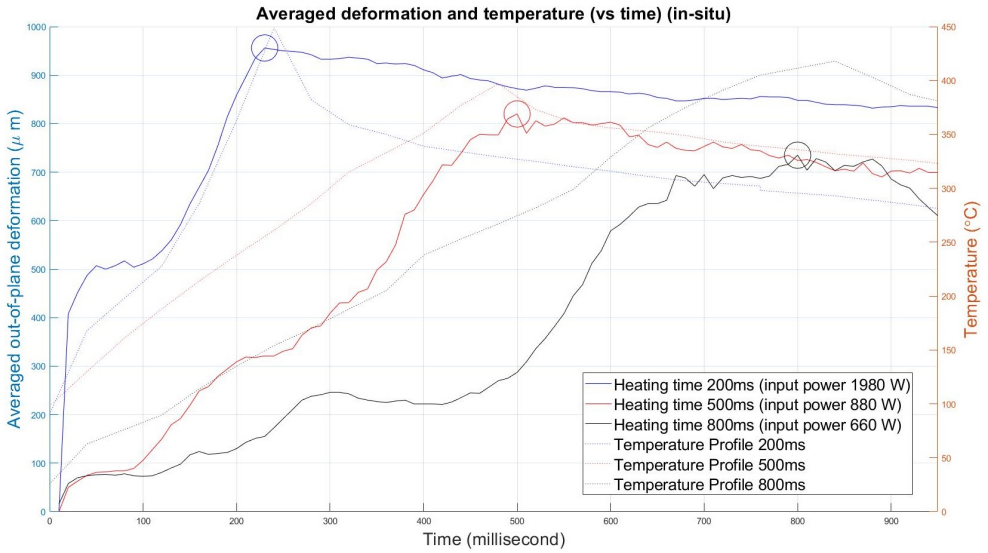

Figure B.4: Closer look at influence of temperature on out-of-plane deformation: verification

C

Appendix C: DoE specimen ANOVA

Table C.1: Recapitulation of configuration settings used in the P-B screening design. High levels are indicated by color shaded cells

Parameter	Unit	Symbol	Configuration											
			1.1	1.2	1.3	1.4	1.5	1.6	1.7	1.8	1.9	1.10	1.11	1.12
Heating time	ms	T_h	800	800	200	800	200	800	200	800	200	200	200	800
Cooling rate	$^oC/s$	R_c	184	184	184	121	121	184	184	121	184	121	121	121
Heated spot length	mm	L_s	80	30	30	30	80	30	80	80	80	30	30	80
Power input	W	-	660	222	600	222	1980	222	1980	660	1980	600	600	660

Table C.2: Recapitulation of configuration settings used in the full-factorial design. Intermediate and high levels are indicated by color shaded cells

Parameter	Unit	Symbol	Configuration								
			2.1	2.2	2.3	2.4	2.5	2.6	2.7	2.8	2.9
Heated spot length	mm	L_s	30	30	50	50	80	30	80	80	50
Heating time	ms	T_h	800	500	800	500	800	200	200	500	200
Cooling rate	^oC/s						121				
Power input	W	-	222	420	320	560	660	600	1980	880	880

Full factorial 3-level design

General Factorial Regression: Max RMS roughness ... e; Heating length

Factor Information

Factor	Levels	Values
Heating time	3	200; 500; 800
Heating length	3	30; 50; 80

Analysis of Variance

Source	DF	Adj SS	Adj MS	F-Value	P-Value
Model	4	5,7876	1,44690	40,35	0,002
Linear	4	5,7876	1,44690	40,35	0,002
Heating time	2	1,9787	0,98933	27,59	0,005
Heating length	2	3,8089	1,90446	53,11	0,001
Error	4	0,1434	0,03586		
Total	8	5,9310			

Model Summary

S	R-sq	R-sq(adj)	R-sq(pred)
0,189363	97,58%	95,16%	87,76%

Coefficients

Term	Coef	SE Coef	T-Value	P-Value	VIF
Constant	9,4346	0,0631	149,47	0,000	
Heating time					
200	-0,4752	0,0893	-5,32	0,006	1,33
500	-0,1629	0,0893	-1,82	0,142	1,33
Heating length					
30	-0,8036	0,0893	-9,00	0,001	1,33
50	0,0138	0,0893	0,15	0,885	1,33

Regression Equation

Max RMS roughness = 9,4346 - 0,4752 Heating time_200 - 0,1629 Heating time_500
+ 0,6381 Heating time_800 - 0,8036 Heating length_30
+ 0,0138 Heating length_50 + 0,7898 Heating length_80

General Factorial Regression: Normalized-out-of-plane ... ating length

Factor Information

Factor	Levels	Values
Heating time	3	200; 500; 800
Heating length	3	30; 50; 80

Analysis of Variance

Source	DF	Adj SS	Adj MS	F-Value	P-Value
Model	4	250866	62717	35,83	0,002
Linear	4	250866	62717	35,83	0,002
Heating time	2	72762	36381	20,78	0,008
Heating length	2	178105	89052	50,87	0,001
Error	4	7002	1750		
Total	8	257868			

Model Summary

S	R-sq	R-sq(adj)	R-sq(pred)
41,8383	97,28%	94,57%	86,25%

Coefficients

Term	Coef	SE Coef	T-Value	P-Value	VIF
Constant	665,6	13,9	47,72	0,000	
Heating time					
200	115,4	19,7	5,85	0,004	1,33
500	-11,6	19,7	-0,59	0,589	1,33
Heating length					
30	-166,2	19,7	-8,43	0,001	1,33
50	-11,6	19,7	-0,59	0,589	1,33

Regression Equation

Normalized-out-of-plane deform. = 665,6 + 115,4 Heating time_200 - 11,6 Heating time_500
- 103,9 Heating time_800 - 166,2 Heating length_30
- 11,6 Heating length_50 + 177,8 Heating length_80

General Factorial Regression: Width increase (arc length) ... ing length

Factor Information

Factor	Levels	Values
Heating time	3	200; 500; 800
Heating length	3	30; 50; 80

Analysis of Variance

Source	DF	Adj SS	Adj MS	F-Value	P-Value
Model	4	12,8204	3,2051	15,37	0,011
Linear	4	12,8204	3,2051	15,37	0,011
Heating time	2	3,2983	1,6492	7,91	0,041
Heating length	2	9,5221	4,7610	22,84	0,006
Error	4	0,8340	0,2085		
Total	8	13,6544			

Model Summary

S	R-sq	R-sq(adj)	R-sq(pred)
0,456613	93,89%	87,78%	69,08%

Coefficients

Term	Coef	SE Coef	T-Value	P-Value	VIF
Constant	3,066	0,152	20,14	0,000	
Heating time					
200	0,580	0,215	2,70	0,054	1,33
500	0,255	0,215	1,18	0,302	1,33
Heating length					
30	-1,339	0,215	-6,22	0,003	1,33
50	0,178	0,215	0,83	0,454	1,33

Regression Equation

Width increase (arc length) % = 3,066 + 0,580 Heating time_200 + 0,255 Heating time_500
- 0,835 Heating time_800 - 1,339 Heating length_30
+ 0,178 Heating length_50 + 1,161 Heating length_80

General Factorial Regression: Void content versus ... e; Heating length

Factor Information

Factor	Levels	Values
Heating time	3	200; 500; 800
Heating length	3	30; 50; 80

Analysis of Variance

Source	DF	Adj SS	Adj MS	F-Value	P-Value
Model	4	4,7984	1,1996	7,46	0,039
Linear	4	4,7984	1,1996	7,46	0,039
Heating time	2	4,4418	2,2209	13,81	0,016

Heating length	2	0,3566	0,1783	1,11	0,414
Error	4	0,6432	0,1608		
Total	8	5,4416			

Model Summary

S	R-sq	R-sq(adj)	R-sq(pred)
0,400988	88,18%	76,36%	40,16%

Coefficients

Term	Coef	SE Coef	T-Value	P-Value	VIF
Constant	3,649	0,134	27,30	0,000	
Heating time					
200	-0,897	0,189	-4,75	0,009	1,33
500	0,079	0,189	0,42	0,696	1,33
Heating length					
30	0,181	0,189	0,96	0,393	1,33
50	-0,277	0,189	-1,47	0,216	1,33

Regression Equation

Void content = 3,649 - 0,897 Heating time_200 + 0,079 Heating time_500
+ 0,818 Heating time_800 + 0,181 Heating length_30 - 0,277 Heating length_50
+ 0,096 Heating length_80

General Factorial Regression: Thickness increase % ... ; Heating length

Factor Information

Factor	Levels	Values
Heating time	3	200; 500; 800
Heating length	3	30; 50; 80

Analysis of Variance

Source	DF	Adj SS	Adj MS	F-Value	P-Value
Model	4	381,78	95,45	3,85	0,110
Linear	4	381,78	95,45	3,85	0,110
Heating time	2	189,00	94,50	3,81	0,118
Heating length	2	192,78	96,39	3,89	0,115
Error	4	99,16	24,79		
Total	8	480,94			

Model Summary

S	R-sq	R-sq(adj)	R-sq(pred)
4,97898	79,38%	58,76%	0,00%

Coefficients

Term	Coef	SE Coef	T-Value	P-Value	VIF
Constant	26,70	1,66	16,09	0,000	
Heating time					
200	-3,01	2,35	-1,28	0,269	1,33
500	-3,46	2,35	-1,48	0,214	1,33
Heating length					
30	6,30	2,35	2,68	0,055	1,33
50	-1,60	2,35	-0,68	0,533	1,33

Regression Equation

Thickness increase % = 26,70 - 3,01 Heating time_200 - 3,46 Heating time_500
+ 6,48 Heating time_800 + 6,30 Heating length_30
- 1,60 Heating length_50 - 4,70 Heating length_80

Screening Design

Screening design model: Max_rms_roughness versus ... Heating length

Analysis of Variance

Source	DF	Adj SS	Adj MS	F-Value	P-Value
Model	3	313,849	104,616	2,49	0,134
Linear	3	313,849	104,616	2,49	0,134
Heating time	1	85,859	85,859	2,04	0,191
Cooling rate	1	2,962	2,962	0,07	0,797
Heating length	1	225,028	225,028	5,36	0,049
Error	8	335,965	41,996		
Lack-of-Fit	4	162,184	40,546	0,93	0,526
Pure Error	4	173,781	43,445		
Total	11	649,814			

Model Summary

S	R-sq	R-sq(adj)	R-sq(pred)
6,48040	48,30%	28,91%	0,00%

Coded Coefficients

Term	Coef	SE Coef	T-Value	P-Value	VIF

Constant	12,23	1,87	6,54	0,000	
Heating time	2,67	1,87	1,43	0,191	1,00
Cooling rate	0,50	1,87	0,27	0,797	1,00
Heating length	4,33	1,87	2,31	0,049	1,00

Regression Equation in Uncoded Units

Max_rms_roughness = -4,2 + 0,00892 Heating time + 0,0158 Cooling rate + 0,1732 Heating length

Alias Structure (up to order 2)

Factor	Name
A	Heating time
B	Cooling rate
C	Heating length

Aliases
I + AA + BB + CC
A - 0,33 BC
B - 0,33 AC
C - 0,33 AB

Screening design model: Thickness_increase versus ... ; Heating length

Analysis of Variance

Source	DF	Adj SS	Adj MS	F-Value	P-Value
Model	3	217,85	72,62	1,42	0,307
Linear	3	217,85	72,62	1,42	0,307
Heating time	1	48,24	48,24	0,94	0,360
Cooling rate	1	73,59	73,59	1,44	0,265
Heating length	1	96,03	96,03	1,88	0,208
Error	8	409,34	51,17		
Lack-of-Fit	4	228,99	57,25	1,27	0,411
Pure Error	4	180,35	45,09		
Total	11	627,19			

Model Summary

S	R-sq	R-sq(adj)	R-sq(pred)
7,15316	34,73%	10,26%	0,00%

Coded Coefficients

Term	Coef	SE Coef	T-Value	P-Value	VIF
Constant	28,06	2,06	13,59	0,000	
Heating time	2,00	2,06	0,97	0,360	1,00
Cooling rate	-2,48	2,06	-1,20	0,265	1,00
Heating length	-2,83	2,06	-1,37	0,208	1,00

Regression Equation in Uncoded Units

Thickness_increase = 42,9 + 0,00668 Heating time - 0,0786 Cooling rate - 0,1132 Heating length

Alias Structure (up to order 2)

Factor	Name
A	Heating time
B	Cooling rate
C	Heating length

Aliases
I + AA + BB + CC
A - 0,33 BC
B - 0,33 AC
C - 0,33 AB

Screening design model: Width increase versus Heating ... ting length

Analysis of Variance

Source	DF	Adj SS	Adj MS	F-Value	P-Value
Model	3	27,4836	9,1612	31,38	0,000
Linear	3	27,4836	9,1612	31,38	0,000
Heating time	1	4,5294	4,5294	15,52	0,004
Cooling rate	1	0,7781	0,7781	2,67	0,141
Heating length	1	22,1762	22,1762	75,97	0,000
Error	8	2,3353	0,2919		
Lack-of-Fit	4	0,3600	0,0900	0,18	0,936
Pure Error	4	1,9753	0,4938		
Total	11	29,8190			

Model Summary

S	R-sq	R-sq(adj)	R-sq(pred)
0,540292	92,17%	89,23%	82,38%

Coded Coefficients

Term	Coef	SE Coef	T-Value	P-Value	VIF
Constant	3,313	0,156	21,24	0,000	
Heating time	-0,614	0,156	-3,94	0,004	1,00
Cooling rate	0,255	0,156	1,63	0,141	1,00
Heating length	1,359	0,156	8,72	0,000	1,00

Regression Equation in Uncoded Units

Width increase = 0,113 - 0,002048 Heating time + 0,00808 Cooling rate + 0,05438 Heating length

Alias Structure (up to order 2)

Factor	Name
A	Heating time
B	Cooling rate
C	Heating length

Aliases
I + AA + BB + CC
A - 0,33 BC
B - 0,33 AC
C - 0,33 AB

Fits and Diagnostics for Unusual Observations

Obs	Width increase	Fit	Resid	Std Resid	
8	2,714	3,803	-1,089	-2,47	R

R Large residual

Screening design model: Void content (%) versus ... te; Heating length

Analysis of Variance

Source	DF	Adj SS	Adj MS	F-Value	P-Value
Model	3	2,5480	0,8493	0,60	0,632
Linear	3	2,5480	0,8493	0,60	0,632
Heating time	1	1,5460	1,5460	1,10	0,326
Cooling rate	1	0,7689	0,7689	0,55	0,481
Heating length	1	0,2331	0,2331	0,17	0,695
Error	8	11,2854	1,4107		
Lack-of-Fit	4	9,1012	2,2753	4,17	0,098

Pure Error	4	2,1842	0,5461
Total	11	13,8334	

Model Summary

S	R-sq	R-sq(adj)	R-sq(pred)
1,18772	18,42%	0,00%	0,00%

Coded Coefficients

Term	Coef	SE Coef	T-Value	P-Value	VIF
Constant	3,780	0,343	11,02	0,000	
Heating time	0,359	0,343	1,05	0,326	1,00
Cooling rate	0,253	0,343	0,74	0,481	1,00
Heating length	0,139	0,343	0,41	0,695	1,00

Regression Equation in Uncoded Units

Void content (%) = 1,65 + 0,00120 Heating time + 0,0080 Cooling rate + 0,0056 Heating length

Alias Structure (up to order 2)

Factor	Name
A	Heating time
B	Cooling rate
C	Heating length

Aliases
I + AA + BB + CC
A - 0,33 BC
B - 0,33 AC
C - 0,33 AB

Screening design model: Normalized max out of plane ... ating length

Analysis of Variance

Source	DF	Adj SS	Adj MS	F-Value	P-Value
Model	3	218958	72986	2,72	0,115
Linear	3	218958	72986	2,72	0,115
Heating time	1	8112	8112	0,30	0,598
Cooling rate	1	16280	16280	0,61	0,459
Heating length	1	194565	194565	7,25	0,027
Error	8	214808	26851		
Lack-of-Fit	4	59907	14977	0,39	0,810

Pure Error	4	154901	38725
Total	11	433766	

Model Summary

S	R-sq	R-sq(adj)	R-sq(pred)
163,863	50,48%	31,91%	0,00%

Coded Coefficients

Term	Coef	SE Coef	T-Value	P-Value	VIF
Constant	564,5	47,3	11,93	0,000	
Heating time	-26,0	47,3	-0,55	0,598	1,00
Cooling rate	36,8	47,3	0,78	0,459	1,00
Heating length	127,3	47,3	2,69	0,027	1,00

Regression Equation in Uncoded Units

Normalized max out of plane def = 149 - 0,087 Heating time + 1,17 Cooling rate + 5,09 Heating length

Alias Structure (up to order 2)

Factor	Name
A	Heating time
B	Cooling rate
C	Heating length

Aliases
I + AA + BB + CC
A - 0,33 BC
B - 0,33 AC
C - 0,33 AB

Fits and Diagnostics for Unusual Observations

Obs	Normalized max out of plane def	Fit	Resid	Std Resid	
7	1053,3	754,6	298,7	2,23	R

R Large residual

Bibliography

[1] J. Hale. Boeing 787 from the ground up. *Aero. 4. 17-24.*, page 18, 2006.

[2] Hexcel. Hexcel ready to fly on the A350 XWB. *Reinforced Plastics 57(3): 25-26*, 2013. doi: https://doi.org/10.1016/S0034-3617(13)70089-4.

[3] J.M. Marchello N.J. Johnston, T.W. Towell and R.W. Grenoble. Automated fabrication of high performance composites: an overview of research at the Langley research center. In *Proceedings of ICCM–11, Gold Coast, Australia; 14–18th July 1997. p. 85–1*, 1997.

[4] Thermoplastic composites gain leading edge on the A380. Retrieved on: 15 December 2018. https://www.compositesworld.com/articles/thermoplastic-composites-gain-leading-edge-on-the-a380.

[5] Frederic Neil Cogswell. *5 - Processing science and manufacturing technology*, pages 107–159. Butterworth-Heinemann, 1992. ISBN 978-0-7506-1086-5. doi: https://doi.org/10.1016/B978-0-7506-1086-5.50011-2. URL http://www.sciencedirect.com/science/article/pii/B9780750610865500112.

[6] Tencate Advanced Composites. Inside a thermoplastic composites hotbed. https://www.tencatecomposites.com/media/3d4e6a1f-98e8-4f55-bb7e-33e9dcc7d1f8/x526ZQ/TenCate%20Advanced%20Composites/Documents/Articles/TenCate_CW_InsideThermoplasticHotbed_Daher_Socata_Cetex.pdf, 2018. Retrieved on: 15 November 2018.

[7] Daniel B. Miracle and Steven L. Donaldson. *60.1 Applications*. ASM International, 2001. ISBN 978-0-87170-703-1. URL https://app.knovel.com/hotlink/pdf/id:kt007PSCM2/asm-handbook-volume-21/fiber-plac-applications.

[8] Muhammad Amir Khan, Peter Mitschang, and Ralf Schledjewski. Identification of some optimal parameters to achieve higher laminate quality through tape placement process. *Advances in Polymer Technology*, 29(2):98–111, 2010. ISSN 0730-6679. doi: 10.1002/adv.20177. URL https://doi.org/10.1002/adv.20177.

[9] M. A. Khan and R. Schledjewski. Influencing factors for an online consolidating thermoplastic tape placement process. In *ICCM International Conferences on Composite Materials (2009)*. URL https://www.scopus.com/inward/record.uri?eid=2-s2.0-80052057156&partnerID=40&md5=969843c96d11486ae0a451b296ff4589.

[10] A. J. Comer, D. Ray, W. O. Obande, D. Jones, J. Lyons, I. Rosca, R. M. O' Higgins, and M. A. McCarthy. Mechanical characterisation of carbon fibre–peek manufactured by laser-assisted automated-tape-placement and autoclave. *Composites Part A: Applied Science and Manufacturing*, 69:10–20, 2015. ISSN 1359-835X. doi: https://doi.org/10.1016/j.compositesa.2014.10.003. URL http://www.sciencedirect.com/science/article/pii/S1359835X14003133.

[11] L. Ye, Z. R. Chen, M. Lu, and M. Hou. De-consolidation and re-consolidation in cf/pps thermoplastic matrix composites. *Composites Part a-Applied Science and Manufacturing*, 36(7):915–922, 2005. ISSN 1359-835x. doi: 10.1016/j.compositesa.2004.12.006. URL <GotoISI>://WOS:000230195100005.

[12] Muhammad Amir Khan, Peter Mitschang, and Ralf Schledjewski. Parametric study on processing parameters and resulting part quality through thermoplastic tape placement process. *Journal of Composite Materials*, 47(4):485–499, 2012. ISSN 0021-9983. doi: 10.1177/0021998312441810. URL https://doi.org/10.1177/0021998312441810.

[13] Thijs Kok, W.J.B Grouve, Laurent L. Warnet, and Remko Akkerman. Quantification of tape consolidation during laser assisted fiber placement. In *Proceedings of 3rd International Symposium on Automated Composites Manufacturing, ACM 2017*, 2017.

[14] J. S. U. Schell, J. Guilleminot, C. Binetruy, and P. Krawczak. Computational and experimental analysis of fusion bonding in thermoplastic composites: Influence of process parameters. *Journal of Materials Processing Technology*, 209(11):5211–5219, 2009. ISSN 0924-0136. doi: https://doi.org/10.1016/j.jmatprotec.2009.03.008. URL http://www.sciencedirect.com/science/article/pii/S0924013609000983.

[15] Q. Chu, Y. Li, J. Xiao, D. Huan, X. Zhang, and X. Chen. Processing and characterization of the thermoplastic composites manufactured by ultrasonic vibration–assisted automated fiber placement. *Journal of Thermoplastic Composite Materials*, 31(3):339–358, 2018. doi: 10.1177/0892705717697781. URL https://www.scopus.com/inward/record.uri?eid=2-s2.0-85042521698&doi=10.11772f0892705717697781&partnerID=40&md5=a6874e95832ec7ea469c0cbf3e84dbcc.

[16] W. J. B. Grouve, L. Warnet, R. Akkerman, S. Wijskamp, and J. S. M. Kok. Weld strength assessment for tape placement. *International Journal of Material Forming*, 3(SUPPL. 1):707–710, 2010. doi: 10.1007/s12289-010-0868-z. URL https://www.scopus.com/inward/record.uri?eid=2-s2.0-78651589295&doi=10.1007%2fs12289-010-0868-z&partnerID=40&md5=ea236e2abe201b751a70c2cd905cbe57.

[17] W. J. B. Grouve, L. L. Warnet, B. Rietman, H. A. Visser, and R. Akkerman. Optimization of the tape placement process parameters for carbon–pps composites. *Composites Part A: Applied Science and Manufacturing*, 50:44–53, 2013. ISSN 1359-835X. doi: https://doi.org/10.1016/j.compositesa.2013.03.003. URL http://www.sciencedirect.com/science/article/pii/S1359835X13000742.

[18] R. Schledjewski and A. Miaris. Thermoplastic tape placement by means of diode laser heating. In *International SAMPE Symposium and Exhibition (Proceedings)*, volume 54, 2009. URL https://www.scopus.com/inward/record.uri?eid=2-s2.0-74949090025&partnerID=40&md5=2357bda5e4ebd4afc93e2ff91763d678.

[19] C. M. Stokes-Griffin, P. Compston, T. I. Matuszyk, and M. J. Cardew-Hall. Thermal modelling of the laser-assisted thermoplastic tape placement process. *Journal of Thermoplastic Composite Materials*, 28(10):1445–1462, 2015. ISSN 0892-7057. doi: 10.1177/0892705713513285. URL <GotoISI>://WOS:000368902000010.

[20] E. Beyeler, W. Phillips, and S. I. Güçeri. Experimental investigation of laser-assisted thermoplastic tape consolidation. *Journal of Thermoplastic Composite Materials*, 1(1):107–121, 1988. doi: 10.1177/089270578800100109. URL https://www.scopus.com/inward/record.uri?eid=2-s2.0-84965567423&doi=10.1177%2f089270578800100109&partnerID=40&md5=3a1a56f67af1e77e4652c3888ffef79f.

[21] C. M. Stokes-Griffin, S. Ehard, A. Kollmannsberger, P. Compston, and K. Drechsler. A laser tape placement process for selective reinforcement of steel with cf/pa6 composites: Effects of surface preparation and laser angle. *Materials & Design*, 116:545–553, 2017. ISSN 0264-1275. doi: 10.1016/j.matdes.2016.12.013. URL <GotoISI>://WOS:000393726600060.

[22] J. Tierney and J. W. Gillespie Jr. Modeling of heat transfer and void dynamics for the thermoplastic composite tow-placement process. *Journal of Composite Materials*, 37(19):1745–1768, 2003. doi: 10.1177/0021998035188. URL https://www.scopus.com/inward/record.uri?eid=2-s2.0-0141883922&doi=10.1177%2f0021998035188&partnerID=40&md5=d152edd4034f1ccac65e2a995b870716.

[23] P Tsotra, M Toma, A Pascual, F Schadt, C Brauner, and C Dransfeld. Thermo-oxidative degradation of peek at high temperatures. In *ECCM18 - 18th European Conference on Composite Materials (Proceedings), 2018*.

[24] M. A. Lamontia and M. B. Gruber. Remaining developments required for commercializing in situ thermoplastic atp. In *International SAMPE Symposium and Exhibition (Proceedings)*, volume 52 (2007). URL https://www.scopus.com/inward/record.uri?eid=2-s2.0-34748923505&partnerID=40&md5=d39ffc016460cf179c26a6453057e0d3.

[25] Thijs Kok. *On the consolidation quality in laser assisted fiber placement: The role of the heating phase*. PhD thesis, University of Twente, Netherlands, 9 2018.

[26] Z. Han, Z. Cao, Z. Shao, and H. Fu. Parametric study on heat transfer for tow placement process of thermoplastic composite. *Polymers and Polymer Composites*, 22 (8):713–722, 2014. URL https://www.scopus.com/inward/record.uri?eid=2-s2.0-84908137260&partnerID=40&md5=a21447de4c699a012e85a4b27fbdc0bc.

[27] M. B. Gruber, I. Z. Lockwood, T. L. Dolan, S. B. Funck, J. J. Tierney, P. Simacek, J. W. Gillespie Jr, S. G. Advani, B. J. Jensen, R. J. Cano, and B. W. Grimsley. Thermoplastic in situ placement requires better impregnated tapes and tows. In *International SAMPE Technical Conference (2012)*. URL https://www.scopus.com/inward/record.uri?eid=2-s2.0-84863911733&partnerID=40&md5=ad38329288df8ab328074a47604aa5d3.

[28] R. Schledjewski and A. K. Schlarb. In-situ consolidation of thermoplastic tape material effects of tape quality on resulting part properties. In *International SAMPE Symposium and Exhibition (Proceedings)*, volume 52 (2007). URL https://www.scopus.com/inward/record.uri?eid=2-s2.0-34748922266&partnerID=40&md5=d2754d5614cd78d5cd97f420e1379e61.

[29] M. A. Lamontia, M. B. Gruber, and B. J. Jensen. Optimal composite material for low cost fabrication of large composite aerospace structures using nasa resins or poss nanoparticle modifications. In *SAMPE Europe - 27th International Conference and Forums (2006)*.

[30] Christophe Ageorges, Lin Ye, Yiu-Wing Mai, and Meng Hou. Characteristics of resistance welding of lap shear coupons.: Part ii. consolidation. *Composites Part A: Applied Science and Manufacturing*, 29(8):911–919, 1998. ISSN 1359-835X. doi: https://doi.org/10.1016/S1359-835X(98)00023-2. URL http://www.sciencedirect.com/science/article/pii/S1359835X98000232.

[31] M. Brzeski and P. Mitschang. Deconsolidation and its interdependent mechanisms of fibre reinforced polypropylene. *Polymers & Polymer Composites*, 23(8):515–524, 2015. ISSN 0967-3911. doi: Doi10.1177/096739111502300801. URL <GotoISI>://WOS:000362143100001.

[32] J. Wolfrath, V. Michaud, and J. A. E. Manson. Deconsolidation in glass mat thermoplastic composites: Analysis of the mechanisms. *Composites Part a-Applied Science and Manufacturing*, 36(12):1608–1616, 2005. ISSN 1359-835x. doi: 10.1016/j.compositesa.2005.04.001. URL <GotoISI>://WOS:000232899100002.

[33] Meng Lu, Lin Ye, and Yiu-Wing Mai. Thermal de-consolidation of thermoplastic matrix composites—ii. “migration” of voids and “re-consolidation”. *Composites Science and Technology*, 64(2):191–202, 2004. ISSN 0266-3538. doi: https://doi.org/10.1016/S0266-3538(03)00233-1. URL http://www.sciencedirect.com/science/article/pii/S0266353803002331.

[34] Mattia Di Francesco, Laura Veldenz, Giuseppe Dell’Anno, and Kevin Potter. Heater power control for multi-material, variable speed automated fibre placement. *Composites Part A: Applied Science and Manufacturing*, 101:408–421, 2017. ISSN 1359835X. doi: 10.1016/j.compositesa.2017.06.015. URL http://www.sciencedirect.com/science/article/pii/S1359835X17302427.

[35] Lin Ye, Meng Lu, and Yiu-Wing Mai. Thermal de-consolidation of thermoplastic matrix composites—i. growth of voids. *Composites Science and Technology*, 62(16):2121–2130, 2002. ISSN 02663538. doi: 10.1016/s0266-3538(02)00144-6. URL http://www.sciencedirect.com/science/article/pii/S0266353802001446.

[36] F. Henninger, L. Ye, and K. Friedrich. Deconsolidation behaviour of glass fibre-polyamide 12 composite sheet material during post-processing. *Plastics Rubber and Composites Processing and Applications*, 27(6):287–292, 1998. ISSN 0959-8111. URL <GotoISI>://WOS:000078664100005.

[37] J. Wolfrath, V. Michaud, and J. A. E. Manson. Deconsolidation in glass mat thermoplastics: Influence of the initial fibre/matrix configuration. *Composites Science and Technology*, 65(10):1601–1608, 2005. ISSN 0266-3538. doi: 10.1016/j.compscitech.2005.02.001. URL <GotoISI>://WOS:000229824500014.

[38] TenCate Advanced Composites. Tencate cetex® tc1220 - product data sheet. Report, TenCate Advanced Composites, 2018.

[39] TenCate Advanced Composites. Tencate cetex® tc1320 - product data sheet. Report, Tencate Advanced Composites, 2018.

[40] Philips GmbH Photonics Aachen G. Derra. *Laser System with Laser Module PPM412-12-980-24-c and Supply Unit PPU104-12 Reference and Installation Manual Version 1.0*. Philips GmbH Photonics Aachen, 2017.

[41] Holger Moench and Günther Derra. High power vcsel systems. *Laser Technik Journal*, 11(2): 43–47, 2014. ISSN 1863-9119. doi: 10.1002/latj.201400024. URL https://doi.org/10.1002/latj.201400024.

[42] Mengxue Yan, Xiaoyong Tian, Gang Peng, Dichen Li, and Xiaoyu Zhang. High temperature rheological behavior and sintering kinetics of cf/peek composites during selective laser sintering. *Composites Science and Technology*, 165:140–147, 2018. ISSN 0266-3538. doi: https://doi.org/10.1016/j.compscitech.2018.06.023. URL http://www.sciencedirect.com/science/article/pii/S0266353818306390.

[43] ASTM E1933 - 14. Standard Practice for Measuring and Compensating for Emissivity Using Infrared Imaging Radiometers. Standard, American Society for Testing and Materials, 2018.

[44] ISO 4287 - 1997. Geometrical Product Specifications (GPS) – Surface texture: Profile method – Terms, definitions and surface texture parameters. Standard, International Organization for Standardization, 1997.

[45] T. K. Slange, L. L. Warnet, W. J. B. Grouve, and R. Akkerman. Deconsolidation of c/peek blanks: on the role of prepreg, blank manufacturing method and conditioning. *Composites Part a-Applied Science and Manufacturing*, 113:189–199, 2018. ISSN 1359-835x. doi: 10.1016/j.compositesa.2018.06.034. URL <GotoISI>://WOS:000444659100019.

[46] Hui Yan, Tai-jiao Du, and Guo-liang Peng. *Meso-scale simulation of temperature field in composite materials under laser irradiation*, volume 10173 of *4th International Symposium on Laser Interaction with Matter*. SPIE, 2017. URL https://doi.org/10.1117/12.2268338.

[47] Beer-Lambert Law. Retrieved on: 15 June 2019. http://www.pci.tu-bs.de/aggericke/PC4/Kap_I/beerslaw.htm.